Simulation and optimisation of batch distillation operations

Frederico da Conceição do Carmo Montes

Thesis to obtain the Master of Science Degree in

Chemical Engineering

Supervisors: **Prof Dr. Henrique A. Matos**

Dr. Charles Brand

Examination Comittee

Chairperson: **Prof. Dr. José M. Lopes**

Supervisor: **Prof. Dr. Henrique A. Matos**

Member of the Committee: **Prof. Dr. Rui M. Filipe**

December 2015

"The struggle you're in today, is developing the strength you need for tomorrow"

Page intentionally left blank

Acknowledgments

In the first place, I would like to show my gratitude to Prof. Dr. Henrique A. Matos, Prof. Dr. Carla Pinheiro and Prof. Dr. Costas Pantelides for the opportunity to work at Process Systems Enterprise Limited in London and improve my knowledge in modelling and optimization.

It would be unfair not to mention the help I received from everyone that works at PSE. I am really grateful to have had Dr. Charles Brand as my PSE's supervisor, for his patience, cheerfulness and wisdom were endless in my times of need. A huge word of appreciation goes to Maria Viseu, Vasco Manaças, Mariana Marques and Marteen Nauta, who supported me when Dr. Charles was not available. My work would not have been finished if it was not for Pierre's skill and knowledge in both optimization and mathematical methods, and for that I am really thankful. To all PSE team: thank you.

London might be labelled as one of the most cold and grey cities in the world. However, I was never bored or sad, thanks to great friends and extraordinary colleagues I have had the pleasure to meet and work with. Thank you Tomasz for welcomingly receiving us, the interns. Thank you Francisco, Mariana Marques, Artur, Renato, Mário, Hugo and Leonor for the trips, for the advices and for all the amazing experiences we had. Thank you Yera, JJ, Byeonggil, Giovanni, Gabriele, Mariana and Helena for sharing this time and experience with me.

To my old housemates, trip companions and above all, friends, I wish all the luck and success on their career. Whatever you are doing Joana, André and Metal, know this: I would love to work again with you, in a future yet to come.

A word of appreciation also goes to my friends at IST, for all the support and help in the last 5 years. I would not be the same person without all the adventures and struggles we have been through. Additionally, many, many thanks to my "Fixolinos", "C.V.P.Lombo" and the C1 family. You were there, when I needed.

Last, but not least, I would like to show my consideration and gratitude to my family. Their love, care and support were endless in every moment of my life.

Page intentionally left blank

Abstract

The present thesis has the objective of simulating and optimizing a model-based batch distillation system for ternary mixtures. Batch distillation is one of the prior choices for the production of high-purity and high-value products in a wide range of industries, from pharmaceutical to waste-water treatment plants. However, the reduction of the operation costs and the implementation of effective control strategies are probably the biggest challenges competitiveness of this method.

Therefore, a case study model was firstly assembled in gPROMS ProcessBuilder® with gML libraries, comprising a one stage distillation operation. This case was used to study and analyse control strategies. A second model was developed regarding a ternary mixture and a multi-stage column distillation. After its validation, the model was optimized by modifying the operational parameters and the time control intervals through three different objective functions.

In the optimization of the process having the recovery of the lightest component as target, there was a time reduction of 50% while improving the lightest component recovery by 5%. The energy consumption has dropped to 57% of the initial value.

In the optimization of the process having the recovery of the lightest and the medium component as target, the operational time has dropped to 60% of the initial value, while increasing the recovery of the lightest and medium component by 10% and 148%, respectively. The energy consumption has dropped to 64% of the initial value.

Finally, when optimizing the recovery of the three components, the time has been reduced by 39%, while reducing the energy consumption to 67% of the initial value. Although the recovery of the heaviest component then the initial simulation by 7%, the lightest and medium component recovery were improved by 9% and 186% respectively. Additionally, the amount of non-recovered components was reduced to 44% of its initial value.

Key-words:

Batch distillation, Dynamic simulation, Dynamic optimization, Distillation control, gPROMS

Page intentionally left blank

Resumo

A presente tese tem o objective de simular e optimizar um modelo de destilação *batch* para misturas ternárias. A destilação *batch* é uma das primeiras escolhas tomadas para a produção de produtos com elevado grau de pureza e de valor, numa grande variedade de indústrias que vão desde a farmacêutica às de tratamento de águas. Porém, a redução de custos e a implementação de estratégias de controlo eficientes são os maiores desafios para a competitividade deste método.

Com esse objectivo, um caso de estudo foi modelado e implementado em gPROMS ProcessBuilder® com as bibliotecas de gML, contendo uma operação de destilação com um andar de equilíbrio. O referido caso foi utilizado no estudo e análise de estratégias de controlo. Um segundo modelo referente a uma destilação ternária numa coluna multi-andar foi desenvolvido. Após validação do mesmo modelo, este foi optimizado, variando parâmetros operacionais e intervalos temporais de controlo para três diferentes funções objectivo.

Na optimização da recuperação do componente mais leve, o tempo de operação foi reduzido em 50% enquanto a recuperação do mesmo componente subiu 5%. O consumo de energia desceu para 57% do valor inicial.

Na optimização da recuperação do componente mais leve e do intermédio, o tempo de operação diminuiu para 60% do valor inicial, enquanto as recuperações do componente leve e intermédio subiram em 10% e 148%, respectivamente. O consumo de energia reduziu em 57% do valor inicial.

Por fim, aquando da optimização da recuperação dos três componentes, o tempo foi reduzido em 39%, enquanto o consumo de energia desceu para 67% do valor inicial. Embora a recuperação do componente pesado tenha diminuído em 7%, o componente leve e o componente intermédio tiveram um aumento da recuperação em 9% e em 186%, respectivamente. Adicionalmente, a quantidade de componentes não recuperados foi reduzida para 44% do seu valor inicial.

Key-words:

Destilação *batch*, simulação dinâmica, optimização dinâmica, controlo de destilação, gPROMS

Page intentionally left blank

Contents

Page intentionally left blank

List of Figures

Page intentionally left blank

List of tables

List of abreviations

CAP	Capacity factor introduced by Luyben
C.p. separator	Constant pressure controlled separator
C.t. separator	Constant temperature controlled separator
F.D.I.	Flow-driven initialization
FL	Feed rate from the middle vessel to the column
MEBAD	Multi-Effect Batch Distillation
MEBC	Multi-Effect Batch column
MERSHQ	Material, Energy, Rate, Sum, Hydrodynamic and eQuilibrium equations
MVBC	Middle-Vessel Batch column
NRTL	Non Random Two Liquid model
PI controller	Proportional integral controller
PSE	Process Systems Enterprise
R.V.S.P.	Reflux valve stem position
SIM-1	Simulation 1
SIM-2	Simulation 2

Page intentionally left blank

Nomenclature

B_0	Initial mixture holdup	mol
C_v	Orifice coefficient	-
C_1	Products value	$
C_2	Raw material cost	$
C_3	Energy and utilities cost	$
$Calculated_{output}$	Proportional gain	-
$D(t_f)$	Amount of recovered product per distillation	mol
d_h	Hole diameter	m
$Distillate_{flowrate}$	Distillate flowrate leaving the column	Mol/h
$Distillate_{purity}\ (n)$	Component n molar purity in the distillate	-
f_i^l	Fugacity of component i in the liquid phase	bar
f_i^V	Fugacity of component I in the liquid phase	bar
g	Constant gravitational acceleration	m/s^2
h_c	Effective clear liquid heigh	m
h_d	Dry vapour pressure drop	m
h_f	Froth height	m
h_l	Aerated liquid pressure drop	m
h_w	Weir height	m
$h_{L,j}$	Liquid specific enthalpy for stage j	J/mol
$h_{V,j}$	Vapour specific enthalpy for stage j	J/mol
h_σ	Residual pressure drop due to surface tension	m
$Heavy_{acum}$	Heavy component accumulation in the reboiler	mol
k_s	Vapour velocity tuning factor	m/s
L_j	Liquid flowrate in stage j	mol/s
$Light_{acum}(n)$	Molar holdup of the n component during light component recovery	mol
$Light_{recov}$	Light component recovery	mol
$M_{L,i}$	Liquid molar holdup of component i on stage j	mol
$M_{V,i}$	Vapour molar holdup of component i on stage j	mol
Max_{mol}	Objective function	mol/h
$Medium_{acum}(n)$	Molar holdup of the n component during medium component recovery	mol
$Medium_{recov}$	Medium component recovery	mol
$Minimum_{DistPurity}(m)$	Minimum distillate purity during *m* component recovery period	-
$Minimum_{TankPurity}(m)$	Minimum acumulation purity during *m* component recovery period	-
$N_{i,j}$	Component i holdup on stage j	mol

P_j^L	Liquid pressure on stage j	bar
P_j^V	Vapour pressure on stage j	bar
$P(t_f)$	Average profit per time per distillation	$/hr
$Product_{recovery}$	Molar holdup recovered from the initial molar holdup	mol
Q	Volumetric flow	m^3/s
$RefluxValve_{StemPosition}$	Instant stem position of the reflux valve	-
$Setpoint_{Valve}$	Desired reflux valve stem position	-
T_c	Distillation maintenance time	hr
T_j^L	Liquid temperature on stage j	K
T_j^V	Vapour temperature on stage j	K
T_{op}	Distillation operation time	hr
U_j	Energy holdup on stage j	J
V	Separator volume	m^3
v_a	Vapour velocity through the active area	m/s
V_h	Vapour velocity through tray holes	m/s
V_j	Vapour flowrate in stage j	mol/s
v^{exp}	Experimental value	-
v^{sim}	Simulation value	-
$Ver_{DistPurity}(m)$	Veracity variable for the distillate purity specifications in the *m* component recovery period	-
$Ver_{TankPurity}(m)$	Veracity variable for the recovery purity specifications in the *m* component recovery period	-
$x_{i,j}$	Liquid molar fraction of component i on stage j	-
$y_{i,j}$	Vapour molar fraction of component I on stage j	-
α	Tuning constant for proportional gain	-
β	Tuning factor for faster change in tangent hyperbolic equations	-
$\mu_{i,j}^L$	Component i chemical potential in the liquid phase on stage j	J/mol
$\mu_{i,j}^V$	Component i chemical potential in the vapour phase on stage j	J/mol
Φ_f	Froth density	kg/m^3
ρ_{mol}	Molar density of the separator mixture	mol/m^3
ρ^L	Liquid density	kg/m^3
ρ^V	Vapour density	kg/m^3
σ	Surface tension	N/m

1. Introduction

1.1. **Motivation**

Batch distillation has always been an important process in the history of mankind. From the simple archaic alembics used for alcohol enrichment to the multi complex pharmaceutical batch columns, batch distillation has improved and is still present in the evolving chemical industry. The flexibility of this method, associated to the high product value, uncertain market demands and lifetimes, makes batch distillation a common separation process nowadays. Additionally, a huge number of chemical industries rely on the batch distillation to separate a multicomponent mixture with only one column, or to distillate a mixture with solid contents.

Although batch distillation is commonly used in industry, it is still one of the most complex processes to simulate, control and optimise. With the growth and evolution of chemical industry, more robust and reliable simulations and optimisation tools are requested to achieve new levels of efficiency and productivity. Therefore, the main purpose of this work is to simulate and optimise batch distillation systems using gPROMS ProcessBuilder® with gML® libraries, validating the existing distillation models and possibly providing feedback or model improvements. In order to achieve this objective, a case study is firstly assembled, and the dynamic behaviour of a simple ternary Rayleigh distillation and the component recovery are studied. Following the case study, a distillation system composed of a 15 tray column, valve models and controller models, is validated against experimental data from a ternary mixture. Different specification strategies are conducted, in order to understand and obtain more realistic results. Furthermore, the same system is used for a sensitivity analysis in the main system operating variables. Finally, the operating parameters behaviour are dynamically optimised for the ternary mixture when: recovering only the lightest component, recovering the lightest and the medium component, recovery all the three components (full distillation optimisation). The minimum time control intervals and their duration are been calculated for the first two cases.

With the present thesis, a strong backup is provided for the powerful simulation tools provided by Process Systems Enterprise Limited (PSE) (see [1]) while providing an optimal operational strategy for the analysed system.

1.2. **State of the art**

An intense literature review is provided in chapter 2 of the current thesis to cover the main and most important developments in batch distillation. These developments include the most common operating policies in batch distillation, the evolution and existent models, different column designs and configurations, and the evolution of the optimisation objectives and problems for the batch distillation.

Many authors dedicated their work in the pursuit of the optimal operating policy for batch distillation column, such as Converse [2] and Robinson [3]. Both compared and analysed the results obtained against the most common operating policies: constant reflux ratio or constant overhead composition. However, most of the early developments made in this area used shortcut models to soften the required computer processing power and the problem complexity. Examples of these shortcuts are the studies realised by authors such as Barolo [4] and Sundaram [5]. With time, nonequilibrium stage models with mass transfer equations from Maxwell-Stefan equation [6] are implemented and modelled for recent papers [7] [8].

Also, different column configurations are presented and their impact in system behaviour studied. Sorensen [9] and Hasebe [10] studied the inverted column configuration, and compared the results with the performance of a regular column. The implementation of a middle vessel in a batch column has been studied by many authors such as Morari [11] who compared the behaviour of a middle vessel batch column (MVBC) against a regular and a inverted column. On the other hand, Demicoli [12] analysed an azeotropic binary mixture and a zeotropic ternary mixture in a MVBC, showing the possibility of reducing the overall mixture temperature and the start-up time. However, it's the multi-effect batch column system (MEBC) that attains all the present attention: Hasebe and Kurooka [13] compared a MEBC with a continuous distillation system, for different multicomponent mixtures with constant relative volatilities, concluding that the separation performance tends to the same value, for both methods, the greater the number of components in the mixture. Skogestad and Wittgens [14] operated a pilot MEBC and tested its feasibility. Although the startup brought some concerns, the column showed an "autonomous" behaviour.

The optimisation objective for batch distillation has always received huge interest from the industry. A choice has always to be taken into account: time problem optimisation (see for example [15]), product recovery optimisation [16], profit optimisation [17], or simply a minimisation of the energy rate [18]. For the present thesis, operational parameters and optimal time control intervals were determined in order to maximixe the capacity factor (CAP) defined by Luyben [19].

1.3. **Original Contributions**

The contributions of this work are the following: preparation and development of a gPROMS ProcessBuilder® case study involving constant pressure and constant temperature controlled separators; validation of gML libraries and column models against experimental batch distillation data publicly available; development of modelling strategies for control and optimal operation of a batch distillation system

1.4. **Dissertation Outline**

The present thesis is organised in the following way:

- Chapter 2 presents a deep and comprehensive literature review on batch distillation. The operating policies, modelling evolution, existent column designs and different optimisation problems are analysed and discussed

- Chapter 3 introduces the gPROMS ProcessBuilder® software and the Multiflash™ physical property package used to develop the models and the thermodynamic properties described in this work;

- Chapter 4 contains a case study of a separator distillation, operating in two different ways: constant pressure and constant temperature;

- Chapter 5 introduces a batch distillation simulation, which is validated against experimental data. Furthermore, a sensitivity analysis is performed in the same system, for some of the operational variables. Finally, optimisation problems are solved for three different cases.

- Chapter 6 presents the final conclusions drawn from this work, as well as suggestions for future work.

Page intentionally left blank

2. Literature Review

Distillation is the most used separation method in chemical industry, relying on different volatilities to separate a liquid mixture into different products. Not only is the most used, it is as well the most ancient one. This process dates back to at least the 1st century A.D., and it started being used in the 11st century to enrich the alcohol content in beverages, in Italy [20]. At that time the distillation operations were carried out in simple one-staged devices, in which the liquid mixture was fed to a heated vessel, condensed, and the dripping vapour recovered into a pot or recovery tank. Today this process is widely known as a Rayleigh distillation. Major developments in this process appeared with the industrial revolution: in 1813, Cellier-Bluementhal developed the first multistage vertical column for continuous distillation; in 1820, the very first packing is applied to a distillation column, consisting of glass spheres; a few years later, sieve trays and bubble cap trays are invented, and the first distillation book is edited by Ernest Sorel [21]. During the 20th century, distillation becomes the main operation for crude oil separation, and today some authors affirm that there are more than 40.000 distillation columns only in the USA, consuming 7% of that country energy [22].

Unlike what was expected in 1950 [23], batch distillation is still a plausible choice in certain separation cases. The need for a flexible separation process is the major choice factor for a batch distillation instead of a continuous one. In addition, it is also considered an efficient choice for mixtures with solids contents, allowing the removal of these by the end of the process [24].

Although batch distillation is considered a low-capital investment, the high energy demand and energy wastes are major negative points [25]. Efforts are being made to find and to implement new column designs and different operating policies in order to improve batch processes.

Operating Policies

In a batch distillation operation, there are two main operating policies: operating with a constant reflux ratio, or operating with a constant distillate composition [26]. The reflux ratio is an instant recycling factor, between the liquid content that leaves the process (distillate) and the liquid that is recycled to the column (see figure 1). At the beginning of the distillation the distillate composition is rich in the most volatile components. With time, the composition starts to get heavier, and the operation is stopped when the recovered product purity meets the required specification. In most distillations, it is highly common to perform an off-cut between product separations. This method allows the recovery of light components in different recovery tanks. The off-cut is recovered in a different recovery tank with off specification mixture, and the distillation ends when the heaviest product meets the specifications inside the reboiler.

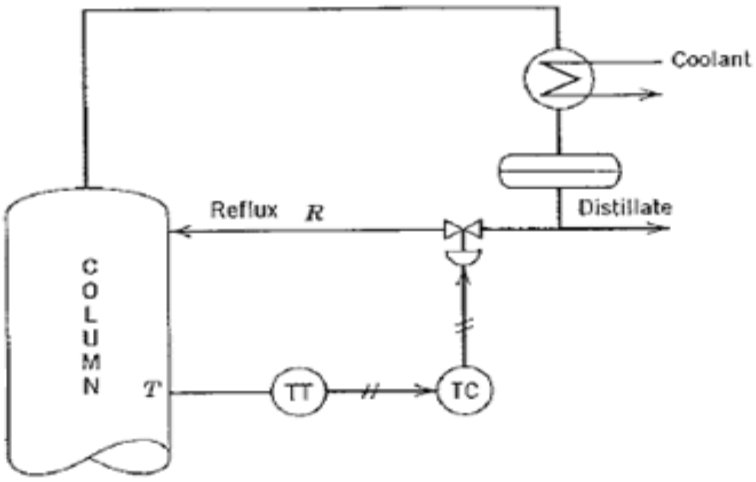

Figure 1 - Distillation column stripping section [23]

Operating with a constant reflux ratio is probably the most common method between the constant distillate composition and the constant reflux ratio policy. In fact, the control strategies and material are the simplest: flow sensors and valve controllers. Assuming no perturbation and constant heat input to the system, it is possible to maintain a constant reflux controlling only the distillate output and the reflux flow. This is achieved by simply using a timed reflux splitter, a ratio controller and a pair of rotameters [24]. However, the off-cut point or distillation end point might be difficult to estimate. This is highly dependent on the method used to estimate the average accumulated distillate product.

Depending on the mixture and system characteristics, both methods will have advantages and disadvantages. Kirster [21] has shown that different policies might have different results for the same system. A constant reflux performed in a three stage column had reduced heat input and up to 25% more product than a constant distillate composition. However, the recovered product had lower purity than a constant distillate policy. A choice has to be made, according to each situation.

However, in most of the time the reflux ratio is a time function variable, divided in time control intervals or manipulated as a constant function. The result is a mixture of the policies presented above, and in most of the cases the results are much more optimistic. Coward [15] was one of the first academics to study and compare an optimal reflux policy. In his work, he minimized the distillation time by only a few per cent, and concluded that the optimal reflux policy was dependent on the still composition.

Other authors included the optimal reflux ratio policy in batch reactive distillations. In 1981, Egly et al. [27] studied the optimum reflux ratio and operating policy for a generic A + B <-> C + D reaction (see figure 2). The optimal reflux policy with a continuous feed of the heaviest reagent achieves a time reduction of around 40%. Mujtaba et al. [28] studied the optimal reflux policy in the production of lactic acid by hydrolysis reaction of methyl acetate, in a batch reactive distillation. Using gPROMS® software, operation time was reduced by 37%, 46% and 48%, using respectively 2, 3, and 4 time intervals. The purity specifications and product recovered have always been met.

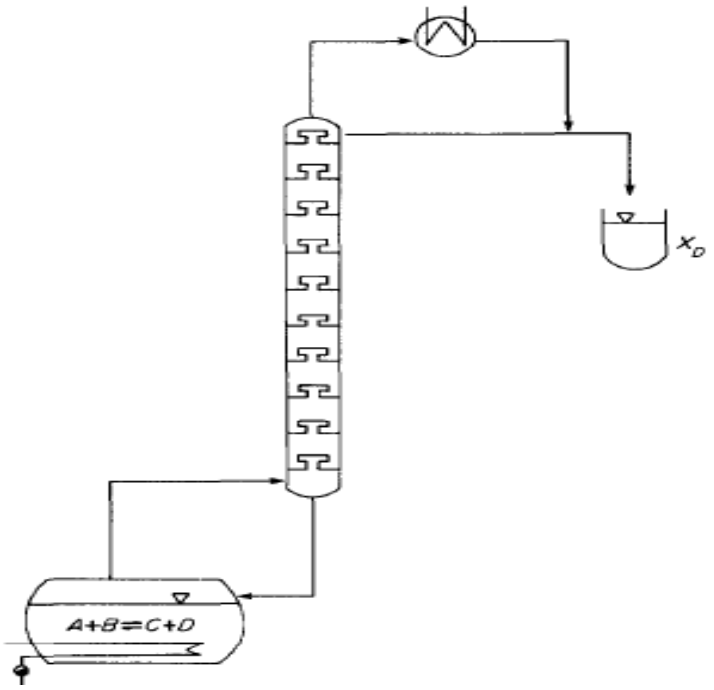

Figure 2- Reactive distillation column schematic [27]

Batch distillation can also be operated using a cyclic operating policy (see figure 3, [29]). This policy is known for repeating the same three operations: filling the condenser, operating at total reflux ratio, and dumping the condenser. The filling of the condenser is determined by the heat input to the system, and can be assumed as the column startup. In simple terms, these steps are performed until the overall composition of the product is met, as well as the recovered amount. During the second period, the column operates at total reflux ratio until the system achieves the steady state. At this point, the purity in the condenser holdup is the highest achievable at that specific time. The last period only empties the drum, and its duration is highly dependent on the maximum distillate flow achievable by the system. Mujtaba [23] affirms that this operating policy is high favorable to laboratory and pilot columns, as it is difficult to control small distillate flows and attain accurate measurements.

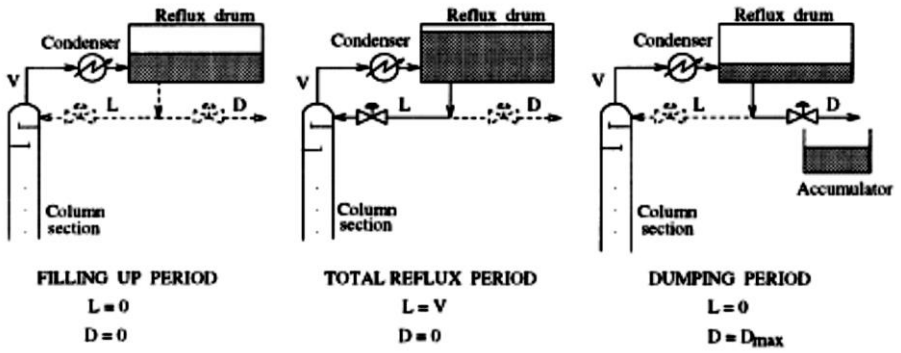

Figure 3- The three cyclic operation policy periods[29]

E. Sørensen [29] discussed the implementation of a cyclic operating policy within different columns configurations. When performing a distillation of a binary mixture with a relative volatility of 1.5, the operation time could be reduced up to 32%. This value is compared to an optimal reflux policy for the same system, in a regular column with 10 trays. Additionally, the cyclic policy was favorable for close boiling mixtures.

All of the above mentioned reflux policies can be improved by recovering or re-utilizing the distillated off-cuts, distillated between two different components [30]. Different authors have studied and analyzed the influence of the off-cut recovery. Luyben [31] has studied the influence of including the distilled off-cut in the following distillation, in a ternary mixture. A pseudo steady state was obtained after three complete distillations, with only 1% difference from the cyclic steady state. Later, in 1990, Luyben and Quintero-Marmol [32] studied different strategies for the off-cut recovery. These strategies englobed including the off-cuts in the following distillation pot (strategy I) (see figure 4), saving and storing the off-cuts until there was enough volume for full off-cut distillation (strategy II), feeding the off-cuts at a specific time and tray during the next operation (strategy III), feeding the heaviest off-cut to the pot and the lightest to the reflux drum (strategy IV), total cyclic operation policy (strategy V), and total cyclic operation policy with reflux drum being filled to its maximum before being dumped (strategy VI).

These strategies have been tested in ternary mixtures with relative volatility of 9/3/1, and for ternary mixtures with relative volatility of 4/2/1 (easy and hard separations, respectively), for minimum purities of 0.95 and 0.99. For all the cases, strategy II has the best results for the lowest required purity (0.95), and strategy V performs the best for the high purity demand (0.99). These strategies have improved the component recovery in average by 38% when compared with the most common method used (strategy I).

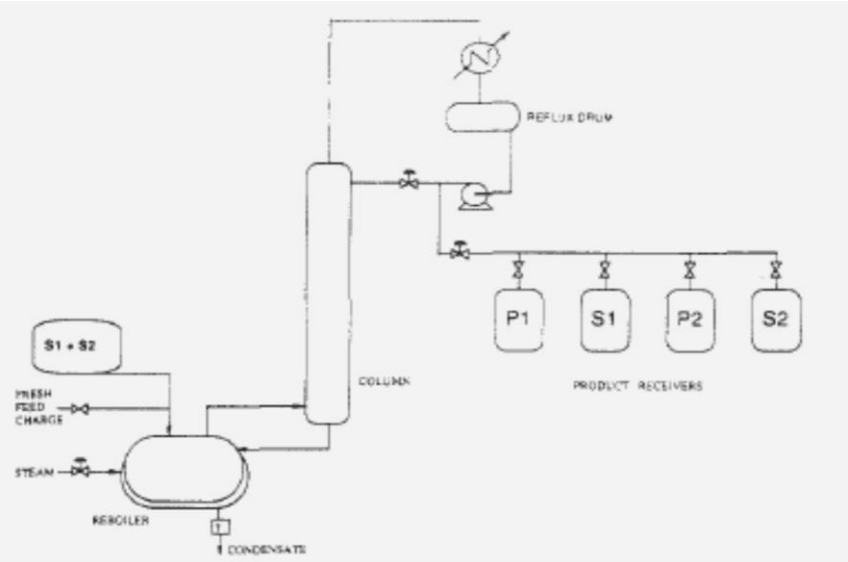

Figure 4- Schematic of the re-distillation of the off-cuts from previous separations (strategy I) [32]

Distillation modelling

Simulating the actual operation (both start-up and product period) of conventional columns has been the subject of much research for more than half a century [23]. The main interest was usually to develop a model (consisting of mass and energy balances, hydraulic model, physical properties, etc.) that could best predict the operation of the column.

The very first column model is the known Rayleigh model [33], but with the constant evolution of computers and processing speed, much more complex and real models have been implemented and created. Other examples of simplified models include the modified Fenske-Underwood-Gilliland (FUG) shortcut model for continuous distillation, and models that assume the constant molar holdup in the plates and condenser, total condensation without sub-cooling and negligible vapour holdup [23].

The so called rigorous models of a distillation column refer to a staged model that includes mass balance and energy balance on each stage. These models also include flow dynamics (with changes in the liquid holdups), and include models for pressure dynamics. Additionally, within these rigorous models, condenser and reboiler models are more detailed [34]. Nevertheless, most of the rigorous models include simplifications, such as assuming perfect mixture between vapour and liquid phases, perfect thermal and thermodynamic equilibrium and neglecting vapour influence in the column behavior. Also, a stage efficiency is usually applied.

For these cases, a typical equilibrium stage model (assuming no feed streams or heat input (see figure 5)) the mass balance may be formulated as:

$$\frac{dN_{ij}}{dt} = L_{j+1} * x_{1+1,j} + V_{i-1} * y_{i-1,j} - L_i x_{i,j} - V_{i,} * x_{i,j} \tag{2.1}$$

where:

$$N_{ij} = M_{li} * x_{ij} + M_{vi} * y_{ij} \tag{2.2}$$

and the energy balance is represented as:

$$\frac{dU_i}{dt} = L_{i+1} * h_{L,i+1} + V_{i-1} * h_{V,i-1} - L_i * h_{L,i} - V_i * h_{V,i} \tag{2.3}$$

where:

$$U_i = M_{L,i} * u_{L,i} + M_{V,i} * u_{V,i} \tag{2.4}$$

additionally, a force balance considers mechanical equilibrium, giving equal pressures for liquid and vapour phases ($P_j^V = P_j^L$). Finally, the thermodynamic model considers an identical chemical potential for both phases, and for each component in the mixture $\mu_{i,j}^V\left(T_j^V, P_j^V, y_{i,j}\right) = \mu_{i,j}^L\left(T_j^L, P_j^L, x_{i,j}\right)$ [35] .

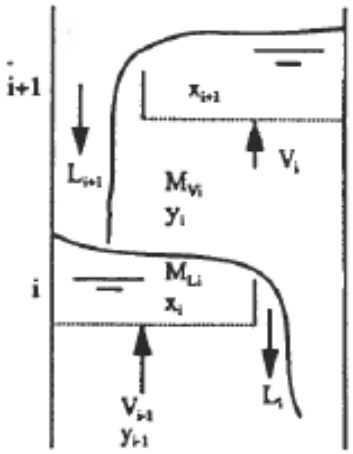

Figure 5- A distillation column stage [34]

The most advanced and realistic models do not assume stage equilibrium. Instead, the model equations for nonequilibrium stages are referred as the MERSHQ equations (Material, Energy balances, Rate of mass and heat transfer, Summation of compositions, Hydrodynamic equation of pressure drop and eQuilibrium) [24]. Vapour and liquid phases are now separated, each one with a mass and energy balance. Mass transfer between these phases is related to the chemical potential gradients using Maxwell-Stefan equations [6] (see for example reactive batch distillation modelling in Gorak et al. [7] and Krishna [8].

Batch column designs and configurations

In 1983 Rippin [36] defended that the ultimate objective for the chemical engineers was to convert batch processes into continuous ones. However, other studies [37] showed that many batch processes were still being operated in the U.K. Moreover, around 80% of those plants were producing for steady or growing markets.

Naturally the academics invested in the batch distillation field, including different and more exotic configurations for a batch distillation column. A background review on some of these designs is hereby presented.

Inverted column

Gilliland and Robinson [9] were the first authors to propose this new column configuration, in 1950 (see figure 6). They stated that the main advantage inverted columns would bring was the collecting of the lightest component being made in the condenser in high purity. This configuration is also called stripping batch column, or complex column, by Hasebe et al. [10]. The same author discussed and analyzed the performance of the inverted column configuration against the regular batch column. Assuming constant relative volatility and equal operating conditions, the separation

efficiency of this configuration was inferior to the regular one. Later, Chiotti and Iribarren [38] presented simplified models for regular and inverted columns. Furthermore, two numerical problems were optimized in terms of annual revenue, and the problem was extended to multicomponent mixtures in regular and inverted columns [39]. For these cases, inverted columns efficiency was superior to regular columns when the heavy component molar fraction was high.

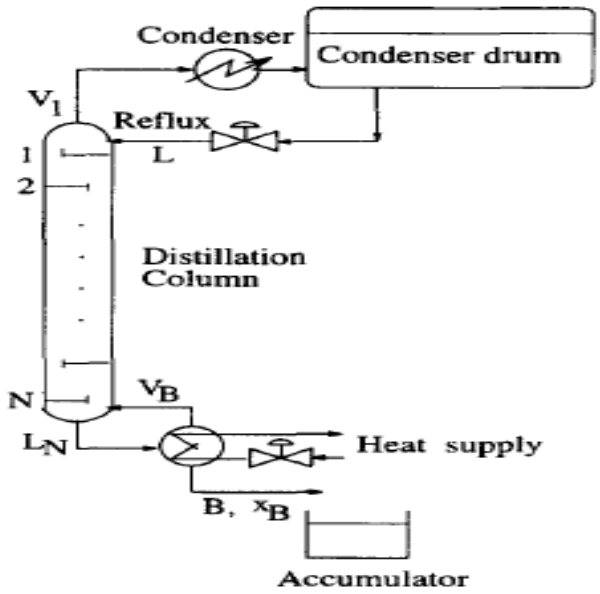

Figure 6- Schematic of an inverted column configuration and operation [9]

Sorensen and Skogestad [9] confirmed the behaviour stated by Chiotti et al. Operating with a binary mixture in a 10 tray column, and assuming a constant volatility of 2, the results where favourable for the inverted column with heavier mixture (see figure 7):

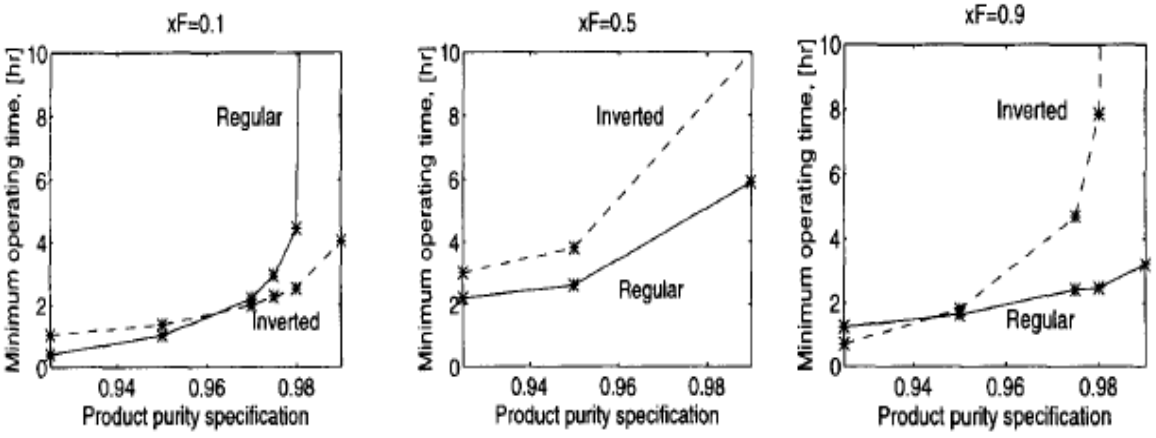

Figure 7- Minimum operating time for different binary mixture composition and purity specification, in the different column designs [9]

Sorensen concluded that the inverted column is the preferable design for heavier binary mixtures. Additionally, the time efficiency was also tested for different volatilities. As a conclusion, for

mixtures richer in heavier components, lower volatilities increased even more the minimum time operation difference between regular and inverted column.

Middle vessel columns

In the earlier 1970´s, Devyatikh [40] proposed a new column configuration composed of a regular batch column and one inversed batch column unified by a middle vessel (see figure 8). The middle vessel batch column (MVBC) has the initial holdup split between the condenser drum, reboiler and middle vessel, and the products are recovered from the bot and the top. Further studies realized in this system show that the new configuration has three main operational parameters: the reflux ratio, the boilup ratio, and the ratio between the liquid coming from the vessel and the vapour flowing to the top part of the column. This ratio is specified as *q* [41].

Morari and Meski [10] compared the time efficiency of the MVBC against an inverted column and a regular column. For the purpose, binary mixtures with different molar composition and with different constant volatilities were testes. As a conclusion, the MVBC required less operating time for any composition and for any relative volatility. The results also support Sorensen [9] conclusions on the inverted column: for compositions richer in heavy components, the inverted column has the best outcome.

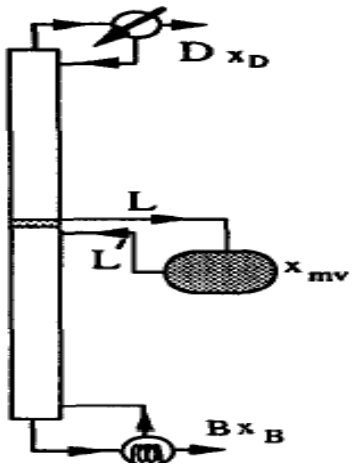

Figure 8- schematic of a MVBC design and operation

However, the *q* ratio might be difficult to set and control. Not only, but as the feed is now made in the middle vessel, the feed rate from the vessel to the column (FL) is also one important parameter to control. Barolo et al. [42] studied operational issues and control strategies for the MVBC. In this paper, the capacity factor (CAP) introduced by Luyben in 1971 [19] is optimized, for different operation policies and FL values. As expected, higher values of FL have a bigger impact in the operation time reduction. This effect is not as effective for the product recovery.

Higher values of FL have also a unique impact in the system behaviour. As a consequence of increasing the feed rate, the condenser and reboiler heat inputs will rise until a steady state in the system hydraulics and liquid/vapour flows is achieved. Also, as the holdup inside the vessel is in equilibrium with its vapour, a high demand in the FL value can cause disturbances. For instance, cavitation can occur in the FL pump. In the same article, a short analysis has been made to the changes in the reboiler steam input, showing some of the issues mentioned above.

Multi effect batch columns

With the introduction of MVBC, the efficiency results obtained were much more promising than regular and inverted batch column. Researchers and academics considered the combination of several regular columns operating together. In this new system, the condenser of the *n* column would be heat integrated with the reboiler of the *n+1* column [13] (see figure 2.9). This configuration was referred as Multi Effect Batch Column (MEBC), and is designated as multi vessel batch column or Multi Effect BAtch Distillation (MEBAD) by other authors.

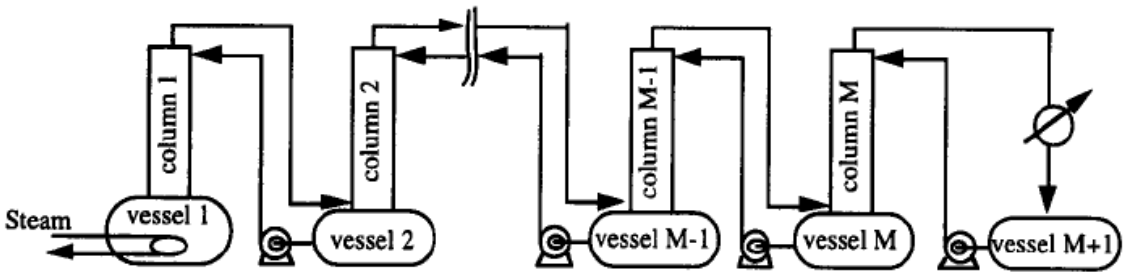

Figure 9- Schematic of a MEBC design and operation

In the same paper, the performance of the new system (MEBC) was compared with a continuous distillation system, for a separation performance objective (amount of product per time per boilup rate). Assuming a constant relative volatility of 3 and a product specification of 0.98, multicomponent mixtures were tested, ranging from 2 to 5. Incredibly, there is no difference for the 5 component mixture. The separation performance has the same value for both systems.

Later, Hasebe et al. [43] optimized the operational policy for binary and ternary mixtures in a MEBC system. While operating at total reflux, two policies where considered: constant holdup policy, and variable holdup policy. In the former, the holdup in the reboiler is optimized during the distillation. On the other hand, for constant holdup policy, only the initial reboiler holdup is optimized. The results show an increase of 61 % of the separation performance for binary distillation (equimolar feed), when operating with a variable holdup policy, instead of a constant holdup policy. The results for ternary mixtures are dependent of the feed composition, but the variable holdup policy has better results in all the cases. The same is verified when comparing a MEBC with a regular batch column, in the same article.

However, the case above considered constant holdup in the system stages, other than the reboiler and reflux drum. The initial distribution of the feed between the system vessels has been

addressed by Pantelides, Furlonge and Sorensen [18]. In this article, a detailed dynamic model was used to compare optimal operating policies in a MEBC with two middle vessels. In this system, an equimolar mixture of methanol, ethanol, n-propanol and n-butanol was studied, in terms of energy reduction per batch time. For the case presented above, different operating strategies have been analyzed:

- Constant holdup: the feed is distributed equally between the vessels, reboiler and reflux drum and is kept constant during total reflux;
- Optimal holdup: The initial feed is totally located in the reboiler or optimally distributed, and the holdup is allowed to vary during the simulation;
- Optimal product withdraw: material is allowed to be withdrawn into accumulators during the operation.
- Feedback control: a feedback control strategy is employed, where the reflux flow rates are adjusted based on temperatures measurements.

The optimal product withdraw achieved the best performance of all the simulations, when the feed distribution was optimized. However, this policy had a greater number of degrees of freedom when compared to the other policies. Therefore, maintaining a constant holdup in all vessels with the feed equally distributed achieves the worst results, as expected. Surprisingly, it has been shown that it is preferable to feed the entire initial holdup to the reboiler than distributing the feed according to its composition among the vessels.

Batch distillation optimization

Through the course of time, batch distillation optimization has changed, in terms of complexity and objectives. The first documented works in this subject have one of two main objectives: the minimization of the distillation time, or the maximization of the product recovery.

For the first objective, the constraints were based on a minimum recovered amount of product, and minimum component purity. Additionally, the model equality equations had to be satisfied. The second objective was optimized during a predefined operational time, while achieving minimum component purity. For both cases, the optimal reflux policy and the heat duty input were the optimized variables. The first papers in this belong to Converse, Robinson, Coward, Mayur, in the middle 60's (see [23] for further information).

Nevertheless, with the improvement of numerical techniques and methods, as well as the growing expenses of utilities due to the oil crisis [44], new optimization objectives were developed. In 1971, Luyben [19] presented a new objective perspective, which would maximize the amount of recovered product or minimize the batch distillation time. Instead, the CAP objective was to maximize the product recovery per unit of time:

$$CAP = \frac{Recovered\ product}{T_{op}+T_c} \quad (2.5)$$

where T_{op} is the distillation operation time, and T_c is the maintenance time (empting, cleaning and refilling column time). The equation presented above has been used by many other authors, such as Barolo et al. [42] for the operation of a MVBC.

By the same time, the first profit objective functions are optimized, for batch distillation systems. Kerkhof and Vissers [17] presented one of the first profit optimizations in 1978. They optimized the average profit per unit operation, taking into account the cost of raw materials, and assuming constant utilities cost:

$$P(t_f) = \frac{C_1 * D(t_f) - C_2 * B_0}{T_{op}+T_c} - C_3 \quad (2.6)$$

where C_1 is the value of the products, C_2 the cost of the raw materials, $D(t_f)$ the amount of recovered product, B_0 the initial mixture holdup, C_3 the cost of the energy and utilities, T_{op} the operation time, T_c the maintenance time and t_f the total distillation time.

Kerkhof and Vissers objective function was accurate to predict and optimize a distillation system in terms of profit. However, they assumed constant energy consumption and utilities costs and had no limit for the final product demand.

For the former, Mujtaba and Miladi [45] optimized and analysed the influence of the number of annual batches performed, for a profit optimization problem. As a conclusion, it was preferable to perform a greater number of batch distillations with lesser holdup and lower operation time, for a fixed value of vapour load. In fact, the profit revenue could be negative if the vapour load was on its maximum allowed value, and the number of batches was minimum. Other variables were also analysed, such as the optimum number of trays and reflux ratio policy.

In terms of energy consumption, it might be of industrial interest to change the operating policy of a column in order to reduce the utility costs. Therefore, a different objective and optimization strategy might be needed, such as the minimization of the energy rate proposed and solved by Furlonge et al. [18].

3. Materials and methods

3.1. gProms Processbuilder®

In the present thesis, gPROMS® ProcessBuilder® v1.0.0 was the platform used for simulation and validation of different batch processes, provided by Process Systems Enterprise ("PSE"). This platform allows the assembling of different flowsheets, using a simple drag and drop system. From the topology tab panel, a whole model can be connected and assembled, starting from an existing model's library, such as gML libraries. Additionally, it is still possible to add or change the different equations and variables in the gPROMS language tab.

Another feature of the gPROMS ProcessBuilder® is the optimisation tool, which is able to optimise a continuous or dynamic behaviour of an assembled flowsheet. For that purpose, it is necessary to provide certain unassigned variables which will be optimised. Constraints and objective function must be provided as well. For the current thesis, the gPROMS® NLPSQP solver has been used to optimise in chapter 5. It solves non-linear problems using a sequential quadratic programing method, optimally determined by the satisfaction of the Karush-Kuhn-Tucker conditions [46].

3.2. gML® Library

The gML® library contains steady state and dynamic models for a huge variety of processes. The models are based on mass balances, momentum, enthalpy and many other physical properties and chemical behaviours. The gML® library includes the models needed for batch distillation and one stage separators. Briefly, some of the models are going to be described in the following section.

3.2.1. Separator

This model describes a two-phase flash vessel (liquid-vapour). It is assumed that there is only one liquid phase, and one vapour phase, and that both are at phase equilibrium. The phase equilibrium is obtained via equality of the fugacities, with the fugacity coefficients being calculated from the physical property package provided (see section 3.3).

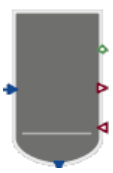

Figure 10- Separator and tank icon used in gPROMS ProcessBuilder®

3.2.2.Tank

The Tank model has the objective to simulate the storage of intermediate/final liquid components/products. The model's dynamics options determine liquid holdup accumulation, after design specifications and geometrical parameters inputs. The model has also the option to remove/add heat to the system, and energy holdups accumulation is calculated through an enthalpy balance.

3.2.3.Sink

The Sink model is the end-point of a flowsheet, where a material stream ends/leaves the flowsheet. The pressure is a specification needed for pressure-driven running mode, but unnecessary in flow-driven mode.

Figure 11- Sink icon used in gPROMS ProcessBuilder®

3.2.4.Source Material

The Source Material model is the beginning point of a material stream into the flowsheet/system, with infinite capacity if wished. The specifications include temperature, component fraction, pressure and/or flows. The physical property package used must be specified as well.

Figure 12- Source material icon used in gPROMS ProcessBuilder®

3.2.5.Controller

The Controller model describes and simulates the actions of a controller with proportional, integral and derivative gain. The action mode needs to be specified (manual, automatic or cascade model), as well as the type of controller (P, PD, PI or PID). Additionally, the model has a selector for direct or reverse action.

Figure 13– Controller icon used in gPROMS ProcessBuilder®

3.2.6.Distillation Column

The distillation column model describes a two-phase (vapour-liquid) distillation column. This column is divided into multiple stages. For each stage there is a mass and energy balance, and by default it assumed that vapour-liquid equilibrium is achieved at each state.

Condenser and reboiler sub-models also assume vapour-liquid equilibrium. Different types of reboiler designs and condenser operating policies can be selected (kettle reboiler, thermosiphon reboiler, partial condenser, total condenser…). Depending on the chosen policy, two or three operational specifications are required. These specifications include the reflux ratio, reboil ratio, distillate flowrate, cooling rate, amongst others.

Trays design and sizing can also be selected. Different correlations options are available for pressure drop, aerated liquid pressure drop, dry vapour pressure drop and clear liquid height. Non ideal trays can be modelled using the Murphree efficiency.

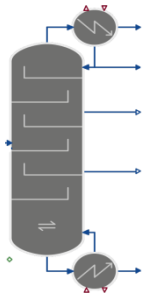

Figure 14- Distillation column icon used in gPROMS ProcessBuilder®

3.2.7.Valve

The Valve model simulates the flow of a fluid through a valve, using mass and energy balances, and flow-pressure drops relations. It is possible to use the valve flow characteristics curves to determine the flow coefficient fraction for linear, quick opening and butterfly valves. If desired, a dynamic behaviour of the valve stem position may be selected (Dynamic option), varying accordingly to a given position setpoint.

Figure 15- Valve icon used in gPROMS ProcessBuilder®

3.2.8.Splitter

The Splitter model divides an inlet stream into multiple outlet streams, depending on the flowrate or split fraction specified.

Figure 16– Splitter icon used in gPROMS ProcessBuilder®

3.2.9.Cooler

The cooler model simulates a heat exchanger that removes heat from a fluid stream. Three main modes are available: “Mass and energy balances only”, “design” and “performance”. The first two allow the heat duty exchanged as an input, while “performance” mode is dependent on the performance of the heat exchanger area and transfer coefficient. Only the third operating mode can be used for dynamic behaviour.

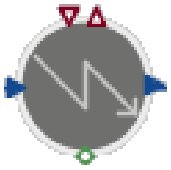

Figure 17- Cooler icon used in gPROMS ProcessBuilder®

3.2.10. Pump

This unit models the behaviour of a fluid through a pump using mass and energy balances. It is possible to use pump characteristic curves while specifying performance mode or, alternatively, specifying the outlet conditions, such as outlet flow or pressure ratio.

Figure 18– Pump icon used in gPROMS ProcessBuilder®

3.3. Physical properties

gPROMS standard physical property package is Infochem Multiflash ™ which is supplied by KBC Advanced Technologies [47]. As Multiflash is designed for equation-oriented modelling, it generates analytical partial derivatives and tight convergence of iterations for variables such as temperature, pressure, composition and density.

The determination of phase equilibrium is based on the fact that a component’s fugacity is equal in all phases, at equilibrium. For a single vapour-liquid system:

$$f_i^V = f_i^L \tag{3.1}$$

where f_i^V is the fugacity of component i in the gaseous state, and f_i^L is the fugacity of the component i in the liquid state. There are two main categories for the Multiflash fugacity models: equation of state methods and activity coefficients method. With an equation of state method, all thermal properties can be derived from an equation of state. On the other hand, an activity coefficient method derives the vapour phase properties from an equation of state, whereas the liquid properties are determined from the summation of the pure component properties to which a mixing term or an excess term has been added.

For the present thesis, the Non Random Two Liquid (NRTL) activity coefficient model was selected. It is a useful model for non-ideal systems and vapour-liquid equilibrium calculations.

Page intentionally left blank

4. Separator simulation: Modelling and scheduling

In this chapter, a Rayleigh separation is presented through a simplified flowsheet of a separator and tanks. The objective is to simulate the behaviour of a one stage semi-continuous distillation with refill and off-cuts schedule, and two different control strategies.

4.1. Case introduction

A simple separator followed by a condenser is the chosen case to exemplify a Rayleigh distillation, as well as to schedule and to observe dynamic behaviour of a simple batch process. The separator is filled with an initial mixture of cyclohexane, heptane and toluene, heat is supplied to the same vessel, and the output of the new vapour formed is guaranteed by a pump. The re-fill composition is the same as Mujtaba [23].

4.2. Flowsheet assembly

The flowsheet assemble in gPROMS® ProcessBuilder is presented in figure 19.

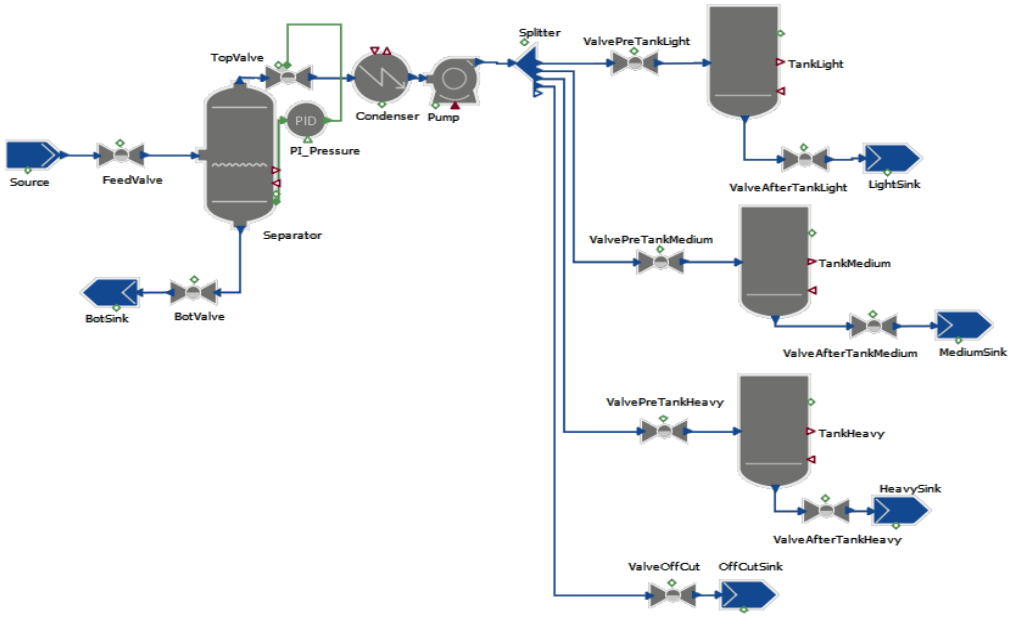

Figure 19- Separator case study assembled flowsheet

In the present flowsheet, all models have been selected to operate in pressure-driven mode excluding the pump model ("**Pump**"), the condenser model ("**Condenser**") and all the valve models. The initial mixture is specified in the separator model ("**Separator**"), assigning the initial desired molar

holdup. The initial pressure inside the separator is 0.7 bar and the heat duty supplied to the separator is 1 MJ/s. The initial holdup and the separator dimensions are shown in table 1:

Table 1– Design and initial molar holdup specifications of the separator model

Component specification		Separator design		
Component	**Initial molar holdup (kmol)**			
Cyclohexane	30	**Vessel heads**	**Separator height (m)**	**Diameter (m)**
Heptane	40			
Toluene	50	Flat	5	3

The source model ("**Source**") is in charge to re-fill the separator whenever the liquid height reaches a critical point (arbitrarily chosen as 1% of the separator's height). The inlet mixture has a temperature of 355 K, and a pressure of 1.013 bar. The molar fraction is the same as [23] or as shown in table 2:

Table 2 - Molar fraction in the feed source

Component	Molar fraction
Cyclohexane	0.407
Heptane	0.394
Toluene	0.199

The condenser has its bottom outlet closed at all times, due to the stem position of the respective valve ("**BotValve**"). The mixture inside the separator leaves in vapour state through the upper outlet, flowing across the upper valve ("**TopValve**"). In the present flowsheet, the valve stem position is the manipulated variable of the system's controller ("**PI_Pressure**").

A proportional-integral type of control was selected for the present controller model, adding a integral term to the steady-state proportional error. A maximum and a minimum value for both manipulated and controlled variables were specified, with values as shown in table 3.

The vapour exiting the separator is promptly condensed in the condenser model ("**Condenser**"), which is set to operate in a "mass and energy balance" mode. The only specification needed for this case is the enthalpy state of the distillate: either in saturated liquid, with a subcooling degree or specified temperature.

Table 3– "PI_Pressure" controller specifications

Controller parameters		Value
Controlled variable: "Separator" pressure	Min. value (bar)	0.2
	Max. value (bar)	1
Manipulated variable: "TopValve" stem position	Min. value	0.01
	Max. value	0.99
Controller action:		direct
Proportional gain		144
Integral time constant (s)		10

For integration matter and to better simulate a liquid pumping (in the following model), a 3 degree subcooling was selected. In reality, other factors would have been taken into account, such as liquid height, in order to prevent cavitation of the pump.

After condensing and subcooling, the distillate is pumped to its final destination, through the pump model ("**Pump**"). Operating in the simplest mode "mass and energy balance", the outlet pressure increase as been specified to 0.15 bar.

The splitter model ("**Splitter**") divides the inlet stream into as many as desired. Due to the operating mode pressure driven, split, ratio or division specifications are not necessary, as the different flows are calculated with rigorous pressure/pressure-drop – flow correlations from gPROMS® gML libraries. As the system operates in a semi-continuous mode (the distillation is continuous, however the separator refill is time dependent), there is no need for deactivating the "inlet low flow protection operating" mode: although it is strictly necessary its deactivation for batch processes due to flow interruption, this option is less robust for gPROMS ProcessBuilder®.

All the tank models presented in the current flowsheet have the same dimensions, same initial molar holdup, same pressure and same behaviour: the valve that controls the tank outlet (and named after the respective tank) is closed at all times, allowing a permanent component accumulation inside each tank, depending on which inlet valve is open. The table 4 has the characteristics of the tank that accumulates the light component ("**TankLight**"), which are equal for the other two tank models ("**TankMedium**" and "**TankHeavy**"):

Table 4 - Tank models specifications and dimensions

Intitial molar Holdup (kg)			Temperature (K)	Pressure (bar)	Diameter (m)	Height (m)
Cyclohexane	Heptane	Toluene	320	0.79	3	6
3	3	3				

Table 5 and 6 shows the specifications chosen for the valve and sink models, as well as additional information about their behaviour through the simulation:

Table 5– Valve models specifications and sizing

Valve model	Initial stem position	Flow coefficient (kg s^{-1} Pa^{-1})	Permanently closed	Dynamics	
				Dyn. mode	Time constant (s)
"FeedValve"	0	1e-3	No	No	---
"BotValve"	0	1e-3	Yes	No	---
"TopValve"	Controller dependent	1e-3	No	Yes	5
"ValvePreTankLight"	0	1	No	No	---
"ValvePreTankMedium"	0	1	No	No	---
"ValvePreTankHeavy"	0	1	No	No	---
"ValveAfterTankLight"	0	1e-3	Yes	No	---
"ValveafterTankMedium"	0	1e-3	Yes	No	---
"ValveAfterTankHeavy"	0	1e-3	Yes	No	---
"ValveOffCut"	0.5	1	No	No	---

"TopValve" dynamics mode was kept activated with the objective to give a time delayed perturbation to the "PI_Pressure" controller model, looking forward to obtaining a more realistic behaviour of its opening/closing action.

Table 6– Valve models specifications and sizing

Sink model	Pressure (bar)	High importance parameter
"BotSink"	1.005	No
"LightSink"	0.6	No
"Mediumsink"	0.6	No
"HeavySink"	0.6	No
"OffcutSink"	0.8	Yes

The pressure specification in the "**OffCutSink**" has, as expected, an impact in the gPROMS ProcessBuilder algorithm: all the pressure calculations, enthalpy and dynamics behaviours are calculated after the end-point pressure specifications. As shown in figure 19 and table 5, only "OffCutSink" preceding valve is not permanently closed. Any other pressure value value than the ones presented in table 6, were conceivable.

4.2.1.Constant pressure target

On the current process, two different operating ways were taken into consideration. For the first way, a constant pressure inside the separator was set as the objective of “PI_Pressure” controller model, with a setpoint of 0.69 bar. As shown in table 3, the “TopValve” stem position was selected as the manipulated variable, with controller specifications explicit in the same table.

With constant heat input the mixture will reach its boiling point, greater amounts of vapour will form and, as expected, the pressure and temperature will rise. By changing the stem position, ranging from 0 to 1 (closed / completely open, respectively), the vapour flow being pumped out of the system varies, allowing pressure to vary accordingly.

4.2.2.Constant temperature target

The second operating way consists of maintaining the temperature constant / under a maximum value, reducing the pressure of the system. The flowsheet for this operating way remains the same, apart from the controller model, which is now manipulating the “**Pump**” energy rate (kJ/s) in order to control the separator temperature.

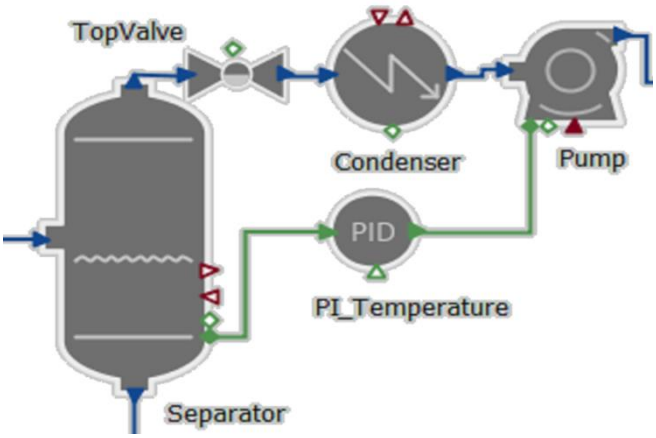

Figure 20 - Changes performed in the initial flowsheet (see figure 19)

The “**PI_Temperature**” model has a new set of specifications, consequence of a new manipulated and controlled variable, and control behaviour.

Table 7 - “PI_Temperature” controller specifications

Controller parameters		Value
Controlled variable: “Separator” temperature	Min. value (K)	340
	Max. value (K)	370
Manipulated variable: “Pump” energy rate	Min. value ($kJ.s^{-1}$)	0.1
	Max. value ($kJ.s^{-1}$)	0.5
Controller action:		direct
Proportional gain		33
Integral time constant (s)		4.5

The setpoint was set to 352 K, and the heat input was kept at 1 MJ/s through the simulation.

4.3. Schedule and objectives

With the initial holdup specified in table 1, the separator model starts at 44% of its total volume. "**FeedValve**" stem position changes its value from 0 (closed) to 0.5 (half-open), allowing the separator to refill its content when the holdup liquid level reaches 1% (5 cm of liquid height). The valve stem position closes right after the holdup liquid level inside the separator achieves 95% of the total height (4.75 m).

Meanwhile, the destination of the distillate is dependent on its mass fraction. If the distillate mass fraction is 0.45 of cyclohexane, "**ValvePreTankLight**" stem position is switched to 0.5, while the other three valve stem position are changed to zero ("**ValvePreTankMedium**", "**ValvePreTankHeavy**" and "**ValveOffCut**"). The same action is scheduled for a mass fraction of 0.45 for heptane, and 0.40 for Toluene.

In the case that two requirements are met, such as 0.45 mass fraction of heptane and 0.40 of toluene, the lightest compound valve has priority.

The simulation is set to occur for a minimum of 23000 seconds (approximately 6 hours and 24 minutes).

4.4. Simulation results

In this sub-chapter, gPROMS® ProcessBuilder results for the separator case study are presented.

4.4.1. Separator model results

The liquid level inside the separator is a non-constant variable during the simulation. Although the liquid level threshold for refilling the separator is the same, the synchronization of both examples is eventually lost, as can be seen in figure 21:

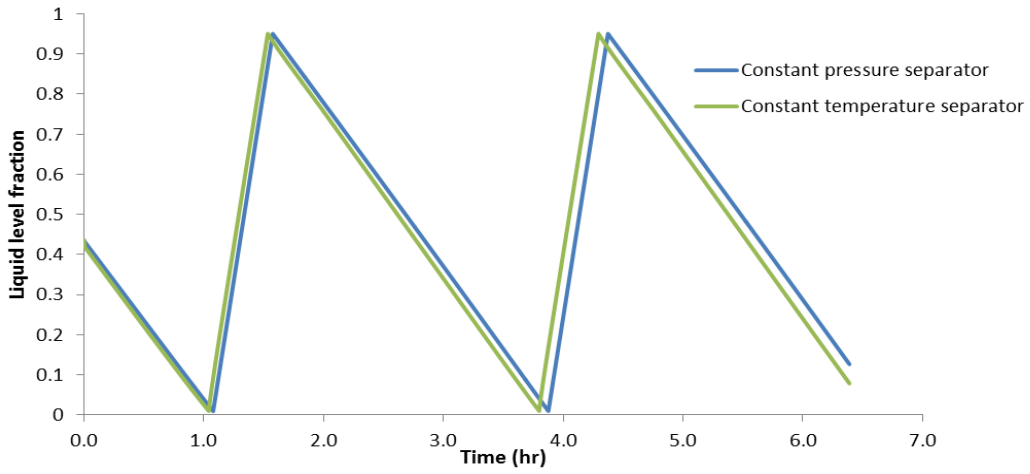

Figure 21– Separator liquid level profile from both simulations

As can be observed from figure 21, the constant temperature simulation tends to distillate faster for the same heat input, consequence of different conditions inside the respective separator. Figure 22 show the dynamic behaviour of both separators temperature and pressure:

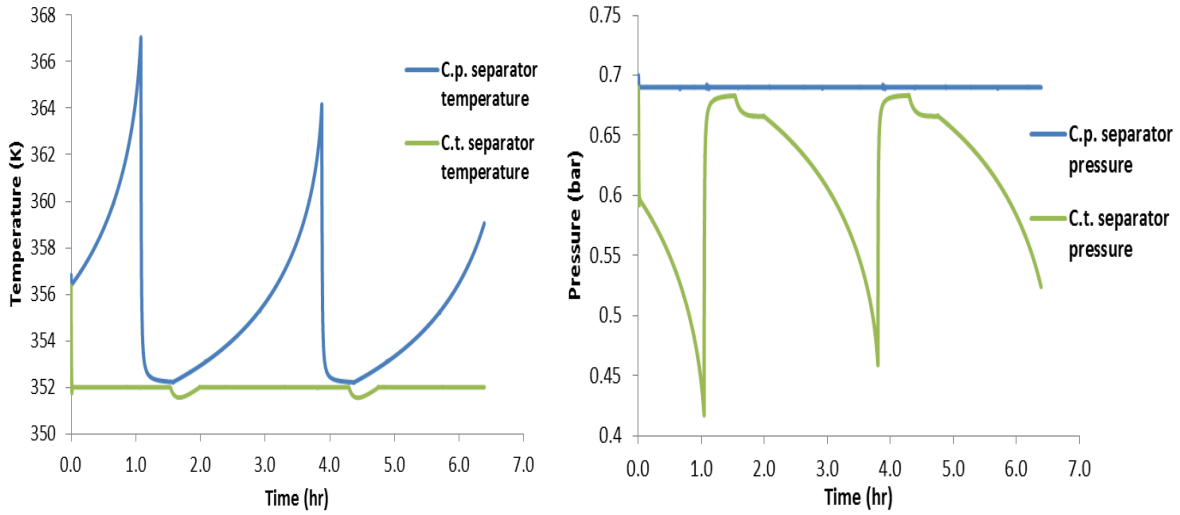

Figure 22– Separator temperature and pressure in both simulations

The first case (constant pressure) has an average temperature of 355.5 K and 0.69 bar average pressure. In comparison with the second case (constant temperature), with 352 K of average temperature and 0.615 bar average pressure, the constant pressure simulation will have a slower output of vapour, due to this operating conditions.

As it can be seen in figure 22, there are abrupt changes in the system behaviour twice: approximately at time 1 and 4. During the first re-fill, the "**Source**" feeds the system through the "**FeedValve**", and the temperature, pressure and composition inside the "**Separator**" tend to the source model values. The inlet flow, which influences the re-fill time, is dependent on the pressure difference between the separator model and the source mode. On the other hand, this pressure difference is calculated with the flow coefficient specified in "**FeedValve**". As expected, the pressure difference is considerably bigger in the constant temperature simulation, leading to a small burst in the feed flowrate until stability is achieved, as can be noticed in figure 23:

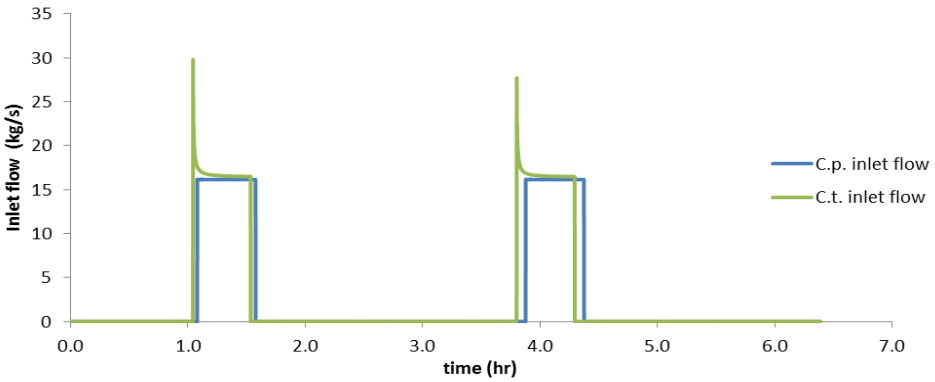

Figure 23– Separator inlet flow

While the separator is being filled, other changes can be noticed: the vapour flow increases substantially, and the composition inside the separator has a turning point, with constant increase in the amount of light components. Also, this change in the composition has a direct impact in the outlet vapour: with constant heat input to the system, the new composition requires less energy to vaporize (as it is richer in light components) and leading to a considerable increase in the vapour formed, as can be observed in figure 24:

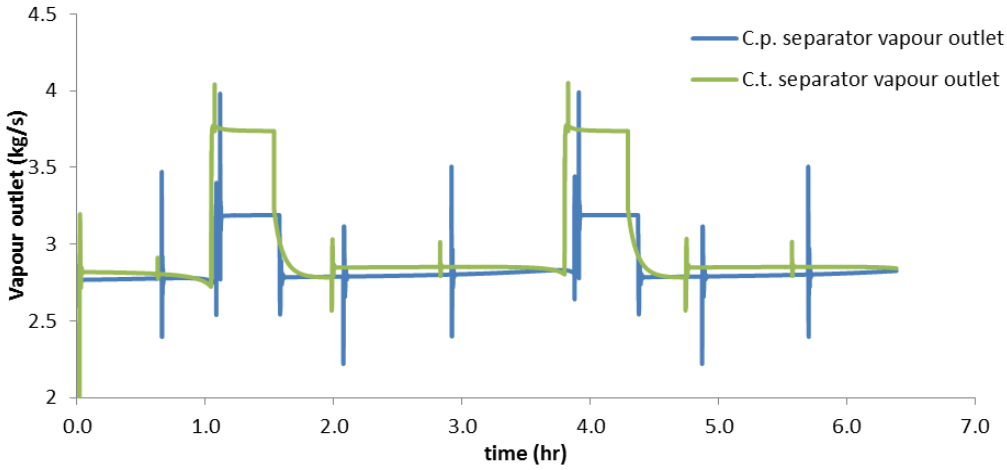

Figure 24– Separator vapour outlet flow

Figure 25 show the variation of the "**Separator"** mass fraction with time for both simulations: with constant pressure and with constant temperature, correspondingly. As explained before, the vapour output is not the same in both simulations, due to operatory conditions. That event can be clearly noticed by the different behaviour of the toluene and heptane mass fraction at the end of the simulation

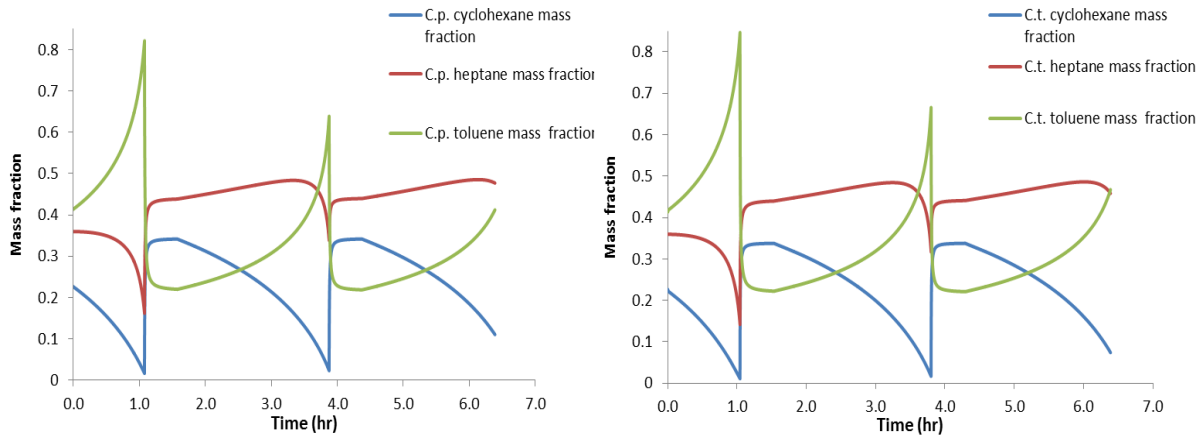

Figure 25– Constant pressure and constant temperature separator mass fraction

4.4.2. Tank models results

In this sub-chapter, only the pressure controlled simulation results will be presented. The molar fraction composition of the tank models and "**OffCutSink**" is shown in figure 61 and 62 from appendix A.1.

The dynamic behaviour of the tank models is a direct consequence of the vapour composition and the vapour flow coming from the "**Separator**". All the condensed vapour is accumulated in either a tank model or in the "**OffCutSink**", when the mass fraction requirements are not met. Figure 26 shows the evolution of the mass holdup of all the tank models and the off-cut sink model:

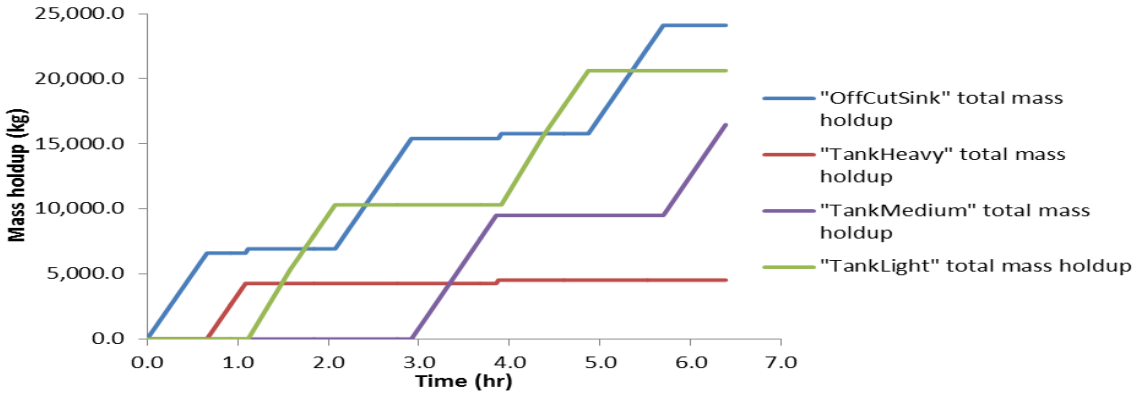

Figure 26– Mass holdup in the tank models and the off-cut sink model

The separation starts with the sink valve model open, as the outlet vapour mass fraction is not rich enough for the "**ValvePreTankHeavy**" stem position to change. That vapour mass fraction, 0.40, is only achieved at 0.7 hr. From that time instant until 1.1 hr, the "**TankHeavy**" is being filled with the separator outlet distillate. As soon as the conditions for the "**FeedValve**" to open are met, a cycle begins:

- In the short time that the separator is being refilled with a new content, the endpoint of the distillate changes twice: first, it is sent to the "**OffCutSink**" when the toluene mass fraction is no longer above 0.4; secondly, when the cyclohexane composition is now the most abundant, the distillate is sent to the "**TankLight**".

- "**TankLight**" is filled for about an hour, until the mass composition is no longer 0.45 of cyclohexane. At this point, neither heptane mass fraction is above the mass fraction specification, which means the distillate is carried to the "**OffCutSink**" again.

- This off-cut between the cyclohexane and the heptane lasts for around 50 minutes. At 2.9 hr, the "**ValvePreTankMedium**" is open, and the medium tank is filled.

- The transition between the medium component and the heavier one (heptane and toluene) is direct, without off-cut. The justification for this event is that the mass fraction requirement for the toluene is lower than the mass fraction requirements for the other components. Additionally, there is a small period of time where both requirements (for the medium and the heavier key) are met and, as

explained in sub chapter 4.3, the priority is given to the lightest component. Therefore, the accumulation of heptane takes longer than the accumulation of toluene.

Figure 27 is presented the profile of the vapour fraction in the outlet vapour of the separator:

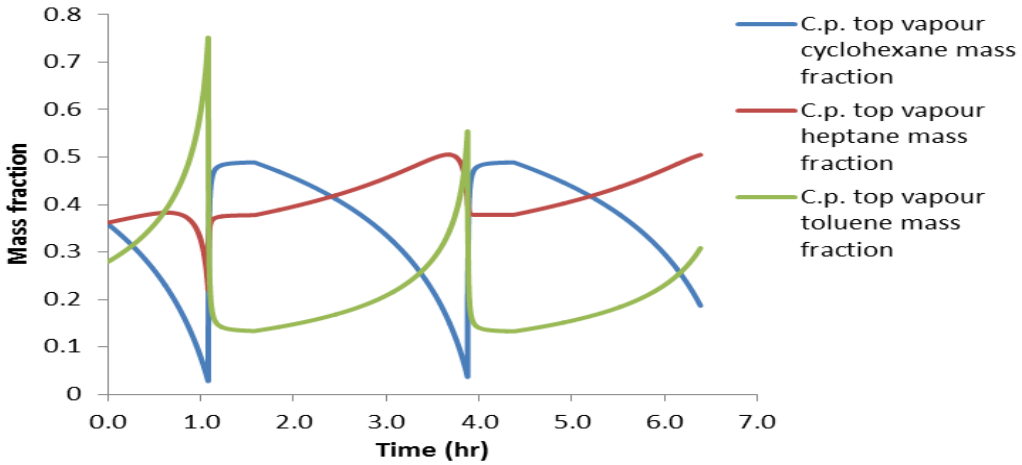

Figure 27– Constant pressure vapour mass fraction

4.4.3. Controller models

In this sub-chapter, the results from the controller models will be presented.

As explained previously in sub-chapter 4.2, two simulations were conducted: one simulation where the separator was controlled to keep its interior pressure constant (manipulating the "**TopValve**" stem position), and a second one where stabilizing its temperature was the controller model objective (manipulating the "**Pump**" energy rate).

Figure 28 presents the profile of the "**TopValve**" stem position variable through time, as well as a more detailed results between 7400 and 7670 seconds of simulation:

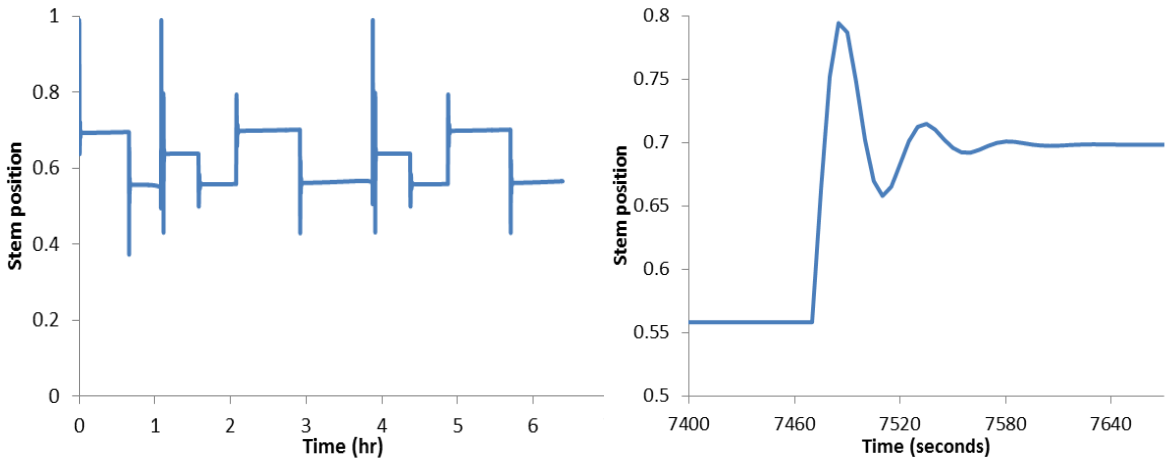

Figure 28– Dynamic behaviour of "TopValve" stem position

From figure 28 is possible to notice 3 main stem position values, with the values 0.69, 0.56 and 0.63, approximately. The first value is obtained when the "**OffCutSink**" is being filled. This model has a slightly bigger value for the assigned pressure than the tanks (0.8 bar compared with 0.79). Therefore, the stem position changes accordingly to reduce the pressure drop, maintaining the pressure inside the separator constant. This can be observed up to 0.8 hr in figure 28. As soon as the distillate destination changes to any of the other tanks, the value of the stem position acquires values near 0.56, as can be observed 0.8 and 1.1 hr of the simulation. This value has an abrupt change at the end of this interval, consequence to a quick change in the distillate destination, between the "**HeavyTank**", the "**OffCutSink**" and the "**LightTank**". Additionally, the "**FeedValve**" is open to refill the tank during this period of time. While the valve remains open, the manipulated variable value stabilizes around 0.63. The new mixture is more volatile than the previous holdup, therefore requiring a slight change in the "**TopValve**" stem position.

For the simulation where the temperature was controlled in order to remain constant, the energy rate from the "**Pump**" was chosen to be the manipulated variable. The lower bound for the energy rate was kept at 100 J/s, in order not to shut down the "**Pump**" (the energy rate would take values of zero during the refill of the separator). Therefore, at the beginning of each refill and for a certain time after, the temperature drops below the setpoint (figure 22, temperature profile of constant temperature simulation). The pump has no operating conditions to keep the system in the desired setpoint, apart from waiting a temperature rising due to the heat input. Figure 29 presents the profile of the "**Pump**" power output through time, as well as more detailed results between 7110 and 7330 seconds of simulation:

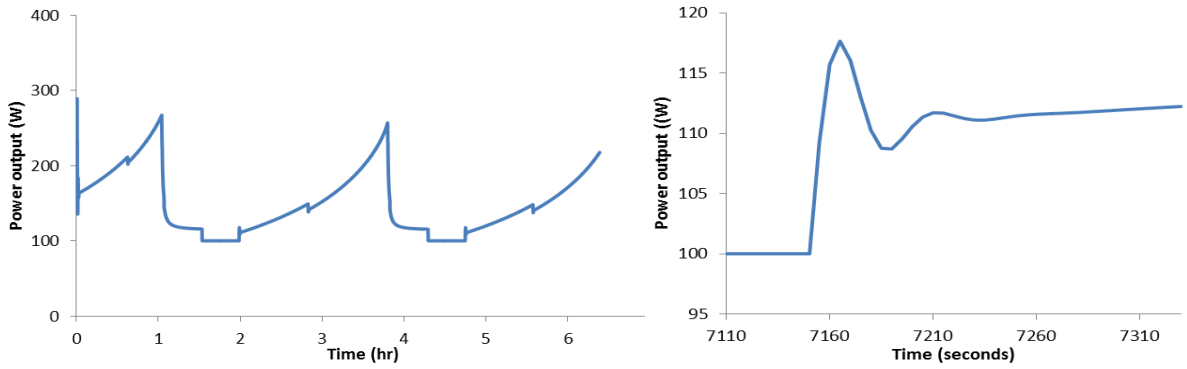

Figure 29– Dynamic behaviour of "Pump" power output

Page intentionally left blank

5. Batch distillation

In this chapter, a model validation, sensitivity analysis of the same model and an optimization problem are presented in detail, all respective to a ternary batch distillation with the same composition as the experimental data available in the papers by Bonsfills and Puigjaner [48]

5.1. Model validation

In the present sub-chapter, a validation of a batch distillation model was achieved through the comparison between the data available in Bonsfills and Puigjaner [48] and the results obtained in the assembled flowsheet.

Bonsfills and Puigjaner present the experimental data from a ternary batch distillation of an equimolar mixture composed by cyclohexane, toluene and chlorobenzene. The initial mixture has a volume of 6L, and is fed to a 6L reboiler, connected to a 15 tray distillation column with a 5 cm inner diameter, and 9 cm outer diameter. Table 8 shows the available data presented in [48] for the distillation of the cyclohexane/toluene/chlorobenzene mixture at the experimental reboiler heat input 681.3 W:

Table 8– Pilot column dimensions and operating conditions [48]

Column	**Column height (m)**	3.75
	Number of trays	15
	Inner diameter (mm)	50
	Outer diameter (mm)	90
	Average operating pressure (mmHg)	760
Reboiler	**Volume (L)**	6
	Maximum heat duty (W)	1400
	Operating heat duty (W)	681.3
Condenser	**Operating mode**	Total condenser
	Distillate flow (mol/min)	0.19
	Reflux ratio	4
Mixture	**Composition**	Equimolar
	Volume (L)	6

With a constant heat duty input of 681.3 W, the column operates at total reflux for 30 minutes, allowing the component distribution to stabilize. After this period of time, the distillate valve is opened and the distillation starts, with a constant reflux ratio of 4 and an average distillate flow of 0.19 mol/min, for 4 hours and 40 minutes. The total time of the experiment is 5 hours and 10 minutes.

The following figure shows the distillate composition profile for the pilot column for the 4 hours and 40 minutes after the opening of the distillate valve:

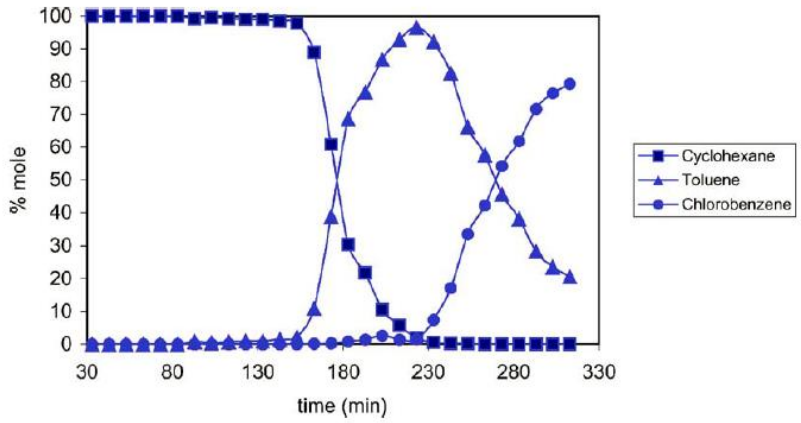

Figure 30– Concentration profile in the distillate, Bonsfills et. Puigjaner results

Using ScanIt software, from AmsterChem [49], the data from figure 30 was condensed in table 9:

Table 9– Experimental data for the distillate composition

Time (min)	Cyclo. purity (%)	Time (min)	Tol. purity (%)	Time (min)	Chlor. purity (%)
32.8	100	32.8	0	32.8	0
44	100	43.3	0	44	0
53.7	100	53	0	53	0
64.2	100	63.5	0	62.8	0
73.3	100	73.3	0	73.3	0
83.7	100	82.3	0	83.7	0
93.5	99.3	92.8	0.7	94.9	0
104	99.6	103	0.4	104	0
114	99.3	113	0.7	113	0
124	98.8	123	1.05	123	0.15
134	98.6	133	1.09	133	0.31
144	98.3	143	1.45	143	0.25
154	97.5	153	2.17	154	0.33
164	89.1	163	10.5	163	0.4
173	61.4	173	38	172	0.6
183	30.4	183	68.1	183	1.5
193	21.4	193	76.8	193	1.8
203	10.5	204	87	203	2.5
213	6.5	213	92.4	214	1.1
223	1.8	223	96	225	2.2
234	0.75	235	92	234	7.25
243	0.4	245	82.2	244	17.4
253	0.3	255	67.2	254	32.5
263	0	264	58.2	265	41.8
273	0	275	45.3	274	54.7
283	0	284	37.7	285	62.3
294	0	295	27.9	295	72.1
303	0	304	23.2	305	76.8
313	0	313	20.7	314	79.3

In addition to the distillate composition, the same paper contains data about the temperature profile in trays 1, 10 and 15, as presented in figure 31:

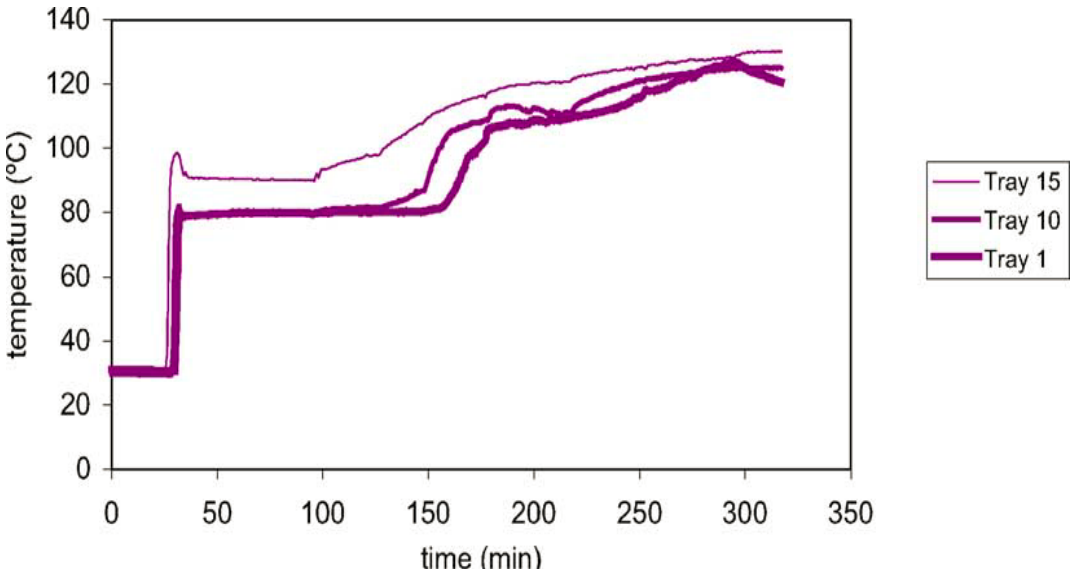

Figure 31 – Temperature profile in the first, tenth and fifteenth tray, Bonsfills et. Puigjaner results

Repeating the procedure used for figure 30, the data from the trays temperature profile (figure 31) was converted into the following table:

Table 10– Experimental data for the trays temperature

Time (min)	Tray 15 temp. (°C)	Time (min	Tray 10 temp. (°C)	Time (min)	Tray 1 temp. (°C)
4.1	30.6	2.9	30.6	0.5	30.6
25	30.2	21.9	30.6	7.8	30.6
28.3	95.4	29.3	31.5	15.8	30.6
30.7	98.6	32.1	79.5	25	30.2
32.6	94.5	49.2	79.5	29.3	31.1
41.8	90.9	70.1	80	30.4	45.7
58.4	90	99.5	80.5	32.1	79.5
83.5	90	129	81.5	49.2	79.5
95.7	90.5	147	87	68.2	80
101	93.3	153	98.4	86	80
119	97.9	162	106	101	80.5
126	97.4	172	108	129	81.5
143	107	180	112	150	81
157	113	194	113	159	85.2
173	117	205	112	170	98.4
183	119	219	113	178	106
193	120	227	116	197	108
208	120	240	120	215	110
224	123	257	122	233	112
243	125	270	123	247	116
262	127	286	126	263	120
284	128	303	125	276	123
297	130	306	125	292	126
305	131	312	126	307	122
316	131	316	126	316	121

5.1.1.Flow-driven flowsheet assembly

The model assembled will start the simulation in a steady-state continuous distillation, as the initial holdup cannot be specified. As a consequence, the component specification in the source model ("**Source_1**") had to be tested and changed until the molar sum of all the trays, condenser and reboiler achieved a composition as close as possible as the Bonsfills experimental data. In addition, a flow-driven model had to be created in order to obtain the valve models flow coefficient, the reboiler and condenser duty, and initial guesses for pressure drop and the distillate flowrate. Figure 32 presents the flow-driven flowsheet assembled:

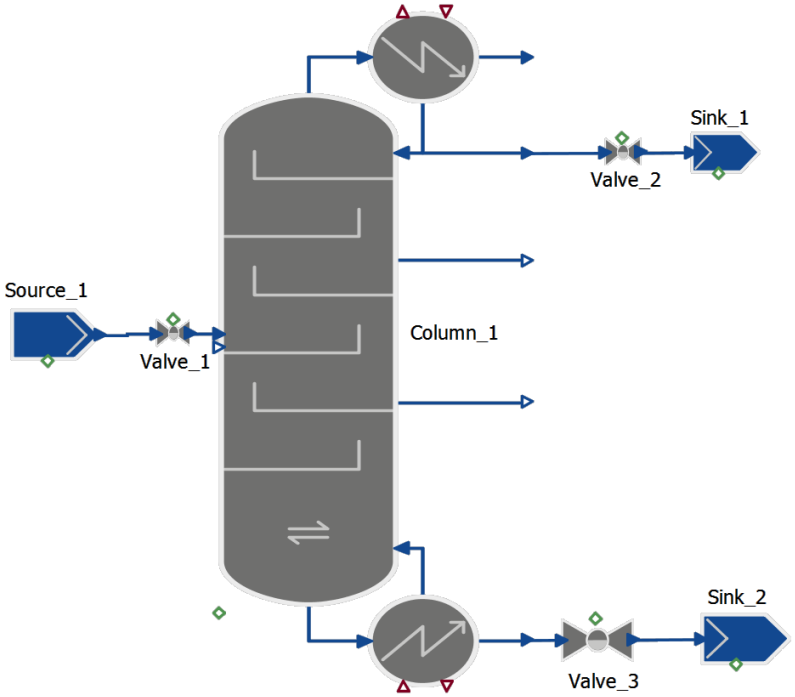

Figure 32– Flow-driven assembled flowsheet flowsheet

The dimensions of the column model (**Column_1**) are presented in table 11. The plate spacing of 0.25m is calculated after the column height of 3.75 m, dividing it by the 15 stages. The active area fraction, hole fraction and weir fraction are calculated after typical values by Seader [20], Perry [24] and Sinnot [26], with the values 0.8, 0.1 and 0.7, respectively. Although the weir height was calculated in order to have an average holdup of 0.036 mol as the published data, the impossibility of specifying the initial holdup has a huge influence in the holdup calculation, as it is calculated based on flowrates, and the flowrates are calculated based on pressure gradients. The weir height was kept at 9.55 mm:

Table 11– Column_1 specifications

Column	**Column diameter (cm)**	5
	Plate efficiency (%)	80
	Plate spacing (cm)	25
	Stages	17
Condenser	**Diameter (cm)**	8
	Volume (L)	1
	Liquid level (cm) / liquid fraction	5.97 / 0.30
	Inlet valve flow coefficient (kg s^{-1} Pa^{-1})	1 x 10^{-4}
	Stem position of the inlet valve	0.5
	Stem position of the reflux valve	0.5
	Reflux ratio normalized	0.8
	Operating mode	Total condenser
Reboiler	**Diameter (cm)**	25
	Volume (L)	0.19
	Liquid level (cm) / liquid fraction	12.12 / 0.85
	Boilup ratio normalized	0.8
Trays	**Active area fraction**	0.8
	Hole area fraction	0.1
	Weir fraction	0.7
	Weir height (mm)	9.55
	Tray thickness (mm)	2
	Hole diameter (mm)	4.5
Pressure	**Dry vapour press. drop correlation**	Bernoulli [appendix A.7.1]
	Aerated liquid press. drop correlation	Bennett [appendix A.7.2]
	Clear liquid height correlation	Bennett [appendix A.7.2]
	Initial guess for press. drop per stage (bar)	4 x 10^{-4}

All the valve models (**Valve_1, Valve_2** and **Valve_3**) have been set to operate in mass and energy balance mode with a pressure drop specification of 0.1 kPa, and a stem position of 0.2.

The data from Bonsfills refers an initial 6 litre mixture of an equimolar mixture of cyclohexane, toluene and chlorobenzene.

Using Multiflash property package, the molar density was calculated, and with it, the initial molar holdup present in the described initial mixture:

$$Ini.molar\ holdup = V * \rho_{mol} \tag{5.1}$$

Table 12 presents the values calculated and obtained from Multiflash:

Table 12– Molar density and initial molar holdup

ρ_{mol} (mol/m^3)	Initial molar holdup (mol)
9.40×10^3	56.43

The feed composition (which is specified in **Source_1**) has been tested several times until the total holdup inside the column had similar values to those of Bonsfills, as presented in table 13:

Table 13– Feed specifications and column holdup relative errors

	Feed molar fraction	Column molar holdup (mol)	Relative error (%)
Chlorobenzene	0.19	18.68	-0.2
Cyclohexane	0.62	18.77	0.2
Toluene	0.19	18.79	0.3
Total	1	56.24	<0.1

.

The specifications needed for the pressure-driven flowsheet are acquired after the results obtained from the flow-driven simulation. These values are presented in table 14:

Table 14– Operational and dimensional results from flow-driven mode

Specification	Model	Value
Flow coefficient *(kg.s^{-1}.Pa^{-1})*	Valve_1	2.46×10^{-5}
	Valve_2	1.08×10^{-5}
	Valve_3	1.38×10^{-5}
Reflux valve flow coefficient *(kg.s^{-1}.Pa^{-1})*	Column_1	4.26×10^{-5}
Pressure *(bar)*	Sink_1	1.012
	Sink_2	1.040
Condenser heat duty *(kJ.s^{-1})*	Column_1	-0.386
Reboiler heat duty *(kJ.s^{-1})*	Column_1	0.389
Distillate flowrate *(kmol.hr^{-1})*	Column_1	9.25×10^{-3}

5.1.2.Pressure-driven (F.D.I) flowsheet assembly

The specifications needed for the pressure-driven with Flow-Driven Initialization (F.D.I) flowsheet are presented in table 14 from 5.1.1 sub-chapter. The initial guesses for the initialization (reflux and boilup normalized ratio, reboiler and condenser liquid levels, and reflux and inlet valve stem position) are presented in table 11 from 5.1.1 sub-chapter.

For the current flowsheet, two PI controllers were added in order to maintain the pressure inside the column and the distillate flowrate constant. Figure 33 shows the pressure-driven (F.D.I.) flowsheet:

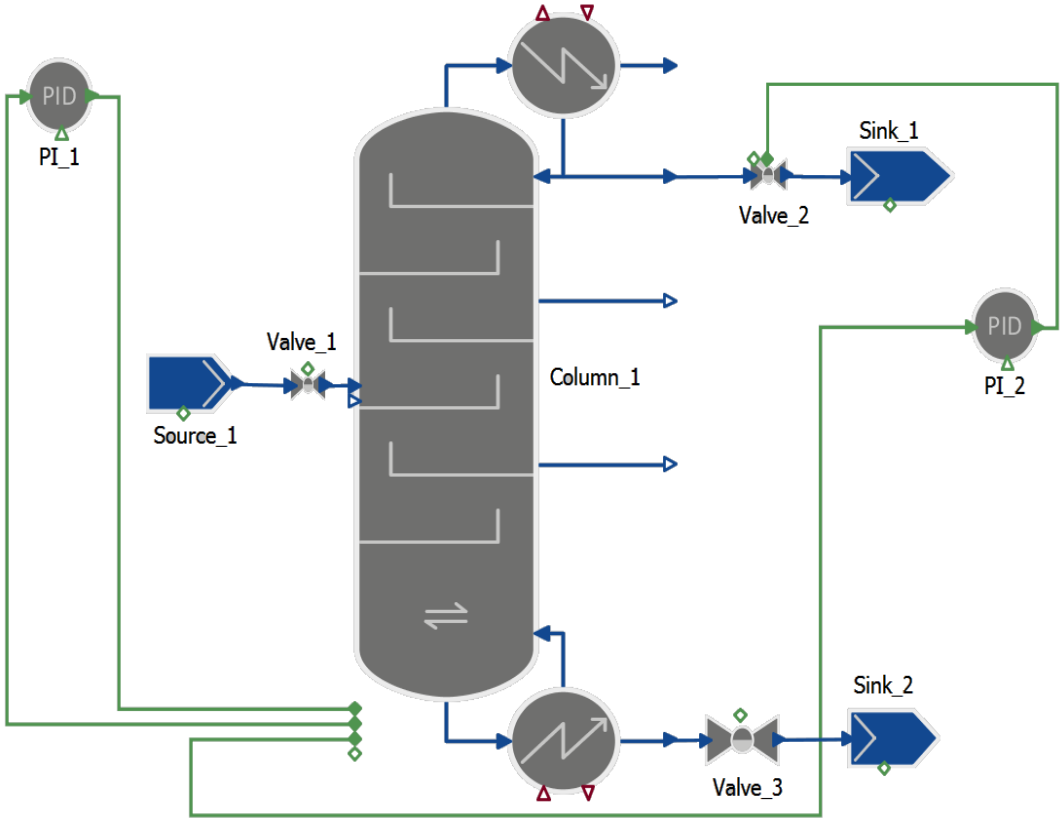

Figure 33– Pressure-driven (F.D.I) flowsheet assembled

The first controller (PI_1) controls the second stage pressure (1st column tray) using the condenser heat duty as manipulated variable. Differently from flow-driven mode, the condenser heat duty is a specification from this operating mode, which does not assure total condensing of the inlet vapour in the condenser, if left untouched. Using this variable as PI_1 manipulated variable, both constant pressure and total condensing problems are solved.

The second controller (PI_2) controls the distillate flowrate using the Valve_2 stem position as a manipulated variable, with values varying between 0 and 1 (fully closed and fully opened, respectively).

Table 15 shows PI_1 and PI_2 specifications and control behaviour:

Table 15– Operational PI_1 and PI_2 controller parameters

	PI_1	PI_2
Manipulated variable	Condenser duty (kJ/s)	Valve_2 stem position
Proportional gain	45	75
Integral time constant	70	6
Controller action	Reverse	Reverse
Setpoint	1.0087 (bar)	9.24 (mol/hr)
Controlled variable	1st tray pressure	Distillate molar flowrate

Both controllers were initially tuned according to the Ziegler-Nichols heuristic method. However, as Valve_2 stem position is now a manipulated variable and no longer an input variable, a bigger value for the proportional gain has been used in order to have a more responsive valve behaviour (faster closing and faster opening).

5.1.3.Schedule plan

By operating in pressure-driven with flow-driven initialisation mode, the simulation begins in steady-state with bottom and top liquid being recovered. At time 0 (after switching to flow-driven) Valve_1 and Valve_3 stem position were set to the value of zero. The same value has been used for PI_2 setpoint, closing the valve in less than 4 seconds. After 100 seconds of simulation, the reboiler heat duty value is changed to match the same value as Bonsfills heat duty (681.3 Watts). The simulation runs for another 1500 seconds in order to stabilize.

At time 1600, PI_2 setpoint is changed to match Bonsfills distillate flowrate (0.19 mol/min, 0.0114 kmol/hr) and the simulation runs until there is no holdup inside the reboiler. Distillate molar faction and trays temperature profiles were then compared.

5.1.4.Results

Both distillate molar fraction profiles were synchronized to start at 30 minutes (when the distillate valve opens), as figure 34 shows:

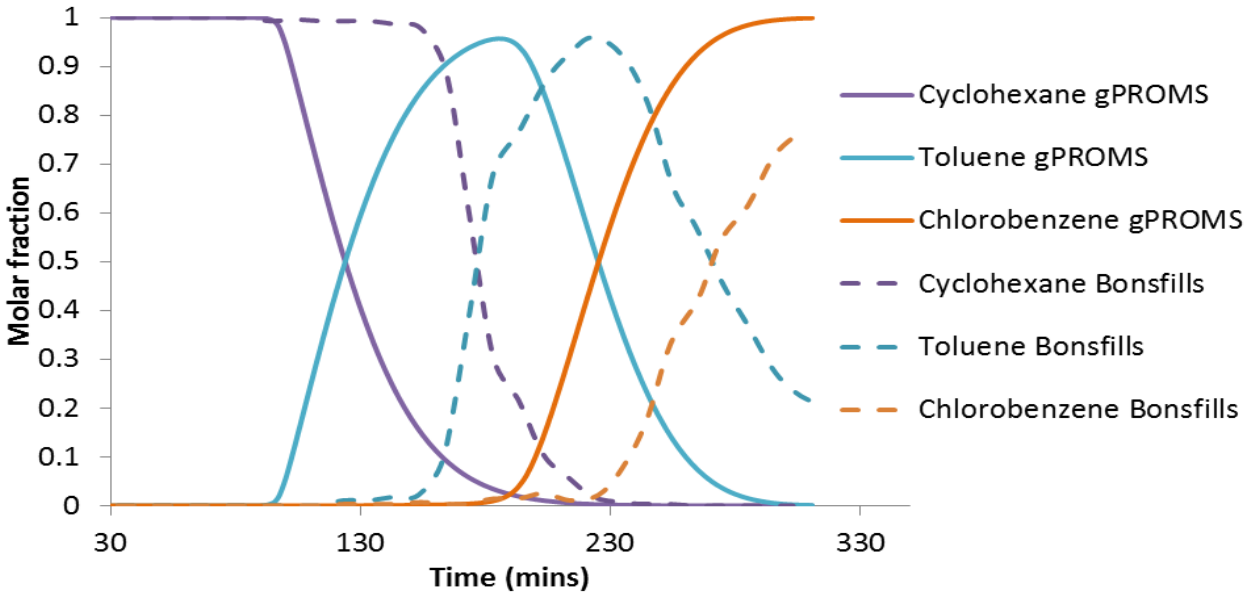

Figure 34– First simulated distillate molar fraction profiles

Figure 34 clearly shows a position shift for the profiles, between Bonsfills results and the simulated ones. The shape between the curves is pretty similar, indicating a good understanding and good results for the component interactions. However, the same figure appears to indicate that a different component composition has been loaded in the same column: the area beneath the cyclohexane profile obtained by Bonsfills is bigger than the one simulated by gPROMS ProcessBuilder. And the opposite happens to the chlorobenzene profiles, presented in the same figure. Table 16 shows the results from the sum of Bonsfills holdup (integration of figure 30 with a constant distillate flow of 0.19 mols per minute) using trapezoidal method:

Table 16– Integration results from Bonsfills distillation profile

	Molar holdup (mol)
Cyclohexane	27.92
Toluene	17.90
Chlorobenzene	7.82
Total	53.84
Difference between initial holdup and distilled mols	3.09

Table 16 clearly shows that exist no equimolarity in the distillation profile curve presented in figure 30. Also, the total molar sum is slightly different from the initial molar holdup calculated in sub chapter 5.1.1, which clearly indicates that part of the initial holdup remains in the column after the distillation, most probably inside the reboiler.

Therefore, two different simulations were conducted:

- One simulation (hereafter known as SIM-1) in which the initial mixture is equimolar, but the initial volume is different. The new volume is calculated with the assumption that all of the initial cyclohexane has been distillate. The total molar holdup is then three times the cyclohexane holdup presented in table 16. The simulated distillate molar fractions profile for SIM-1 is presented in appendix A.2 as well as the simulated trays temperature profile ;
- The second simulation (hereafter known as SIM-2) has the same initial volume, but the composition is the same as table 16. The missing mols were arbitrarily distributed between the heaviest and the intermedium component (80% and 20%, respectively). The simulated trays profile for simulation SIM-2 is presented in appendix A.2;

Steps taken in sub-chapter 5.1.1 and 5.1.2 were repeated for both simulations. Results, relative errors and feed composition for SIM-2 are presented:

Table 17– Column holdup relative errors for SIM-2

	SIM-2 desired holdup (mol)	Simulated results (mol)	Relative error (%)
Cyclohexane	27.92	28.61	-2.5
Toluene	18.22	17.90	1.7
Chlorobenzene	10.29	9.65	6.2
Total	56.43	56.16	0.5

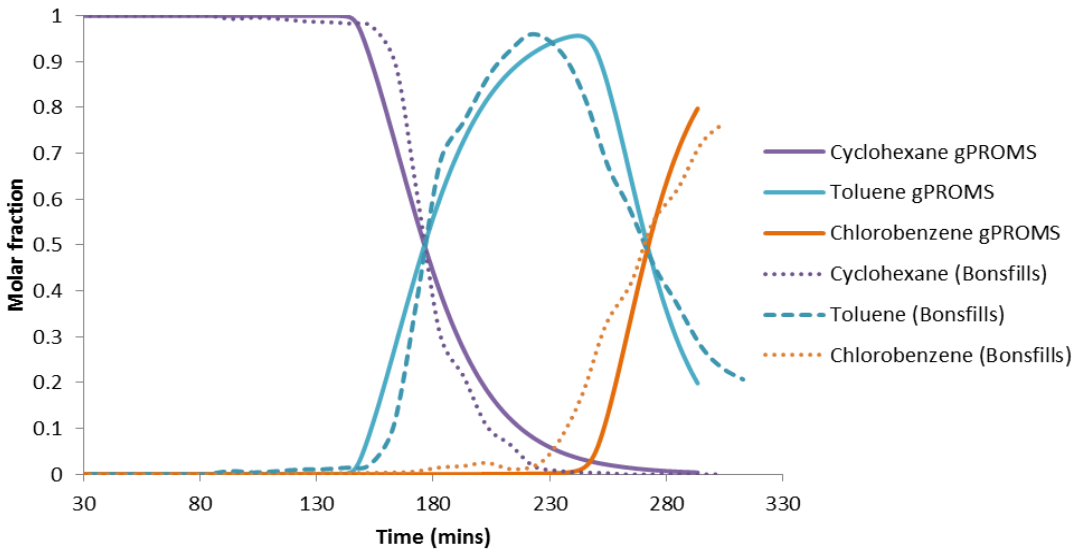

Figure 35–Simulated distillate molar fraction profiles for SIM-2

The results shown in figure 35 show a good prediction of the mixture behaviour. The cyclohexane curve has the best behaviour prediction, slightly missing the time period when the toluene composition gets richer, in the distillate. The interactions between cyclohexane and toluene are well projected by the properties package Multiflash.

The maximum purity achieved for toluene is the same in both cases (Bonsfills results and gPROMS simulation), but a time shift of 10 minutes can be observed between the 0.96 molar fraction maximum value. From this point, the presence of cyclohexane in the distillate can be neglected, and the interactions between the heaviest and medium component are the most important ones. Multiflash, using the NRTL model, assumes that the separation between chlorobenzene and toluene is easily achievable than the results obtained by Bonsfills experiment. As it observable, the maximum purity achieved by gPROMS for the chlorobenzene component is far greater than the results shown by Bonsfills.

The deviation of figure 35 curves is presented in table 18.

As can be observed from the table above, the deviations verified are mostly under 0.05. In fact, the average deviation value for cyclohexane, toluene and chlorobenzene is 0.03, 0.05 and 0.03, (respectively), and the maximum deviation value verified for each of the three components is 0.16, 0.22 and 0.24. These values occur when the distillate composition starts changing in terms of richer component. For instance, cyclohexane has a steady molar fraction at the beginning of the distillation, but the turning point when its molar fraction decreases and toluene composition increases is not well predicted by the simulation.

Table 18– Deviation values between SIM2 and Bonsfills results

Time (min)	Cyclohexane molar fraction			Toluene molar fraction			Chlorobenzene molar fraction		
	Bonsfills	gPROMS	Deviation	Bonsfills	gPROMS	Deviation	Bonsfills	gPROMS	Deviation
32.8	1.00	1.00	**0.00**	0.00	0.00	**0.00**	0.00	0.00	**0.00**
44	1.00	1.00	**0.00**	0.00	0.00	**0.00**	0.00	0.00	**0.00**
53.7	1.00	1.00	**0.00**	0.00	0.00	**0.00**	0.00	0.00	**0.00**
64.2	1.00	1.00	**0.00**	0.00	0.00	**0.00**	0.00	0.00	**0.00**
73.3	1.00	1.00	**0.00**	0.00	0.00	**0.00**	0.00	0.00	**0.00**
83.7	1.00	1.00	**0.00**	0.00	0.00	**0.00**	0.00	0.00	**0.00**
93.5	0.99	1.00	**0.01**	0.01	0.00	**-0.01**	0.00	0.00	**0.00**
104	1.00	1.00	**0.00**	0.00	0.00	**0.00**	0.00	0.00	**0.00**
114	0.99	1.00	**0.01**	0.01	0.00	**-0.01**	0.00	0.00	**0.00**
124	0.99	1.00	**0.01**	0.01	0.00	**-0.01**	0.00	0.00	**0.00**
134	0.99	1.00	**0.01**	0.01	0.00	**-0.01**	0.00	0.00	**0.00**
144	0.98	1.00	**0.01**	0.01	0.00	**-0.01**	0.00	0.00	**0.00**
154	0.98	0.90	**-0.07**	0.02	0.10	**0.08**	0.00	0.00	**0.00**
164	0.89	0.73	**-0.16**	0.11	0.27	**0.17**	0.00	0.00	**0.00**
173	0.61	0.56	**-0.05**	0.38	0.44	**0.06**	0.01	0.00	**-0.01**
183	0.30	0.40	**0.10**	0.68	0.60	**-0.08**	0.02	0.00	**-0.01**
193	0.21	0.28	**0.06**	0.77	0.72	**-0.05**	0.02	0.00	**-0.02**
203	0.11	0.19	**0.08**	0.87	0.81	**-0.06**	0.03	0.00	**-0.02**
213	0.07	0.12	**0.06**	0.92	0.88	**-0.05**	0.01	0.00	**-0.01**
223	0.02	0.08	**0.06**	0.96	0.92	**-0.04**	0.02	0.00	**-0.02**
234	0.01	0.05	**0.04**	0.92	0.95	**0.03**	0.07	0.00	**-0.07**
243	0.00	0.03	**0.03**	0.82	0.96	**0.13**	0.17	0.01	**-0.17**
253	0.00	0.02	**0.02**	0.67	0.89	**0.22**	0.33	0.09	**-0.24**
263	0.00	0.02	**0.02**	0.58	0.70	**0.11**	0.42	0.29	**-0.13**
273	0.00	0.01	**0.01**	0.45	0.49	**0.03**	0.55	0.50	**-0.04**
283	0.00	0.01	**0.01**	0.38	0.32	**-0.06**	0.62	0.67	**0.05**
294	0.00	0.00	**0.00**	0.28	0.20	**-0.08**	0.72	0.80	**0.08**
303	0.00	0.00	**0.00**	0.23	0.20	**-0.03**	0.77	0.80	**0.03**
313	0.00	0.00	**0.00**	0.21	0.20	**-0.01**	0.79	0.80	**0.00**

$$Deviation = v^{sim} - v^{exp} \tag{5.2}$$

As a consequence, the time shift that can be observed in figure 35 creates an increment in the deviation, and the maximum deviation for cyclohexane occurs in this time period. For the toluene, when the maximum purity is achieved for the gPROMS simulation the experimental toluene purity is in decline, with chlorobenzene getting richer in the distillate. This leads to the maximum deviation for both toluene and chlorobenzene.

Based on these results it is possible to conclude that the distillate composition is well predicted for the current model.

5.2. Sensitivity analysis

In this sub-chapter the reboiler heat duty, the reflux valve stem position and the distillate flow setpoint from PI_2 controller were changed to understand their impact in the simulation results. All the variables were changed during the total reflux time in the simulation, and the results analysed afterwards. Additionally, the reflux valve stem position and the reboiler heat duty variables were also changed in a step profile, in order to study different behaviours and the model robustness.

5.2.1.Reboiler heat duty

The reboiler heat duty input was modified, and its influence in the distillate molar fraction analysed. Figures 36, 37 and 38 show the behaviour change of cyclohexane, toluene and chlorobenzene molar fractions (respectively) for different heat duty values and for specific time intervals:

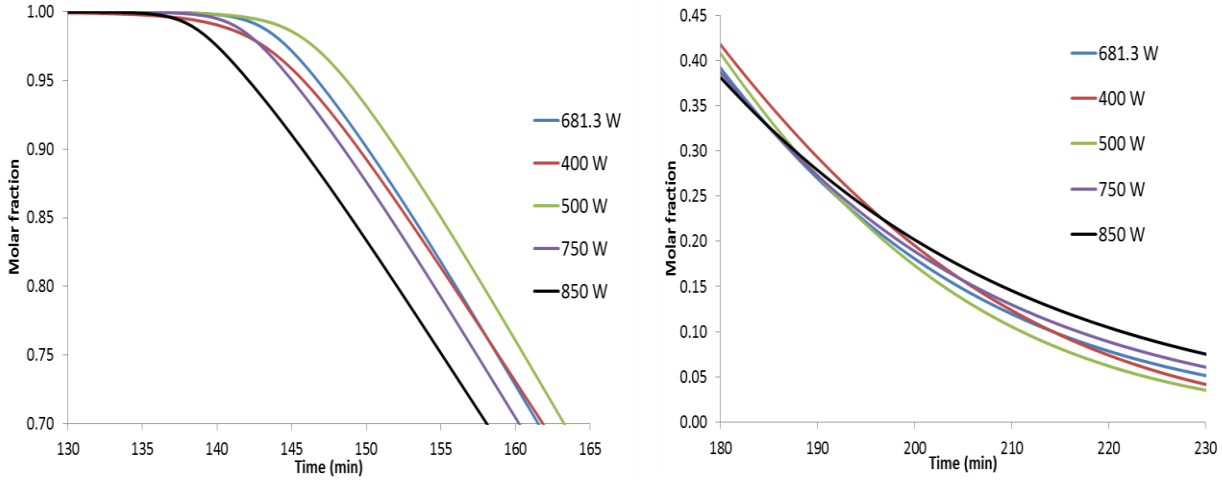

Figure 36– Cyclohexane molar fraction profiles for different heat duty inputs, at different time intervals

It can be observed in figure 36 that higher values for the reboiler heat duty have a negative impact in the component separation. As can be noticed at time 140, the maximum purity achieved is the same for the different tested heat duties. However, the condenser holdup composition (which is the same as the distillate molar fraction) cannot keep that purity for as much time as lower values of heat duty. Additionally, lower heat duty values tend to reach the minimum purity values faster, as can be seen between time 220 and 230.

This effect has an impact in the purity behaviour of the medium component, toluene. Reaching the cyclohexane minimum purity faster achieves higher purity in the toluene profile.

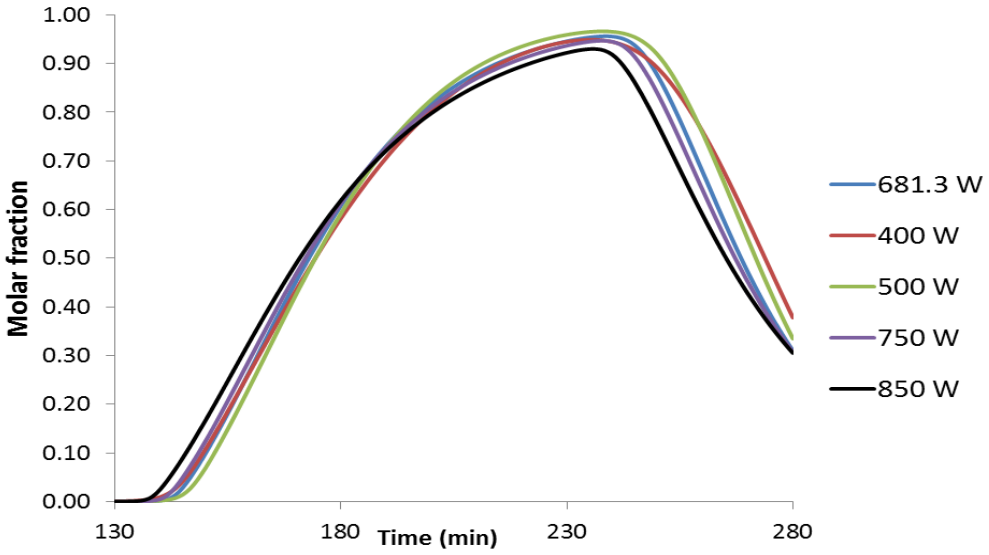

Figure 37 - Toluene molar fraction profiles for different heat duty inputs

At time 190, when the cyclohexane purity decreasing rate tends to stabilize, the same happens to the toluene purity increasing rate. In figure 37 it is possible to notice the difference between the maximum purity achieved for the different heat duty input values. Remarkably, the highest purity does not belong to the lowest heat duty value, 400 W, but to the second lowest, 500 W. Although the maximum purity and the greatest recovered amount of toluene are achieved at 500 W, the same results do not apply to the heaviest and last of the three components, as can be observed at figure 38:

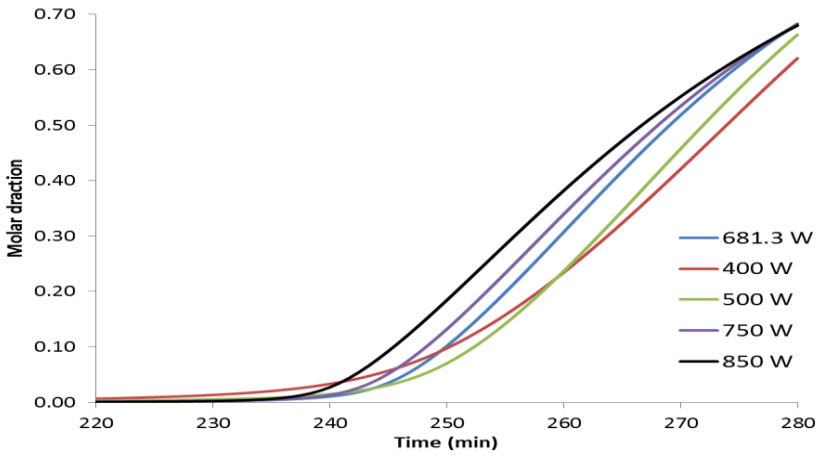

Figure 38– Chlorobenzene molar fraction profiles for different heat duty inputs

The chlorobenzene profiles tend to behave in the same pattern. As soon as the toluene purity in the distillate decreases, the amount of chlorobenzene in the distillate increases. As can be observed, the highest values of heat input will reach higher values of high chlorobenzene concentration first.

Taking a closer look to the condenser liquid holdup fraction profile in figure 39, it can be noticed that for higher values of heat duty there is an increment in the reboiler liquid level after the column stabilization.

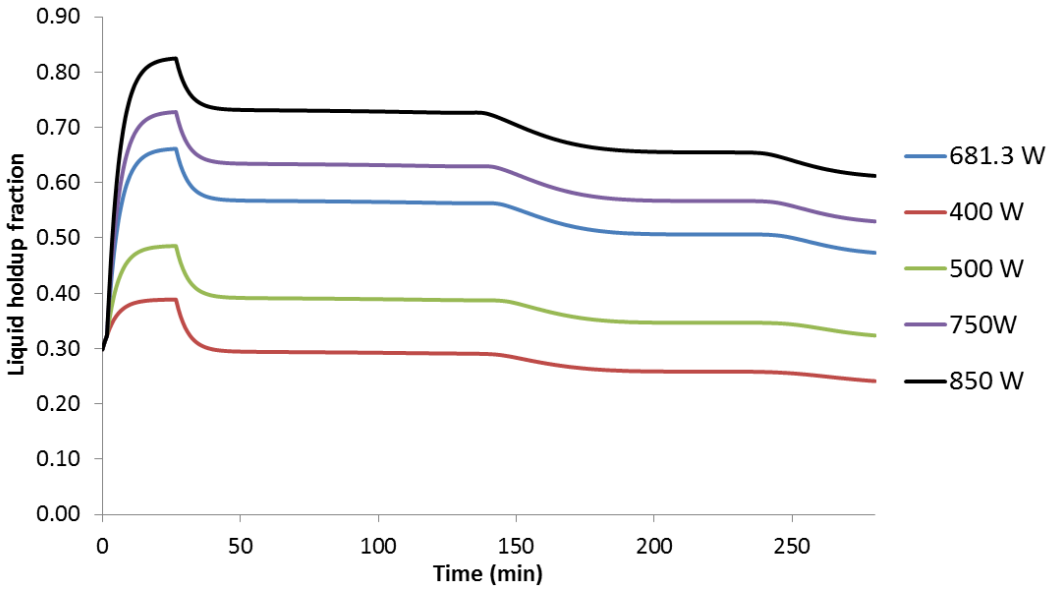

Figure 39– Condenser liquid holdup fraction profile for different heat duty inputs

An increment in the reboiler heat duty will increase the vapour flow leaving the reboiler. This vapour flow increment is responsible for a temporary raise in the system pressure. Controller PI_1 manipulated variable will change accordingly, decreasing the condenser heat duty. During this short period of time, the increment in the system pressure will also decrease the molar flowrate returning to the column from the condenser. Additionally, the decrease of the condenser heat duty will be responsible for a subtle rise in the molar flowrate entering the condenser. As a consequence, the liquid level of the condenser increases until the liquid hydrostatic pressure is enough to stabilize the whole column.

5.2.2.Distillate flow setpoint

The PI_2 controller setpoint (distillate molar flowrate) was altered. Its influence in the distillate molar fraction and in the normalized reflux ratio was also analysed. Figures 40, 41 and 42 show the behaviour change of cyclohexane, toluene and chlorobenzene molar fractions (respectively) for different setpoints and for specific time intervals:

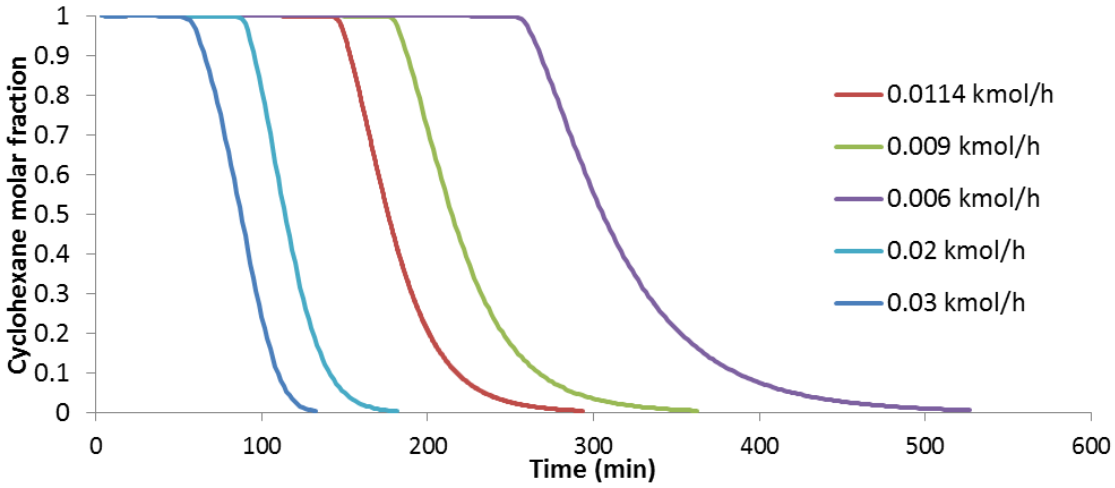

Figure 40– Cyclohexane molar fraction profiles for different PI_2 controller setpoints

The main difference between the different distillate flowrates is the distillation time required for the whole simulation. A bigger flowrate will empty the column faster, and therefore reduce the distillation time. However, without a good reflux valve manipulation, the reflux ratio of the column will decrease with the distillate flowrate increment. This is the main factor for a defective component separation, especially for the toluene component.

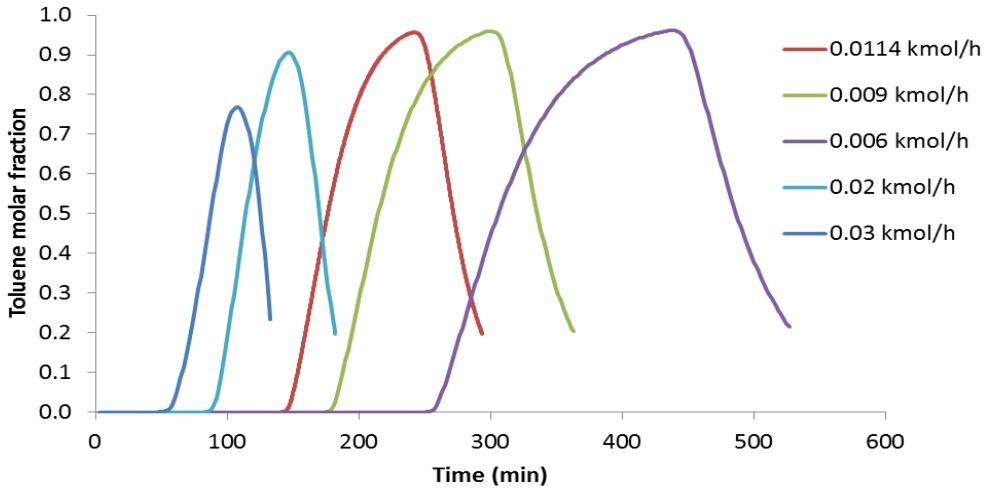

Figure 41– Toluene molar fraction profiles for different PI_2 controller setpoints

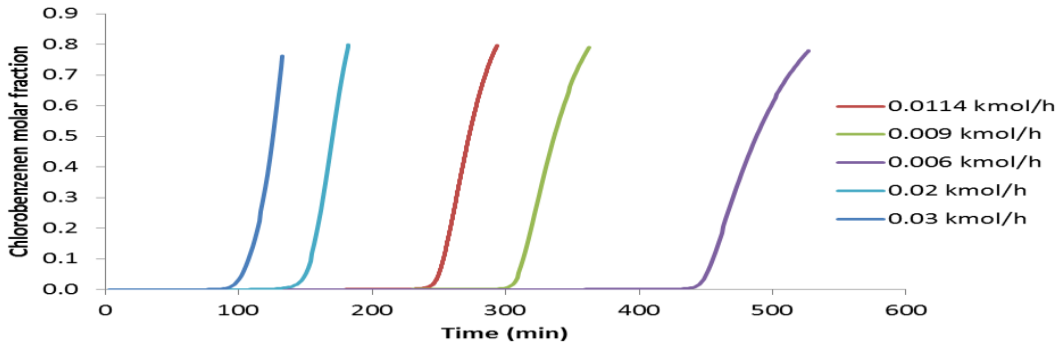

Figure 42– Chlorobenzene molar fraction profiles for different PI_2 controller setpoints

The changes in the distillate flowrate can extent the distillation from 293 minutes to 527, or reduce it up to 133 minutes (30 minutes of stabilization included). In terms of system optimisation, the distillate flowrate is one of the most important factors in time mitigation and/or time control. All of the PI_2 controller setpoints simulations were realised with a fixed value for the reflux valve stem position, and therefore the reflux ratio profiles are different for each setpoint value. The average value for the normalized reflux ratio for each simulation is presented in table 19:

Table 19– Average normalized reflux ratio for each different PI_2 controller setpoint

PI_2 setpoint (kmol/hr)	Average normalized reflux ratio
6.00×10^{-3}	0.92
9.00×10^{-3}	0.88
1.14×10^{-2}	0.85
2.00×10^{-2}	0.74
3.00×10^{-2}	0.61

As was sentenced before, a high normalized reflux ratio will perform a better component separation. Assuming a purity specification higher than 98% for the recovered cyclohexane, table 20 shows the total recovered mols within the specification:

Table 20– cyclohexane recovered mols with 98% purity for each different PI_2 controller setpoint

PI_2 setpoint (kmol/hr)	Cyclohexane recovered mols with 98 % purity (mol)
6.00×10^{-3}	25.35
9.00×10^{-3}	25.26
1.14×10^{-2}	25.16
2.00×10^{-2}	23.45
3.00×10^{-2}	18.04

The distillate molar flowrate backfires for higher values, as lower amounts of components are within the desired specifications. Nevertheless, increasing the distillate molar flowrate by a factor of 5 (from 0.006 to 0.03 kmol/hr) inflicts a 29% molar recovery reduction, in the simulated system.

5.2.3.Reflux valve stem position

The reflux valve stem position was altered and Its influence in the distillate molar fraction was analysed. Figures 43, 44 and 45 show the behaviour change of cyclohexane, toluene and chlorobenzene molar fractions (respectively) for different stem positions, for specific time intervals:

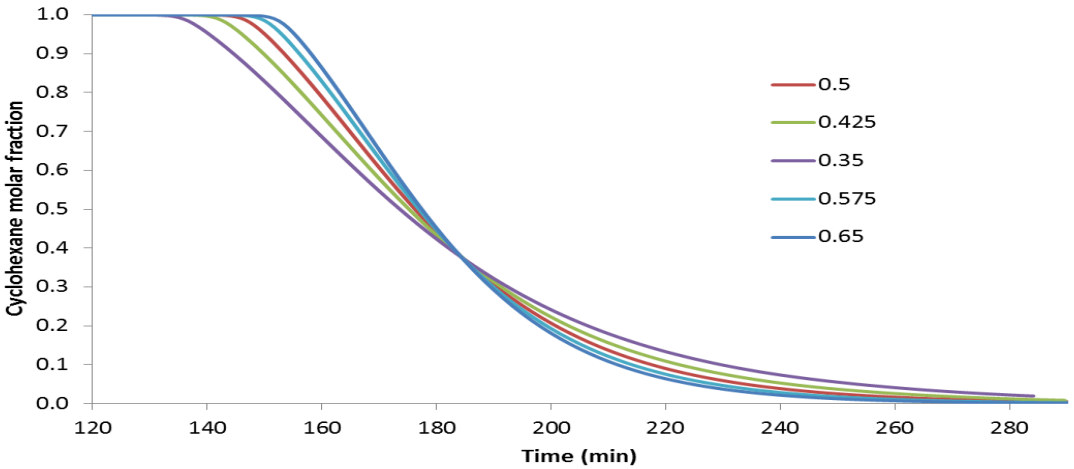

Figure 43– Cyclohexane molar fraction profiles for different reflux valve stem positions

As it can be observed, a more closed valve (lower stem position values) has a faster composition change at the beginning, but a more stable slope by the end of the first component distillation. This effect induces a less effective separation of the components, and a lower amount of recovered cyclohexane above the purity specifications. The same effect can be observed for the intermedium component, where the maximum purity reached is also influenced.

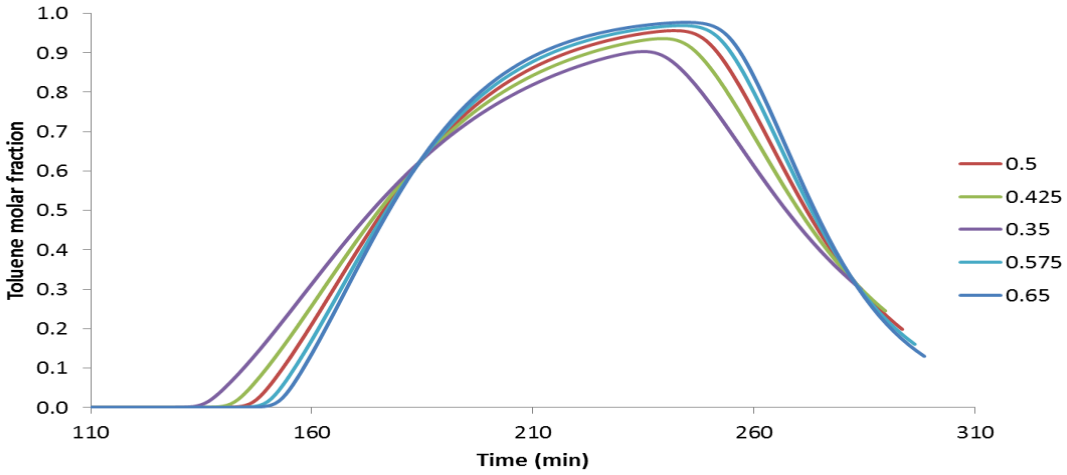

Figure 44– Toluene molar fraction profiles for different reflux valve stem positions

Another consequence of changing the reflux valve stem position is the amount of recovered component after the distillation. A total of 8.28 mol of toluene with 93% purity were recovered from the initial holdup, when operating with a 0.65 reflux valve stem position value. For an operating value of 0.425, the recovered amount only achieves 2.07, and the minimum purity threshold is not achieved when operating at 0.35. On the other hand, when setting the chlorobenzene minimum purity to 80%, only two out of the 5 stem positions reach such value. However, the distillation end-time is different for the 5 simulations: there is a 14 minute difference between the minimum and the maximum of the different stem position simulated, as can be observed in figure 45:

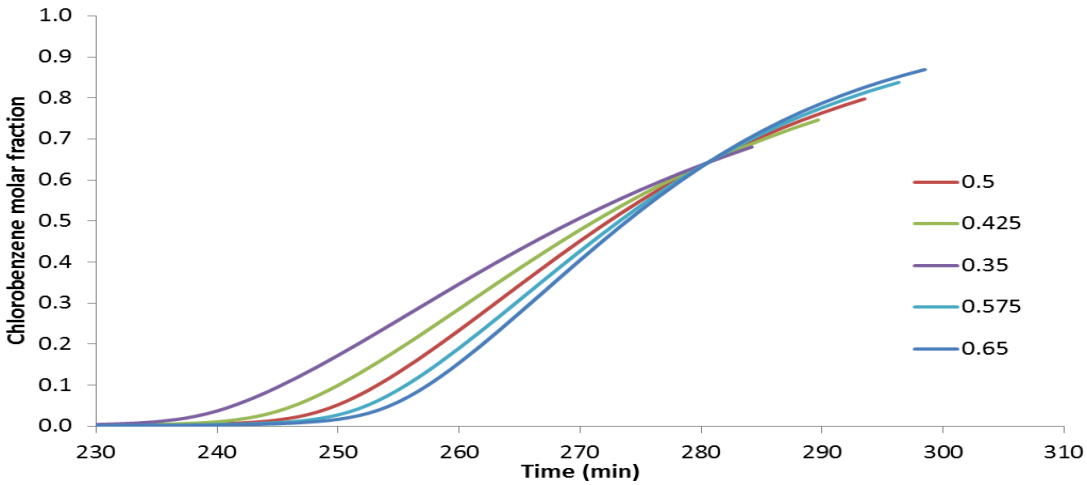

Figure 45 – Chlorobenzene molar fraction profiles for different reflux valve stem positions

The starting position of the reflux valve has a direct influence in the condenser liquid level at the beginning of the very same distillation. A valve with a reduced stem position value (closer to zero) will increase the pressure drop in that valve. Therefore, a higher liquid level is required in order to reach the equilibrium state. Figure 46 shows the liquid holdup fraction profile in the condenser for the different simulated stem positions:

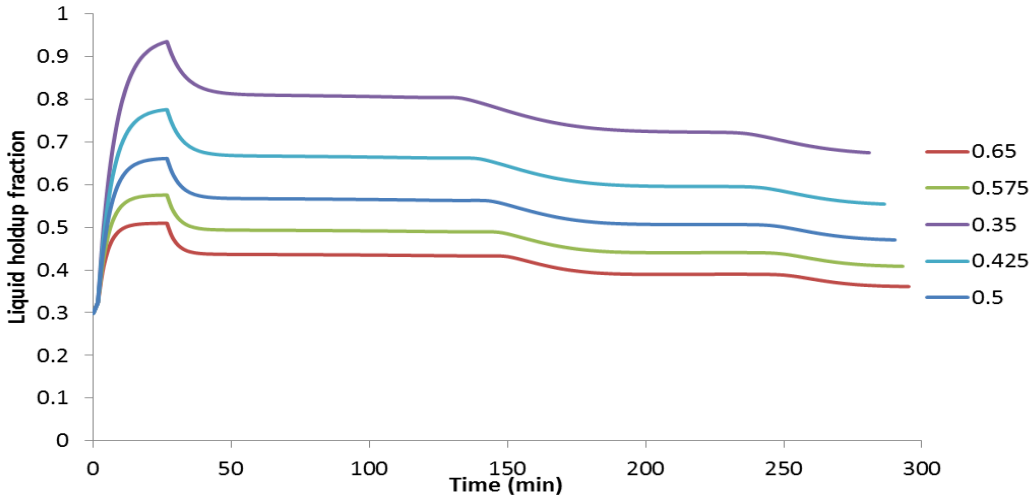

Figure 46 - Condenser liquid holdup fraction for different reflux valve stem positions

The liquid height in the condenser has an important influence in the distillate profile as the liquid inlet composition will change the condenser holdup molar fraction. Until time 140, cyclohexane is the richer component in the condenser. However, the liquid inlet is getting richer with toluene, and the distillate composition starts to change. Depending on the molar holdup (which is proportional to the liquid level), that change is either faster or slower. For slower changes, such as the 0.35 stem position simulation, higher purities are never achieved during the time period that the inlet liquid is richer in toluene.

5.2.4.Step sensitivity analysis: reboiler heat duty and RVSP

An additional sensitivity analysis has been made for both reboiler heat duty and the reflux valve stem position (RVSP). Step variations in the two variables were made during the simulation, in order to analyse the system behaviour and possible mathematical integration problems. Figure 47 shows the step variations conducted in the reboiler heat duty, and the 15th tray liquid flowrate behaviour:

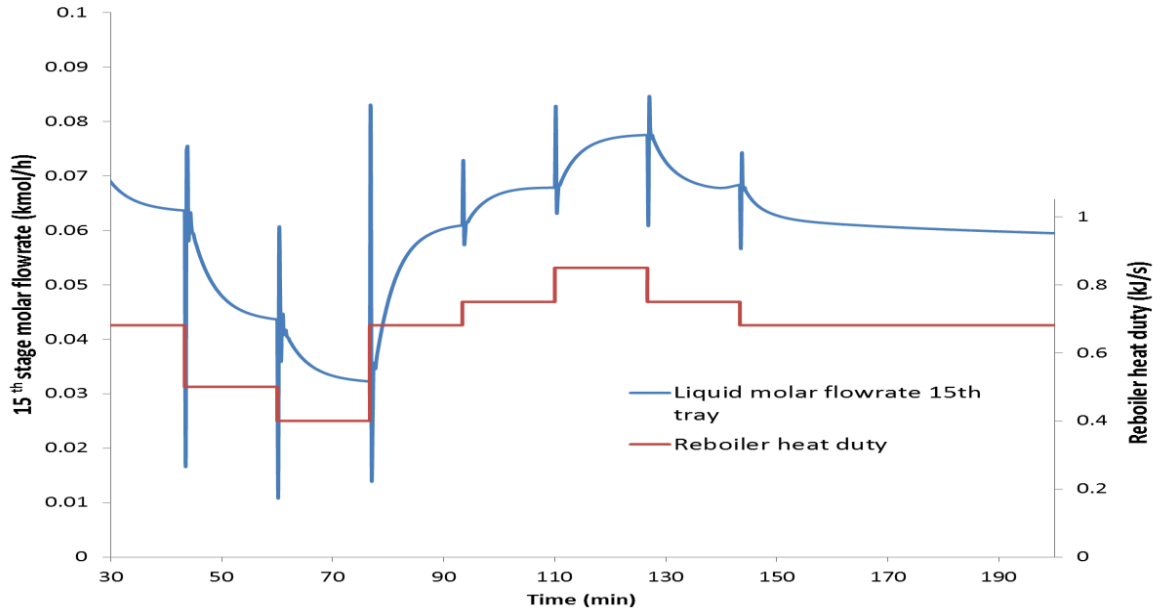

Figure 47– 15th tray liquid molar flowrate profile for reboiler heat duty step variations

As can be observed, a spike arises each time the reboiler heat duty input change. Such sudden variations carry difficult integration problems for the gPROMS® ProcessBuilder simulation solver. These difficulties are greater the bigger the difference between the new and the previous reboiler heat duty value, as can be noticed at the 76th minute.

In order to solve and overcome the problems presented in figure 47, a new controller model was added to the flowsheet, as well as an Energy Source model and an Energy Sink model: figure 48 presents the final assembled flowsheet for Pressure-driven (F.D.I.) and table 21 contains the PI_3 controller operational parameters:

Table 21– Operational PI_3 controller parameters

	PI_3
Manipulated variable	Energy rate (kJ/s)
Proportional gain	0.1
Integral time constant	28
Controller action	Reverse
Setpoint	0.389 (kJ/s)

Controlling the reboiler heat duty by manipulating the energy rate creates continuous and delayed change in the controlled variable. Consequently, the behaviour of the system will change accordingly, such as the liquid molar flowrate. Figure 49 displays the 15th tray liquid molar flowrate for reboiler heat duty step variations, within the final assembled flowsheet:

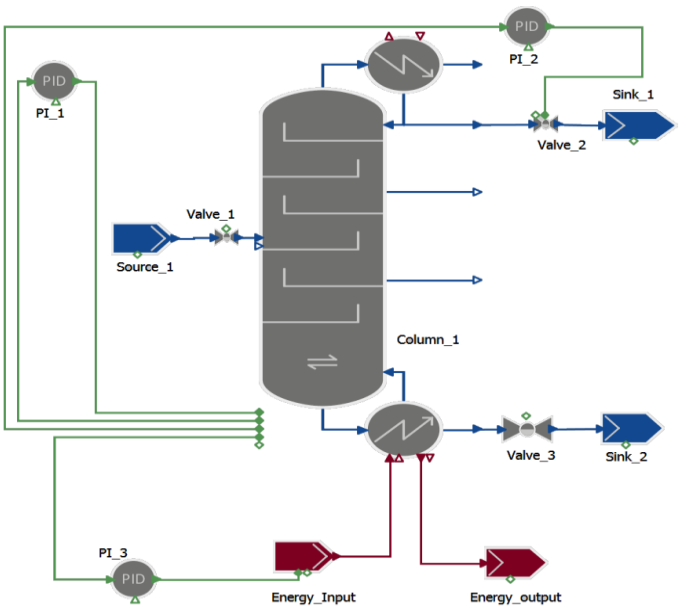

Figure 48– Pressure-driven (F.D.I) final assembled flowsheet

Similar results were obtained for the reflux valve stem position step variations, presented in appendix A.3. The instantaneous opening or closing of the reflux valve has a tremendous impact in the liquid molar flowrate, as a drastic cut (or increase) in the valve pressure drop will vary the liquid flowrate returning to the column from the condenser. The same alteration in the retuning liquid flowrate will have repercussions in the trays liquid molar flowrate, possibly creating temporary flooding or dryness.

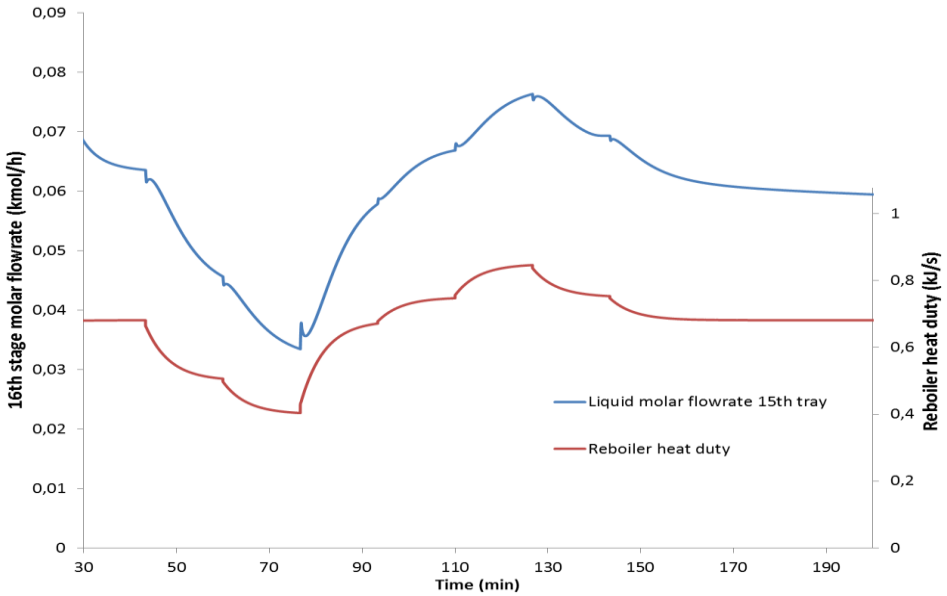

Figure 49– 15th tray liquid molar flowrate profile for reboiler heat duty step variations, within the final assembled flowsheet

In order to overcome this behaviour, a proportional gain to the reflux valve stem position was added. This method allows the reflux valve stem position to converge to a desired value, instead of abruptly changing to the new input. The proportional gain is added as the time integration of the difference between the desired value and the current value. A constant is then multiplied with the proportional gain, in order to tune the behaviour of the respective variable. The equations are:

$$Setpoint_{Valve} = RefluxValve_{StemPosition} + \alpha * Calculated_{Output} \tag{5.3}$$

$$Calculated_{Output} = \int RefluxValve_{StemPosition} \, . dt \tag{5.4}$$

Where $Setpoint_{Valve}$ is the desired reflux valve stem position (new input variable), $RefluxValve_{StemPosition}$ is the instant stem position of the reflux valve, α is the tuning constant for the proportional gain, and $Calculated_{Output}$ is the proportional gain. α was set as 40 for all of the following simulations and results. The results obtained after the model modifications are presented in appendix A.3.

The system behaviour has slightly softened and the reflux valve takes approximately one minute to accomplish its new value. The system is now able to accomplish a full simulation while varying the reboiler heat duty and the reflux valve stem position, without the risk of simulating negative molar flowrates.

5.3. Optimisation

In the following chapter an optimisation problem applied to the SIM-2 system, with the changes presented in sub-chapter 5.2.5, is solved in a constant-piecewise operation. The Capacity factor (CAP) [19] presented by Luyben has been set as base for optimisation objective. Three different optimisations were realised: optimisation of the lightest component distillation, optimisation of the lightest and medium component distillation, and optimisation of the whole distillation. The results for the first two optimisations are presented in the appendix A.4 and A.5 and the results commented in this chapter.

5.3.1. Objective functions

The CAP factor presented by Luyben takes into consideration the amount of distillate recovered per unit of operating time. The operating time is the sum of the distillation time with maintenance time, which includes the column cleaning, discharging and refilling. However, due to the lack of information regarding the maintenance time, this constant was ignored. Therefore the CAP factor is calculated and maximized in a different approach, and named Max_{mol} in all of the following work:

$$Max_{mol} = \frac{Product_{recovery}}{Time} \tag{5.5}$$

where the $Product_{recovery}$ is the molar holdup recovered from the initial column holdup within purity specifications (mol), and *Time* is the simulation time (hours). The $Product_{recovery}$ variable is different for each of the three optimisations, depending on which component recoveries are being maximised. Table 22 presents the different $Product_{recovery}$ equation for each of the optimisation problems:

Table 22– Different Productrecovery equations for the different optimisation problems

	$Product_{recovery}$
Light component optimisation	$Light_{recov}$
Light and medium component optimisation	$Light_{recov}$ + $Medium_{recov}$
Full distillation optimisation	$Light_{recov}$ + $Medium_{recov}$ + $Heavy_{acum}$

where $Light_{recov}$ is the light component recovery (mol), $Medium_{recov}$ is the medium component recovery (mol), and $Heavy_{acum}$ is the heavy component accumulation in the reboiler (mol).

$Light_{recov}$ and $Medium_{recov}$ variables were modelled as accumulation variables, behaving as tanks. These variables are written as:

$$Light_{recov} = \sum_1^n Light_{acum}('n') \tag{5.6}$$

$$Medium_{recov} = \sum_1^n Medium_{acum}('n') \tag{5.7}$$

where $Light_{Acum}$ *('n')* variables are the molar holdup of the *'n'* component during the light component recovery (mol), and the $Medium_{Acum}$ variables are the molar holdup of the respective components during the medium component distillation (mol). Using the $LightAcum_{Cyclo}$ as an example, this variable is modelled as:

$$Light_{acum}('n') = \int Distillate_{flowrate} * Distillate_{Purity}('n') * Constraints('m') \ .dt \tag{5.8}$$

where $Disitillate_{flowrate}$ is the distillate molar flowrate leaving the condenser (mol/h) and the $Distillate_{purity}$*('n')* is the molar fraction of the *n* component. *'m'* stands for the recovery period, either light component recovery period or medium component recovery period. The variable *Constraints('m')* acquires values between 0 and1, and has the objective to nullify or validate the $Light_{acum}$ *('n')*. That objective is achieved by using a modified hyperbolic tangent equation in which "true / false" statements are converted into 0 or 1 numerical values:

$$Constraints('m') = \frac{\tanh[\,(Ver_{DistPurity}('m') + Ver_{TankPurity}('m') - 0.5) * \beta]}{2} + 0.5 \tag{5.9}$$

$$Ver_{DistPurity}('n') = \frac{\tanh[\,(Distillate_{purity}('m') - Minimum_{DistPurity}('m') - 0.5) * \beta]}{2} + 0.5 \tag{5.10}$$

$$Ver_{TankPurity}('m') = \frac{\tanh[\,(Light_{fraction}('n') - Minimum_{TankPurity}('m') - 0.5) * \beta\,]}{2} + 0.5 \tag{5.11}$$

$$Light_{fraction}('n') = \frac{Light_{acum}('n')}{Light_{recov}} \tag{5.12}$$

where $Ver_{DistPurity}$ *('m')* and $Ver_{TankPurity}$ *('m')* are verification variables regarding the distillate purity and the accumulation purity, depending on which component is being distilled. The $Minimum_{DistPurity}$ *('m')* and $Minimum_{TankPurity}$ *('m')* variables are the minimum distillate purity and the minimum accumulation purity desired for the respective *'m'* distillate period. β is an adimensional tuning factor responsible for a faster function change between 0 and 1. This tuning factor was set as 500.

Table 23 contains the minimum distillate purity and the minimum tank purity for the different distillation periods ('m'):

Table 23– Minimum$D_{istPurity}$ and Minimum$_{TanlPurity}$ values for the different recovery periods

'm'	Minimum$_{DistPurity}$	Minimum$_{TankPurity}$
Cyclohexane recovery period	0.979	0.981
Toluene recovery period	0.929	0.931

The $Heavy_{acum}$ variable is written in slightly different way than Light$_{Acum}$ and Medium$_{Acum}$:

$$Heavy_{acu} = Reboiler_{holdup} * Constraints_{Heavy} \quad (5.13)$$

where the $Reboiler_{holdup}$ is the molar holdup inside the reboiler, and the $Constraints_{Heavy}$ is a variable responsible for nullify or validate the $Medium_{Acum}$ term, acquiring values between 0 and 1:

$$Constraints_{Heavy} = \frac{\tanh[(Ver_{HeavyHoldup}+Ver_{HeavyPurity}-1.9)*\beta]}{2} + 0.5 \quad (5.14)$$

$$Ver_{HeavyPurity} = \frac{\tanh[(ReboilerMolarFraction_{Chlorobenzzene}-Minimum_{ChlorobenzenePurity})*\beta]}{2} + 0.5 \quad (5.15)$$

$$Ver_{HeavyHoldup} = \frac{\tanh[(Reboiler_{holdup}-minimum_{ReboilerHoldup})*\beta}{2} + 0.5 \quad (5.16)$$

where the $Reboiler_{Holdup}$ is the molar holdup inside the column reboiler, the $Reboiler_{MolarFractionChlorobnzene}$ is the molar fraction of chlorobenzene inside the reboiler, $Ver_{HeavyHoldup}$ and $Ver_{HeavyPurity}$ are verification variables and the $Minimum_{ChlorobenzenePurity}$ and $Minimm_{ReboilerHoldup}$ are the minimum molar fraction and the molar holdup desired for the optimisation problems.

Table 24 contains the minimum molar fraction and the minimum molar holdup specifications:

Table 24– Minimum$_{ReboilerHoldup}$ and Minimum$_{ChlorobenzenePurity}$ values

Minimum$_{ReboilerHoldup}$ (mol)	Minimum$_{ChlorobenzenePurity}$
4	0.93

With the objective to have a fair comparison for the Light component optimisation, the initial case simulation (SIM-2) is simulated while the $Ver_{DistPurity}$ ('Cyclohexane') or the $Ver_{TankPurity}$ ('CyclohexaneRecoveryperiod') are 1. The same strategy is applied for the Medium and Light component distillation, with the $Ver_{Distpurity}$('Toluene') and the $Ver_{TankPurity}$ ('TolueneRecoveryPeriod').

5.3.2.Decision variables

For the present system, the decision variables optimised were the same as in sub-chapter 5.2 sensitivity analysis: PI_3 setpoint (reboiler heat duty, kJ/s), PI_2 setpoint (distillate valve stem position) and reflux valve stem position. The sensitivity analysis realized in the same sub-chapter shows that this set of variables detains great influence in the distillation time and system equilibrium.

These variables are fixed at the beginning of the simulation, replicating the same behaviour as previous chapters. The decision variables optimisation is realised after the distillation valve opening, at 1601 simulated seconds.

In addition, the optimisation has been divided in different time intervals after the opening of the distillation valve, each one with its own set of decision variables. For the light component and the medium plus light component distillation, the minimum number of time intervals has been found.

Table 25 shows the decision variables operating range, the maximum and minimum time intervals simulated for the first and second optimisation problems, and the number of time intervals simulated for the full distillation problem:

Table 25– Minimum and maximum operational values for the decision variables and optimised time intervals, and simulated number of intervals for full distillation problem

Minimum operating value	Decision variable	Maximum operating value
0.006	PI_2 setpoint (kmol/h)	0.03
0.4	PI_3 setpoint (kJ/h)	0.85
0.35	$Setpoint_{Valve}$	0.7
Light component optimisation		
Min. time intervals simulated: 1		Max. time intervals simulated: 5
Medium and light component optimisation		
Min. time intervals simulated: 7		Max. time intervals simulated: 14
Full distillation problem		
Number of simulated time intervals: 10		

5.3.3.Constraints

The optimisation problems were carried out with a set of constraints, in order to maintain a minimum level of purity and recovered product. Table 26 shows the purity, recovery and time constraints for the different optimisation problems:

Table 26– Optimisation constraints for the different simulations

	Minimum recovery (mol)	Minimum purity
Cyclohexane	24	0.98
Toluene	8	0.93
Chlorobenzene	4	0.91

Light component optimisation			
Min. interval duration (s)	Max. interval duration (s)	Min. total time (s)	Max. total time (s)
300	3000	3000	16000
Medium and light component optimisation			
Min. interval duration (s)	Max. interval duration (s)	Min. total time (s)	Max. total time (s)
300	4000	4000	17000
Full distillation problem			
Min. interval duration (s)	Max. interval duration (s)	Min. total time (s)	Max. total time (s)
300	5000	6000	17000

5.3.4.Results of Light component distillation problem

The results from Light component for 4 time control intervals are presented in appendix A.4.

The MaxMol profile for the Light component optimisation tends to an oblique asymptote. The distillate molar flowrate (controlled by the PI_2 setpoint) operates at its maximum value from the opening of the distillate valve, until the very end of the optimisation.

The system maintains a high level of purity in the distillate by closing the reflux valve at the beginning of the distillation (opening of the distillate valve). By doing so, the liquid level in the condenser rises, while both heat duty and the distillate molar flowrate are operating at their maximum value. The reflux valve stem position increases its value at each interval, momentarily increasing the reflux ratio and allowing a better component separation.

When the toluene composition increases in the rising vapour, the reboiler heat duty decreases to the minimum operational value, as it can be observed.

Increasing the distillate molar flowrate to its maximum operational value, while keeping a controlled level in the condenser and a controlled uprising of the toluene composition, leads to an effective time reduction of the distillation time. In fact, the time distillation time has reduced in approximately 50%, from 159.7 minutes to 79.6. Additionally, the time reduction has repercussions in the heat duty consumptions, both in the reboiler and in the condenser. Although the instant values of these variables are greater than the SIM-2 ones, the optimised time results in a total energy reduction. This reduction can be observed in figure 50:

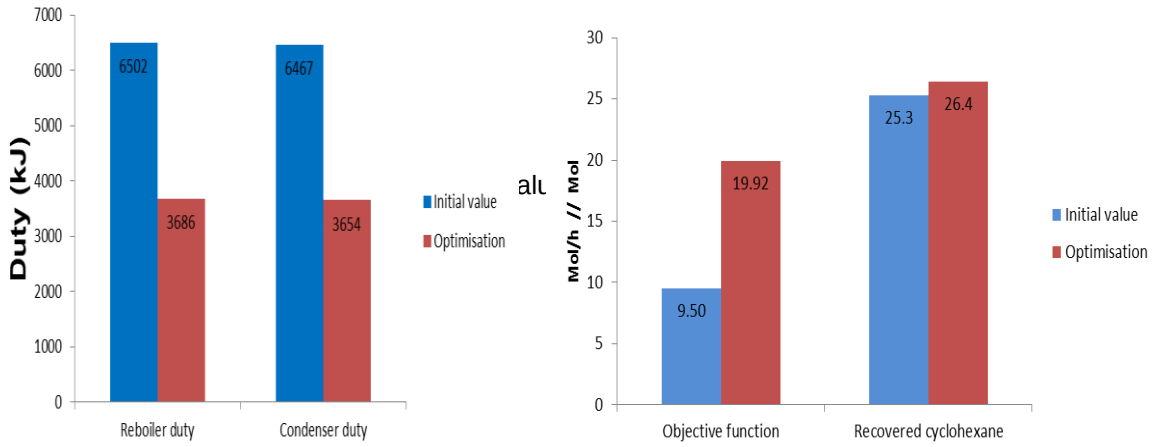

Figure 50– Reboiler duty, Condenser duty, Objective function and Recovered cyclohexane optimised values for Light component optimisation

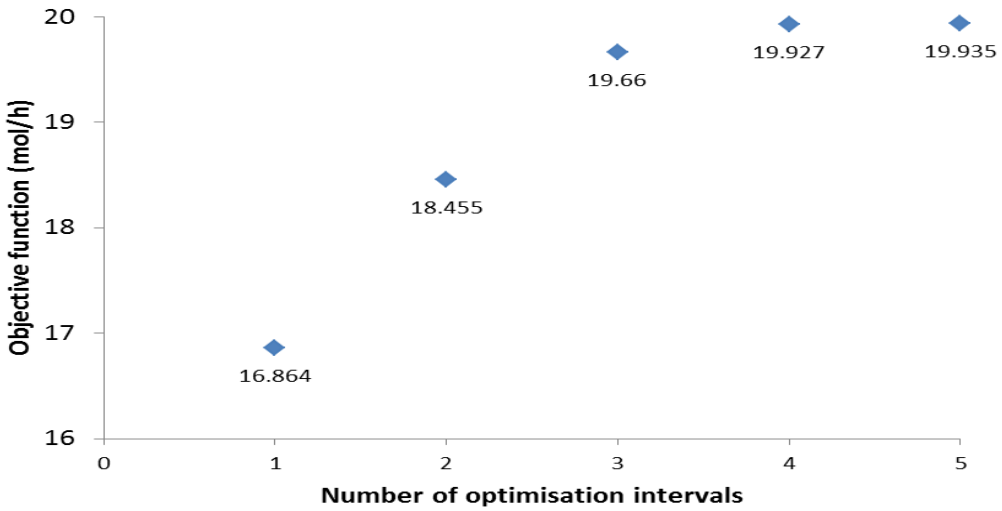

Figure 51– Optimised MaxMol values for different time control time intervals

The MaxMol variable stabilizes after the fourth control interval. In fact, the reflux valve stem position requires three time intervals until it achieves its maximum position, and stabilizes. The reboiler heat duty has an abrupt change at the last time interval, and it remains in the lowest possible value until a hypothetical off-cut, as in Medium and Light component optimisation. Therefore, 4 is the minimum number of required control intervals to achieve the optimal solution for the Light component optimisation.

5.3.5.Results of Medium and Light component distillation

The MaxMol profile from the Medium and Light component optimisation has three local maximum values, shown in appendix A.5. These are a direct influence of the PI_2 setpoint, observable in figure 52:

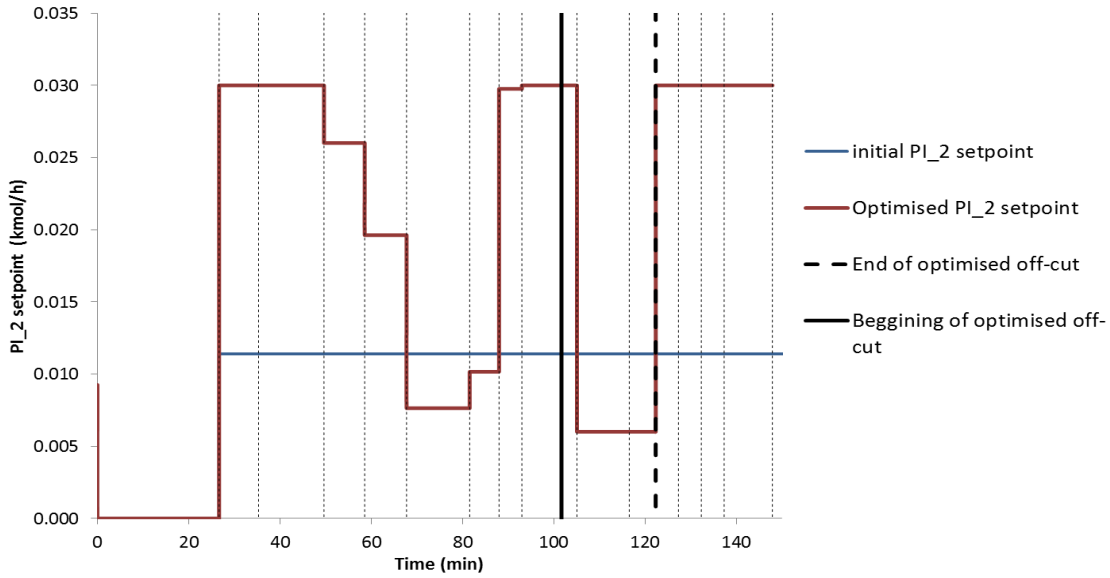

Figure 52– optimised and initial PI_2 setpoint forMedium and Light component optimisation

The PI_2 setpoint profile reveals four time intervals in which the optimised PI_2 setpoint variable has a lower operating value than the initial PI_2 setpoint. In these control intervals, the MaxMol value decreases, as the distillate flowrate is not high enough to overcome the time influence in the objective function. The first time interval, between 67 and 88 minutes, coincides with a constant increment of the reflux valve stem position value. This course of action increases the reflux ratio of the system, leading to a slight increase in the cyclohexane purity in the condenser, as it can be observed in figure 53:

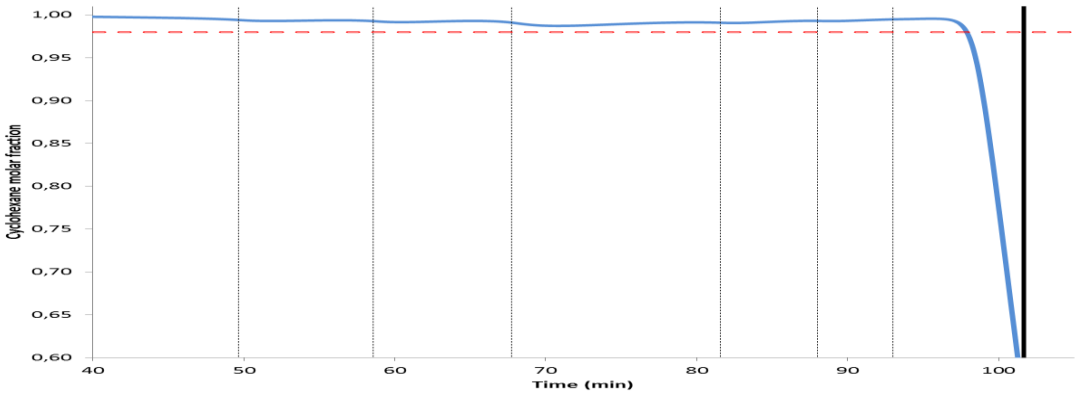

Figure 53– Optimised cyclohexane molar fraction in the condenser, between 40 and 105 minutes

By the end of this time period, the distillate molar flowrate increases to its maximum allowed value, and the condenser is literally emptied. The MaxMol variable increases until it achieves a new local maximum: the end of the cyclohexane recovery, and the beginning of the off-cut.

The off-cut is a critical operational time for the optimisation: a good balance between the system purification and the expelling of not recoverable product is extremely important, while trying to perform so in the minimum time possible.

Five minutes after the beginning of the off-cut, the distillate molar flowrate operates at 0.03 kmol/h, the maximum allowed value for this variable. The system is purging the maximum off-specification distillate as possible. After this time, the distillate valve reduced its opening, and the distillate molar flowrate reduces its value to the minimum possible, ultimately leading an increased reflux ratio, and a quicker enrichment of toluene in the distillate. Figure 54 presents the reflux ratio profile for the optimised Medium and Light component distillation and figure 55 shows the toluene molar fraction profile in the distillate, between 100 and 150 minutes:

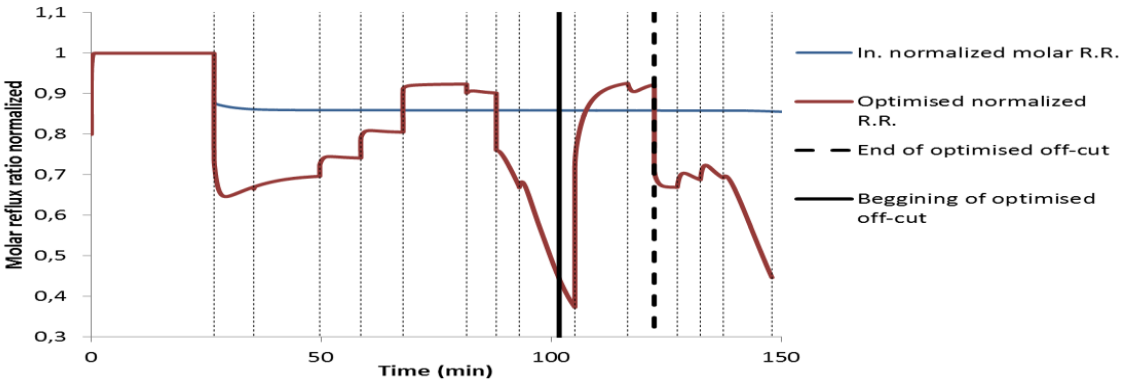

Figure 54– Molar reflux ratio normalized for the Medium and Light component optimisation

The end of the off-cut represents the beginning of the toluene recovery, represented as the third positive slope in the figure 62 in appendix A.5. From this point, the distillate valve is operating at its maximum value until the distillate is off-specification and the toluene accumulation reaches 93%.

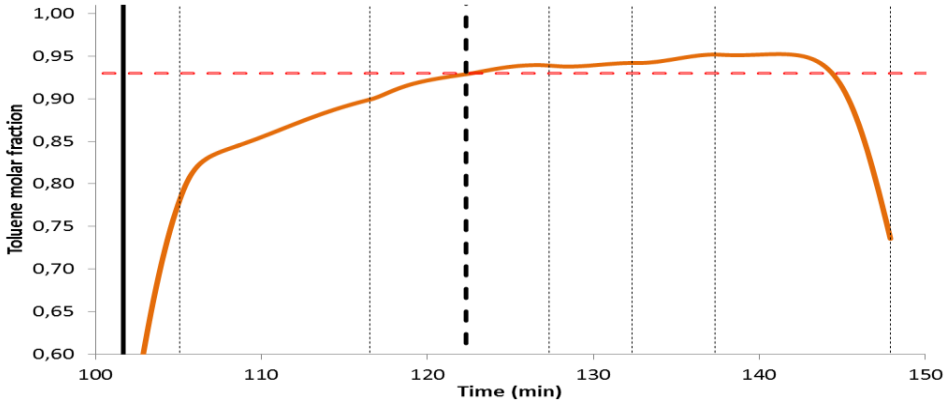

Figure 55 – Toluene molar fraction in the distillate, between 100 and 150 minutes

Figure 56 shows the comparison between initial and optimised values for the recovered toluene and cyclohexane, the off-cut and the objective function (MaxMol):

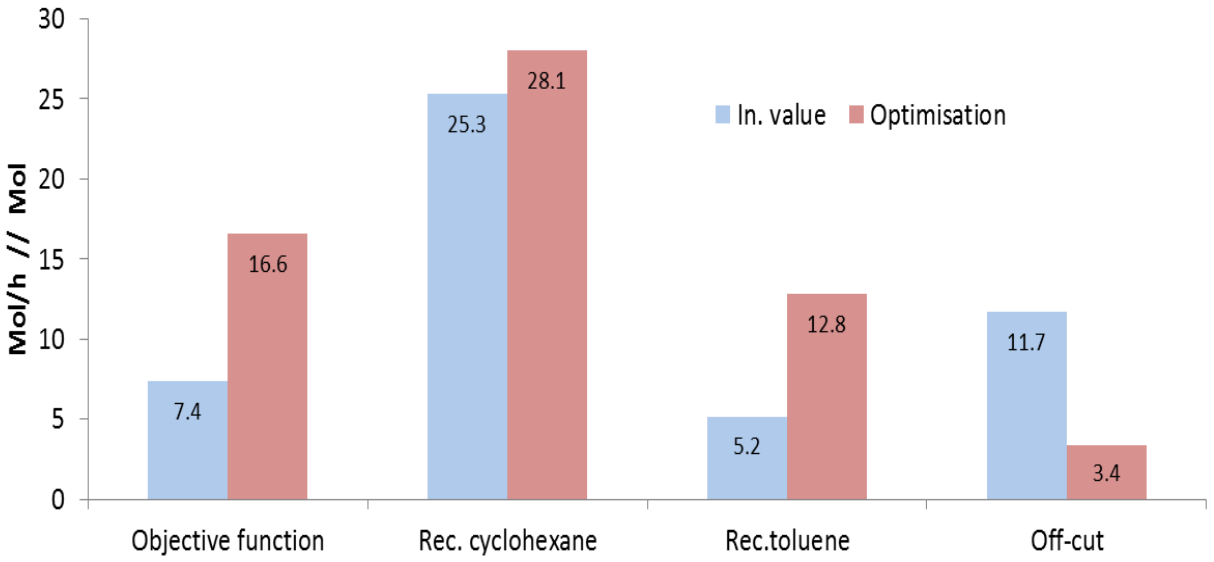

Figure 56– Comparison between initial and optimised values for toluene recovery, cyclohexane recovery, off-cut, and the objective function, for the Medium and Light component optimisation

Other optimised variables can also be consulted in table 27, as well as their variation and improvement:

Table 27– Comparison between initial and optimised variables, and their variation, for Medium andLight component optimisation

	Initial value	Optimised value	Variation (%)
Max_{mol} (mol/h)	7.4	16.6	125.4
Time (min)	248.6	147.9	-40.9
Cyclohexane recovery (mol)	25.3	28.1	10.9
Toluene recovery (mol)	5.2	12.8	147.7
Off-cut (mol)	11.7	3.4	-71.0
Total reboiler heat duty (MJ)	10.1	6.5	-35.5
Total condenser heat duty (MJ)	10.0	6.5	-35.6

Remarkably, the most improved variables (other than the objective function) are the toluene recovery and the off-cut: altogether, there was a reduction of 8.3 moles from the off-cut, and an improvement of 7.6 moles in the toluene recovered. Additionally, the distillation time has been reduced in 40.9 %, consequently reducing the total energy spent by the system.

Figure 57 presents the different Objective function values for different sets of time control intervals:

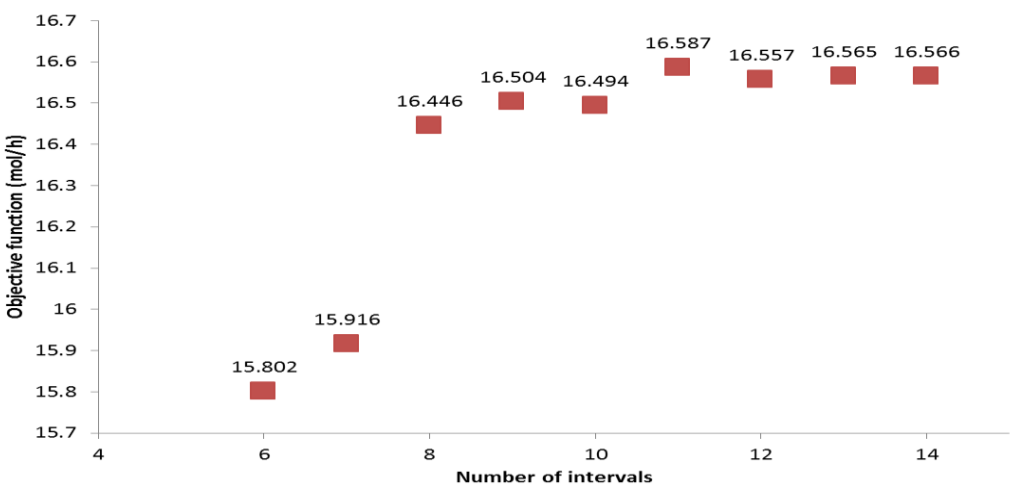

Figure 57– Objective function results for different sets of time control intervals, for Medium and Light component optimisation.

Optimising the two component distillation requires a minimum of 8 time control intervals to achieve an optimal solution. The fluctuations occurring after the 10th time interval are originated due to mathematical integration problems and numerical noise with the optimisation solver.

5.3.6.Results of full distillation

Figure 58 presents the profile of MaxMol variable for full distillation optimisation:

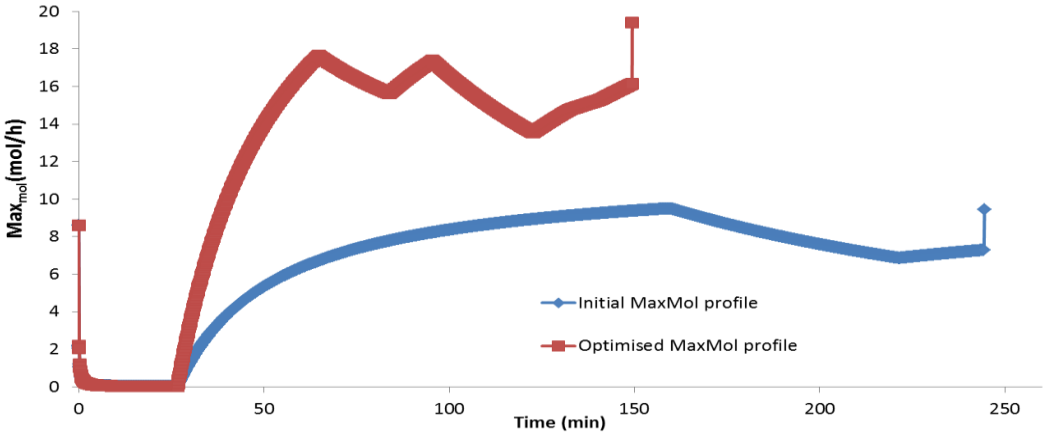

Figure 58– Initial MaxMol profile and optimised MaxMol profile for full distillation optimisation

Figure 58 shows 3 maximum points for the optimised MaxMol profile, and 2 maximum points for the initial MaxMol profile. The maximum point at the end of both profiles is the “activation” of the hyperbolic tangent function for the chlorobenzene component. This “activation” occurs when the molar fraction of chlorobenzene reaches 0.91 inside the reboiler, and the reboiler molar holdup is accounted into the MaxMol calculation.

The two initial maximum values are the initial recovery of cyclohexane, followed by a temporary purification of the system, and the distillation of the remaining in-spec cyclohexane, as explained in sub-chapter 5.3.5. After the off-cut, toluene is distilled until it runs out of specification in the condenser. However, the optimisation has matched this time event with the enrichment of chlorobenzene in the reboiler. By the time the recovery of toluene is finished, the chlorobenzene purity has reached the desired 91%. Comparing with the initial MaxMol profile, the toluene distillation was still ongoing when the chlorobenzene purity achieved 91%.

Table 28 compares the optimised and initial values for the components recovery, energy consumption and MaxMol variable.

Table 28– Comparison between initial and optimised variables, and their variation, for full distillation optimisation

	Initial value	Optimised value	Variation (%)
Max_{mol} (mol/h)	9.4	19.4	105.7
Time (min)	244.5	149.4	-38.9
Cyclohexane recovery (mol)	25.3	27.7	9.3
Toluene recovery (mol)	4.4	12.5	186.3
Chlorobenzene (mol)	8.8	8.1	-7.4
Off-cut (mol)	11.7	4.4	-62.6
Total reboiler heat duty (MJ)	9.9	6.7	-32.7
Total condenser heat duty (MJ)	9.9	6.6	-32.9

Comparing with the Medium and Light component optimisation, the cyclohexane recovery and the toluene recovery is slightly lower, and the off-cut value has an increased value. However, this is the ultimate optimisation, in which all the components are treated as equal and their recovery is optimised while trying to do so in the minimum time possible. Therefore, forfeiting some distillate that could be purified, reduces the distillation time, and that can be noticed by the difference in the MaxMol value, and in the distillation time (which is practically the same, for two component or for a full distillation optimisation).

Ultimately, it is now possible to compare the distribution of the initial holdup through the different components recovery and the off-specification product. Figure 59 contains the component distribution for the initial simulation, with the initial operating parameters:

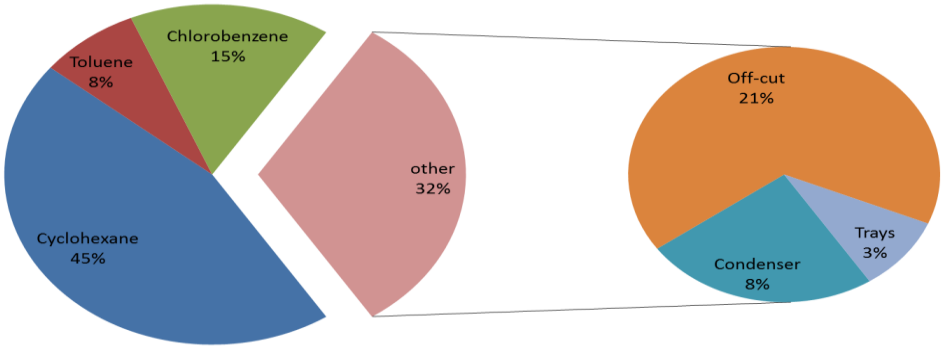

Figure 59– Final distribution of the initial holdup, in the initial simulation

As can be noticed, approximately one third of the initial holdup is not recovered, with 21% of the initial holdup being wasted in the distillation off-cut. The other 11% are distributed between the condenser and in the trays, being carried over for a following distillation. On the other hand, the toluene has the lowest recovery of all of the three components even though the initial holdup has approximately 18 moles of toluene and roughly 11 moles of chlorobenzene.

The optimised distillation has an increased recovery of all the components but the chlorobenzene. Nevertheless, more than half of the previous not recovered product has now been recovered, reducing the total percentage of off-cut, trays and condenser to 14%, as can be observed in figure 60:

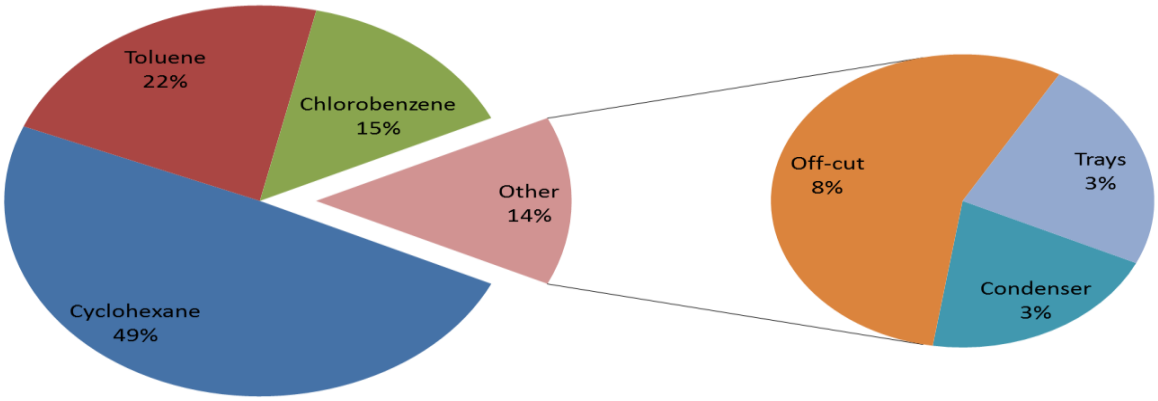

Figure 60– Final distribution of the initial holdup, in the full distillation optimisation

The off-cut has been reduced by almost a third, and the condenser and tray liquid holdup is now only 6%, which is carried over for the next distillation. Optimising the system has almost tripled the recovery of the most difficult separation (toluene) while reducing the operation time and the system energy consumption.

Page intentionally left blank

6. Conclusions and future work

6.1. Conclusions

The prediction and the exact comprehension of a batch distillation system is the most needed and expected result from the present and upcoming modelling challenges, in the current field. However, the greatest challenge is still the implementation of rigorous and capable control strategies for the simulation of the same model systems.

Using the case study of the present thesis as an example: one separator has been assembled to separate a ternary mixture at either constant pressure or constant temperature. All the other initial variables and conditions are the same. The most impressive results are the intense changes in the vapour outlet flow from both separators. The spikes presented are the result of the simulator re-initialisation, due to the opening and closing of valves. The major spike, which occurs twice for each of the different, is due to the fresh feed occurring during this period of time. As the feed composition is richer in light component than the composition of the separator holdup, there is an increment in the mixture evaporation rate. Also, during this period of time, the system has the feed valve opened which results in a system disturbance that can be observed in the manipulated variables behaviour. For the constant temperature separation case, the manipulated variable operates at its minimum allowed value in two distinct time periods. As a consequence, the pressure profile has a perturbation to its behaviour between 1.6 and 2 hours, and between 4.3 and 4.7 hours.

In terms of separation, the results would be the same as if this separation occurred in a one-stage distillation column. For the specification arbitrarily chosen, the off-cut sink holds 37% of the entire product that was separated. The light component, cyclohexane, only achieves 31%, followed up by the 25 % of heptane and 7% of toluene. However, the initial holdup is different from the feed specification. Thus, a steady cyclic state is not achieved in this study case.

For a complete model validation, simulation results have been compared with experimental data available in the literature. The batch distillation system has been simulated using a continuous column system which is not directly prepared to perform batch distillation. Therefore, the whole system had to be initialized in steady state in a flow-driven procedure. This allowed re-specifying the column feed characteristics until the holdup inside the column was approximately the same as the experimental data. The dynamic initialisation and simulation was realised after such procedures were taken.

From the results obtained, the operating strategy chosen for the modelled system is different from the operating policy in the available data. However, Bonsfills work was not explicit about which of the following variables was constant during the distillation: the reflux ratio, or the distillate flowrate. Therefore, after verifying a displacement of the distillate composition curves, an integration of the published curves operating at the referred reflux ratio has been made, and afterwards compared.

The behaviour of the lightest component is by far the best of the ternary mixture. A time lapse can be noticed at the time period that the distillate cyclohexane composition starts to drop. This can easily be explained by differences in the condenser holdup. Bonsfills laboratory column had no reflux drum included, therefore there was no holdup variation. However, this has not been the case for

the system simulation. Additionally, the system could not predict the toluene – chlorobenzene interactions as good as the cyclohexane – toluene interactions. The biggest deviation obtained (0.24) is indeed during the enrichment of chlorobenzene in the distillate. Nevertheless the average deviation is small for all the components, and the system behaviour is well predicted, and validated.

The influences of the condenser holdup are wider than the distillate curve misplacement. The sensitivity analysis has revealed that changes in the heat duty and in the reflux valve have a huge impact in the distillate purity. For greater values of condenser holdup fraction, lower the maximum purity achieved will be. However the changes performed in the heat duty show that there is an optimum value for the condenser holdup influence in the separation. The best separation results obtained were not achieved with the lowest heat duty tested, 400 W. Instead, the 500 W obtained the highest purity in the toluene separation.

Similar conclusions can me made out of the results obtained from the sensitivity analysis realised to the reflux valve stem position. The initial position of this valve is of high importance to the initial condenser liquid holdup fraction. Comparing the product recovery obtained in the reflux valve analysis realised, a difference greater than 6 mols is achieved by starting the distillation with the valve in a 0.65 position, instead of 0.425 (0 = closed valve). If the valve closes even more, the purity specification is not met, for toluene.

From the step sensitivity analysis realised, it is possible to notice that there were some modelling issues. By changing the reflux valve stem position or the reboiler heat duty input during the distillation, the system behaviour was too intense, especially in the liquid molar flowrates. Although such behaviour is not expected, changes in these variables should not be “instantaneous”. The same procedure happening in reality would require some time to take effect. Therefore a new control strategy had to be considered for the heat input, and a dynamic behaviour for the reflux valve has been implemented.

A set of optimisation problems has been addressed: optimising the recovery rate of the light component, optimising the recovery rate of the medium and the lightest component, and optimising the recovery rate of the whole distillation. These problems shared the same purity constraints for the respective components, and the initialisation procedure was equal for all the three problems.

The optimal operating policy for the system has been found, considering the heat duty input, the reflux valve and the distillate flowrate as control variables. The minimum number of control intervals has also been found for the first two problems, being 5 and 8, respectively. Using the capacity factor (CAP) as an objective function, the results were 19.9, 16.6 and 19.4 mol/hr respectively. The difference between the middle value and the others can be explained by the time factor: it is required a greater operation time to effectively separate the toluene from the cyclohexane component, but by the time this is achieved, the chlorobenzene specification in the reboiler is met. However, the biggest amount of cyclohexane and of toluene recovered belongs to the second optimisation.

In all the optimisation problems referred, the time and energy consumption have been reduced.

6.2. Future work

Regarding the system assembly, column models require special attention in the initial system definition. A initial holdup specification might be considered, with an assumption of a mixture distribution between the column stages. Additionally, some of the column sub models can be improved in terms of dynamic behaviour, such as the condenser inlet and reflux valve position, and the possibility to operate with a constant reflux ratio

For the system assembled, further work can be done in the optimisation of the distillation. Not only by changing the objective function to a profit one, but also to analyse the recovery of the off cut and tray and condenser holdup. The deep investigation of this problem leads to the cyclic steady state of this system, which is the ultimate optimisation objective of many industrial batch operations.

Lastly, the comparison of a new operating strategy for the assembled model can be of great interest in terms of additional validation. As it was stated before, the operating policy followed in this thesis is different than the one adopted in the experimental results.

Page intentionally left blank

Bibliography

[1] - [Online] Available: http://www.psenterprise.com/ [last accessed on: 05/11/2015]

[2] – Converse A. O., Gross G.D., *Optimal distillate-rate policy in batch distillation*, I & EC Fundamentals, volume 2, 1963

[3] – Robinson E. R., *The optimisation of batch distillation operations*, Chemical Engineering Science, vol 24, pgs. 1661 – 1668, 1969

[4] - M. Barolo, F. Botteon, *Simple method of obtaining pure products by batch distillation*, vol. 43, 1997.

[5] - S. Sundaram, L. Evans, *Shortcut procedure for simulating batch distillation operations*, vol. 32, 1993.

[6] - R. Krishna, J. Wesselingh, *The Maxwell-Stefan approach to mass transfer*, Chemical Engineering Science*,* vol. 52, pgs.. 861-911, 1997

[7] - Schneider R., Noeres C., Kreul L.U., Górak A., *Dynamic modelling and simulation of reactive batch distillation,* Computer and chemical engineering, pgs.423-426, 1999

[8] - Baur R., Taylor R., Krishna R., *Dynamic behavior of reactive distillation columns described by a nonequilibrium stage model*, Chemical Engineering Science 56, pgs. 2085-2102, 2001

[9]– Sorensen E., Skogestad S., *Comparison of regular and inverted Batch Distillation,* Chemical Engineering Science, Vol. 51, pgs. 4949 – 4962, 1996

[10] - Hasebe S., Abdul Aziz B., Hashimoto I., Watanabe T., *Optimal design and operation of complex batch distillation column*, Proceedings of the IPAC workshop, 1992

[11] – Morari M., Meski G. A., *Design and Operation of a Batch Distillation Column with a Middle Vessel*, Computers Chemical Engineering, vol. 19 , pgs. 5597 – 5602, 1995

[12] – Demicoli D., Stichlmair J., Warte M., *Operation of a batch distillation column with a middl vessel: experimental results for the separation of zeotropic mixtures*, Chemical Engineering and Processing, vol 43, pgs. 263 – 272, 2004

[13]– Hasebe S., Kurooka T., *Comparison of the separation performance of a Multi-Effect batch distillation system and a continuous distillation system,* DYCORD+'95, Copenhagen Denmark, 1995

[14]– Skogestad S., Wittgens B., *Closed Operation of Multivessel Batch Distillation: Experimental Verification,* AIchE jornal, vol. 46, 2000

[15]- I. Coward, *The time-optimal problem in binary batch distillation***,** Chemical Engineering Science, 1967, Vol. 22, pp. 503-516

[16]– Keith F. M., Brunet J., *Optimal Operation of a Batch packed Distillation Column,* The Canadian Journal of Chemical Engineering, vol 49, 1971

[17]– Vissers H. J. M., Kerkhof L. H. J., *On the profit of optimum control in batch distillation*, Chemical Engineering Science, vol 33, pgs. 961 – 970, 1978

[18]– Pantelides C. C., Furlonge H. I., Sorensen E., *Optimal Operation of Multivessel Batch Distillation Columns,* AIChE Journal, vol. 45, 1999

[19]– Luyben W. L., *Some Practical aspects of Optimal Batch Distillation Design,* Ind. Eng. Chem. Process Des. Dev., vol 10, pgs. 54-59, 1971

[20] - J. Seader, E. Henley and K. Roper, *Separation Process Principles*, New York: John Wiley & Sons, 2011.

[21] - H. Kister, *Distillation Design*, New York: McGraw-Hill, 1992.

[22] - E. G. Azevedo, A. M. Alves, *Engenharia de Processos de Separação,* IST Press, first edition, 2009

[23]- I.M. Mujtaba, *Batch Distillation – Design and Operation,* Imperial College Press, vol 3, 2004

[24]- R. H. Perry and D. W. Green, *Perry's Chemical Engineers' Handbook*, McGraw-Hill, 1999

[25]- Babu, G.U.B., Aditya, R. & Jana, A.K., *Economic feasibility of a novel energy efficient middle vessel batch distillation to reduce energy use*., *Energy,* vol. 45, pp.626–633, 2012

[26]- R. Sinnott, *Chemical Engineering Design*, Elsevier, 2005.

[27]- Egly H., Ruby V., Seid B., *Optimum design and operation of batch rectification accompanied by chemical reaction*, Comp. and Chem. Engineering, Vol 3, pgs. 169-174, 1979

[28] - Elmahboub A. E., Mujtaba I. M., Emtir M., *Optimal operation of different types of batch reactive distillation columns used for hydrolysis of methyl lactate to lactic acid*, Chemical Engineering Journal 172, pgs. 467– 475, (2011)

[29]– E. Sorensen, *A cyclic operating policy for batch distillation – theory and practice*, Computers and Chemical Engineering 23, pgs. 533- 542, 1999

[30]- Y.-L. Kao and J. D. Ward, "Design and optimisation of batch reactive distillation processes with off-cut," *Journal of the Taiwan Institute of Chemical Engineers,* vol. 45, pp. 411-420, 2014

[31] - Luyben, W. L., *Multicomponent Batch Distillation. 1. Ternary Systems with Slop Recycle*. Ind. Eng. Chem. Res. 1988.

[32] – Luyben W. L., Quintero-Marmol E., *Multicomponent Batch Distillation 2. Comparison of alternative slop handling and operation strategies*, Ind. Eng. Chem Res., 1990

[33] - Rayleigh, L., *Phil. Mag. 4* **,** 527,1902

[34] – Skogestad S., *Dynamic and control of distillation columns – a critical survey*, Modelling identification and control, vol.18, pgs.177-217, 1997

[35] – Viseu, M., *Dynamic Modelling of Batch Distillation Columns*, Chemical engineering master thesis, Instituto Superior Técnico, 2014

[36] – Rippin D.W., Computer Chemical Engineer 7, pg 137, 1983

[37] – Parakrama R., The Chemical Engineer, September, 1985.

[38]– Chiotti O. J., Iribarren O. A., *Simplified models for binary batch distillation,* Comput. Chem. Engineering, vol 15, 191

[39]– Chiotti O. J., Salomome H. E., Iribarren O. A., *Selection of multicomponent batch distillation sequences,* Chem. Eng. Commun, 1993

[[40]– Devyatikh G. G., Churbanov M. F., *Methods of high purification*, Znanie, USRR, 1976

[41]– Davidyan A. G., Kiva V. N., Meski G. A., Morari M., *Batch distillation in column with a middle vessel*, Chem. Eng. Science, 1994

[42]– Barolo M., Guarise G. B., Ribon N., Rienzi S., Trotta A., *Some issues in the design and operation of a batch distillation column with a middle vessel*, Computers chem. Eng. , vol 20, pg 537 – 542, 1996

[43]– Hasebe S., Noda M., Hashimoto I., *Optimal operation policy for multi-effect batch distillation system,* Computers chem. Eng. , vol 21, pg 1221 – 1226, 1997

[44]– Alpanda S., Peralta-Alva A., *Oil crisis, energy-saving technological change and the stock market crash of 1973-74*, Review of Economic Dynamics 13, pg 824-842, 2010

[45]– Mujtaba M., Miladi M. M., *Optimisation of design and operation policies of binary batch distillation with fixed product demand,* Comp. and Chem. Engi., vol 28, pgs. 2377-2390, 2004

[46]– Process Systems enterprise Limited, “gPROMS ModelBuilder Guide”, London 2015

[47]– “KBC Advanced Technologies” 2015, [Online]: Available at: http://www.kbcat.com/infochem-software/flow-assurance-software-multiflash (Assessed: 14 November 2015)

[48] – Bonsfills A., Puigjaner L., *Batch distillation: simulation and experimental validation*, Chemical engineering and Processing 43, pgs. 1239 – 1252, 2004

[49] – [Online] Available: http://www.amsterchem.com/scanit.html [last accessed on: July 2015]

Appendices

A-1. Separator results

In this appendix, the evolution of the mass fraction profiles of each tank and sink models are presented, for constant pressure simulation:

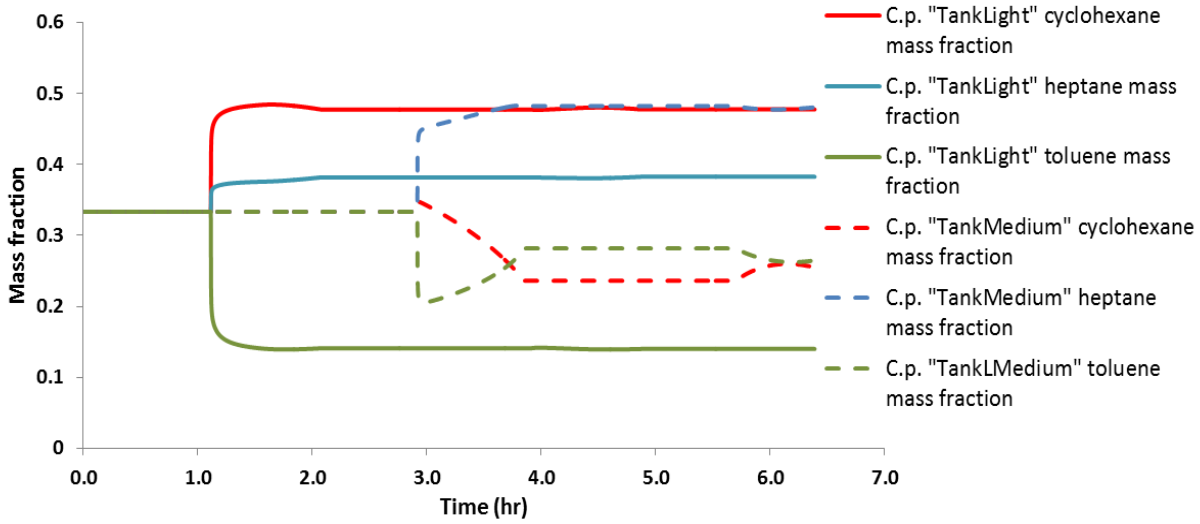

Figure 61 - "TankLight" and "TankMedium" mass fraction profile, for constant pressure simulation

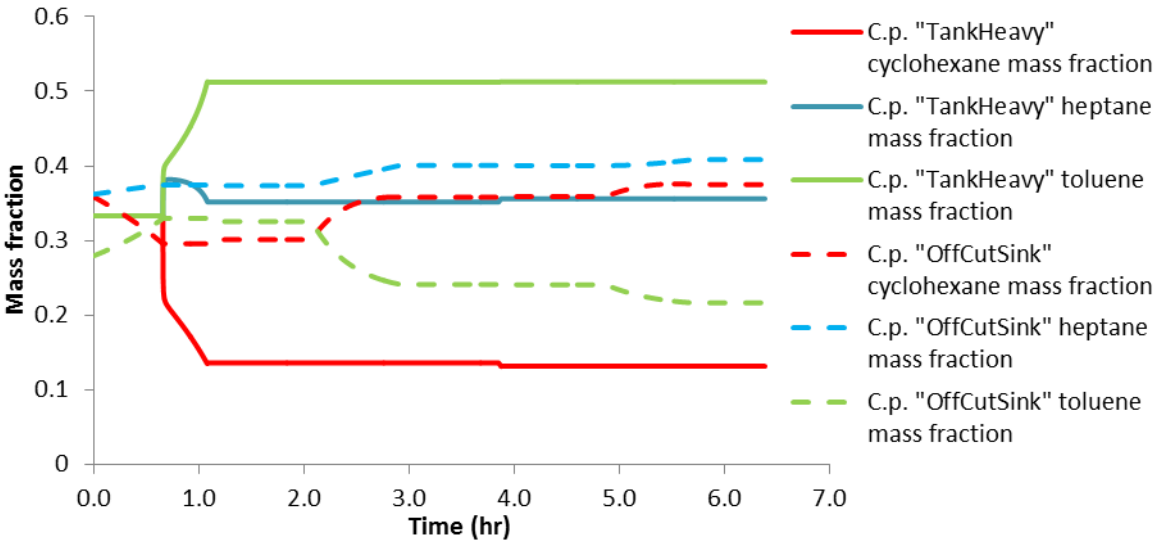

Figure 62– "TankHeavy" and "OffCutSink" mass fraction profile, for constant pressure simulation

A-2. SIM-1 and SIM-2 results

In the present appendix, SIM-1 distillate molar fraction profiles and trays temperature profiles are presented, as well as SIM-2 trays temperature profile:

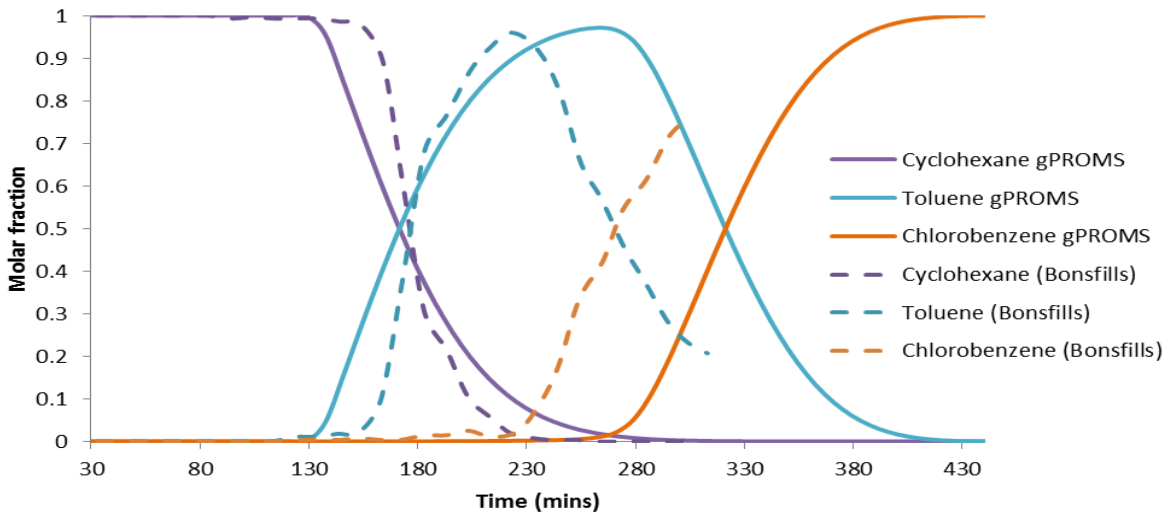

Figure 63 - Simulated distillate molar fraction profiles for SIM-1

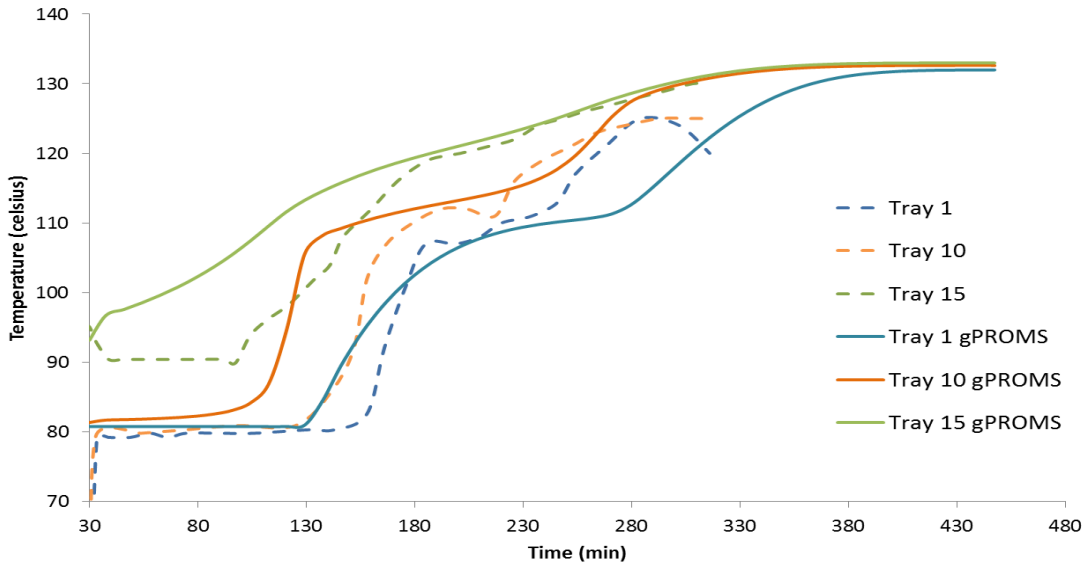

Figure 64 – Comparison between experimental and SIM-1 trays temperature profiles

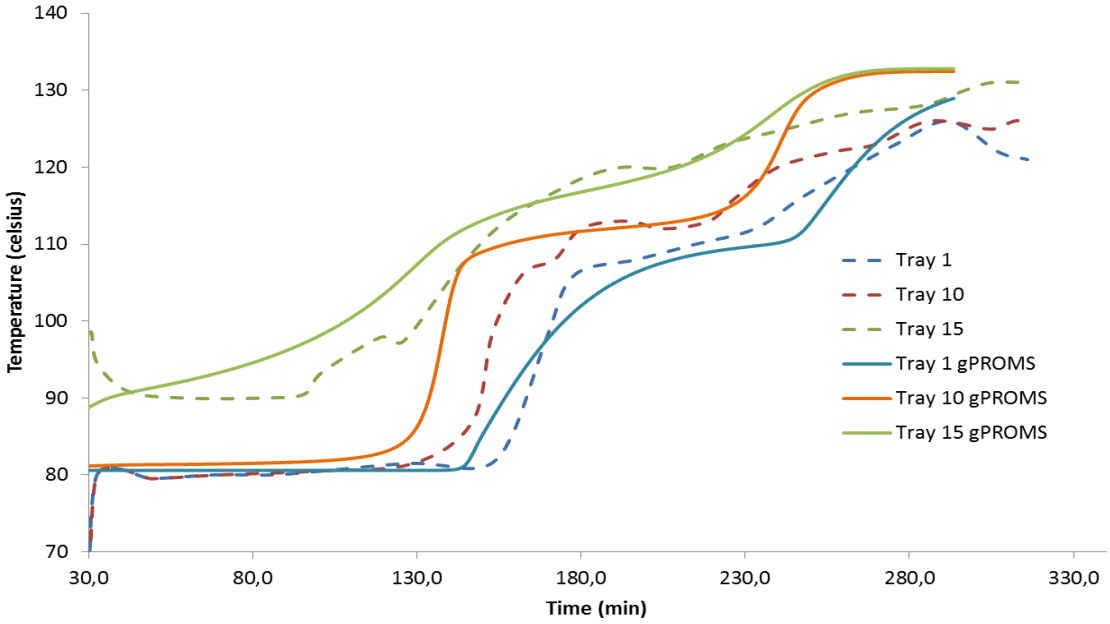

Figure 65– Comparison between experimental and SIM-2 trays temperature profiles

Page intentionally left blank

A-3. Reflux valve stem position step analysis

In the present appendix, the step analysis performed in the reflux valve stem position input variable, and the influences in the liquid molar flowrate are presented. The behaviour change after the model alterations is also shown:

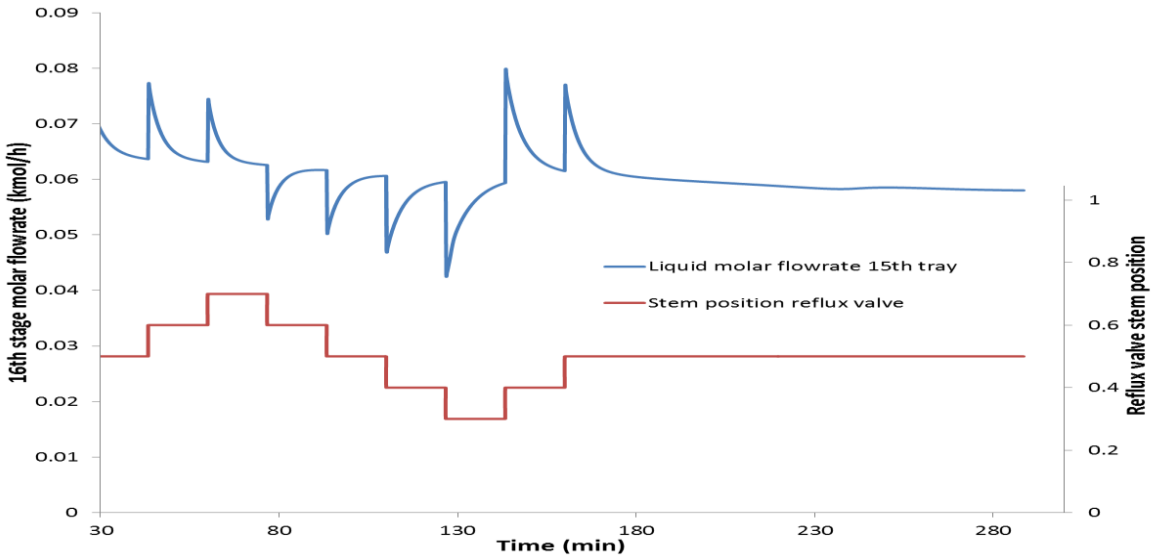

Figure 66 - 15th tray liquid molar flowrate profile for reflux valve stem position step variations

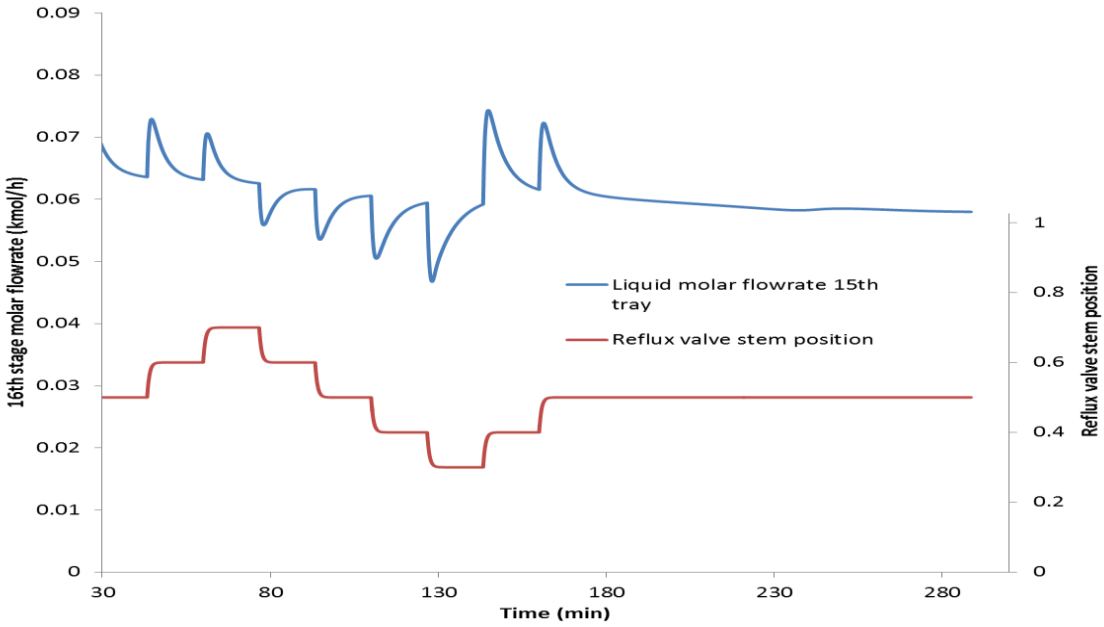

Figure 67 -15th tray liquid molar flowrate profile for reflux valve stem position step variations after model modifications

Page intentionally left blank

A.4 – Light component distillation problem

In this appendix, the objective function profile for the light component distillation problems is presented, as well as the optimised control variables profiles. Additionally, table 29 presents the optimisation result values for the controlled variables in the 4 time intervals optimisation:

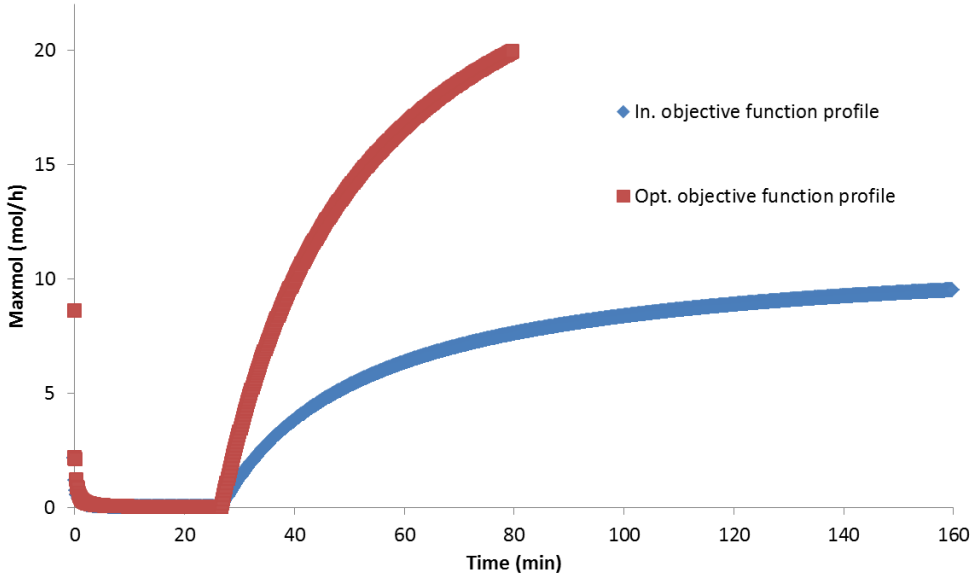

Figure 68 - Initial MaxMol profile and optimised MaxMol profile for light component distillation optimisation

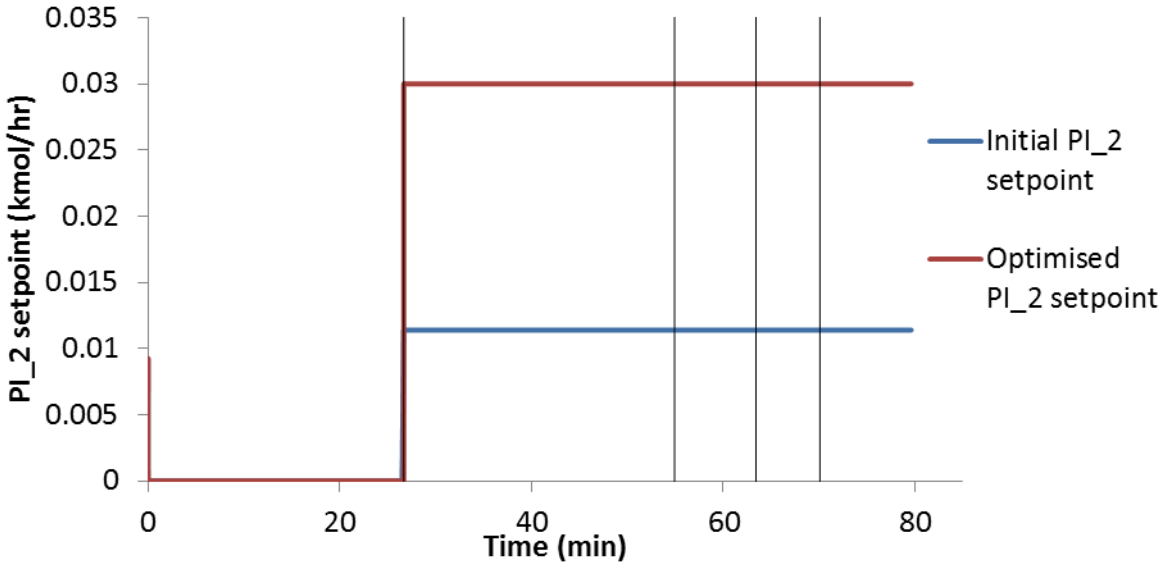

Figure 69 - Initial PI_2 setpoint profile and optimised PI_2 setpoint profile for light component distillation optimisation

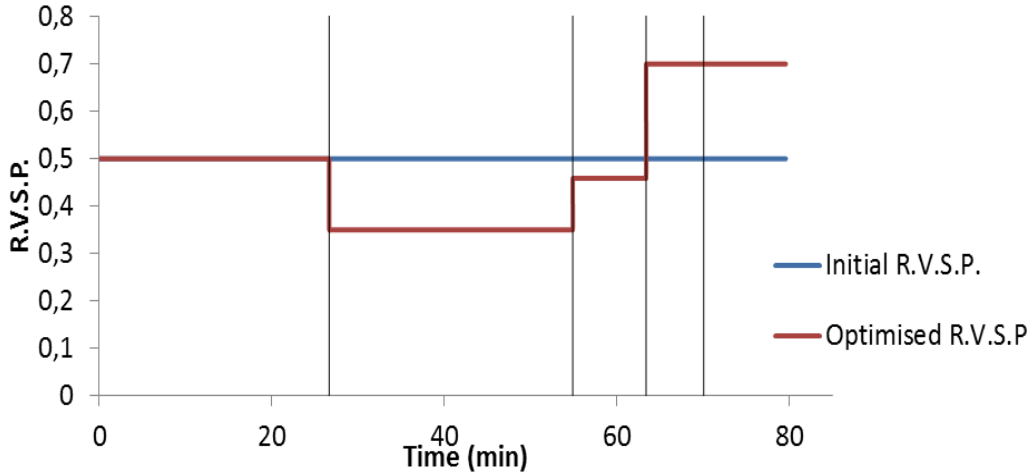

Figure 70 - Initial reflux valve stem position profile and optimised reflux valve stem position profile for light component distillation optimisation

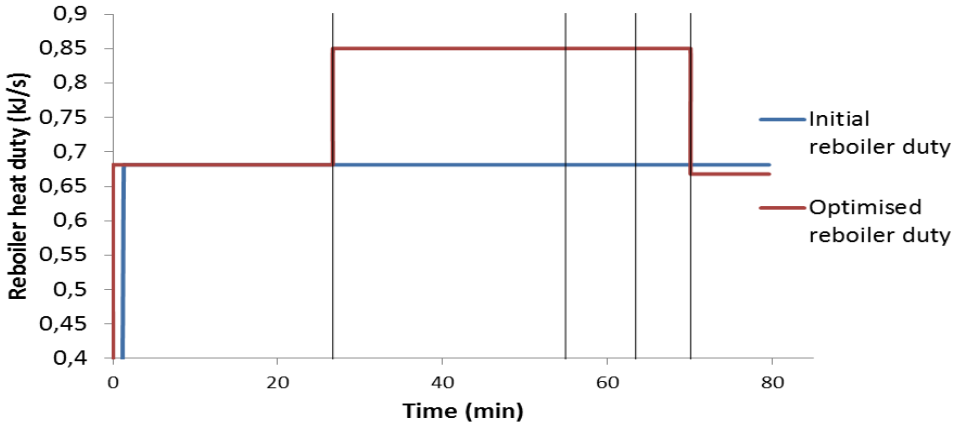

Figure 71 - Initial reboiler duty profile and optimised reboiler duty profile for light component distillation optimisation

Table 29 – Optimisation results for the optimised control variables in the light component distillation problem, for 4 time intervals

Interval	Duration (s)	Final time (min)	PI_2 setpoint (kmol/hr)	RVSP	Reboiler heat duty (kJ/s)
1	1694	54.9	0.03	0.35	0.85
2	510	63.4	0.03	0.46	0.85
3	400	70.1	0.03	0.70	0.85
4	571	79.6	0.03	0.70	0.67

A.5 – Medium and light component distillation problem

In this appendix, the objective function profile for the medium and light component distillation problems is presented, as well as the optimised reboiler heat duty and the reflux valve stem position profiles. Additionally, table 30 presents the optimisation result values for the controlled variables in the 14 time intervals optimisation:

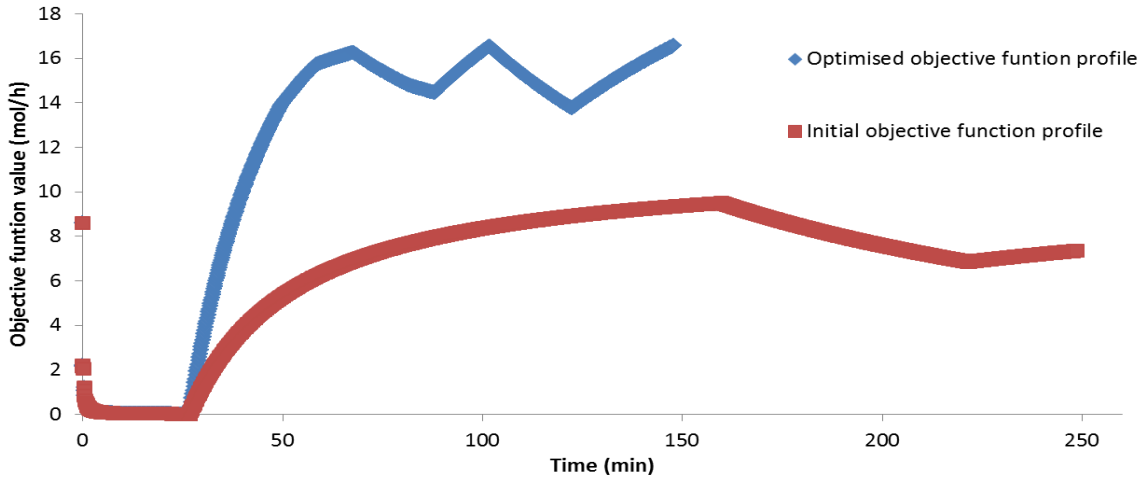

Figure 72- Initial objective function profile and optimised objective function profile for medium and light component distillation optimisation

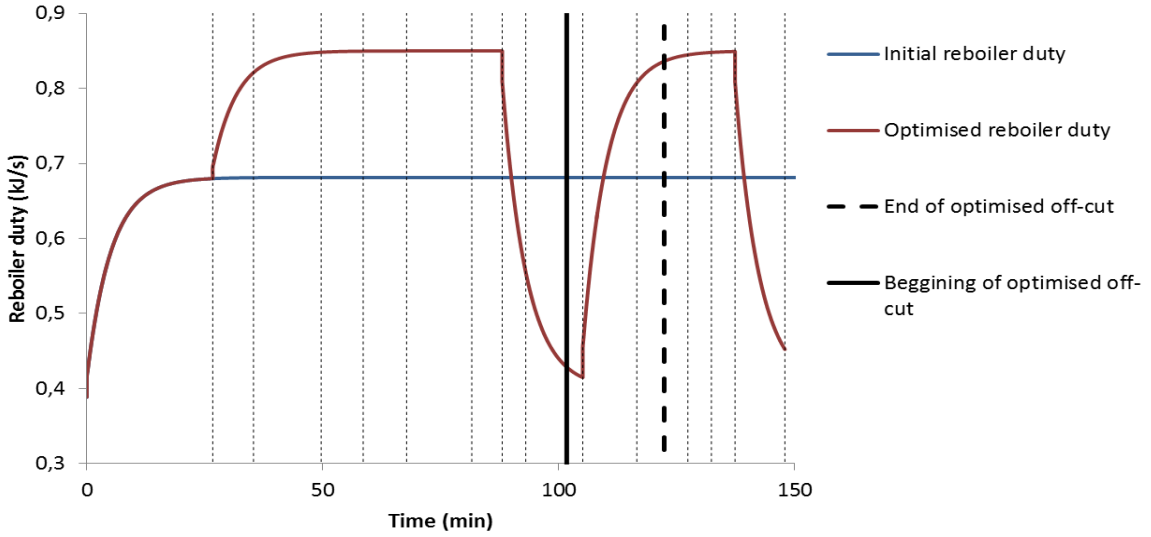

Figure 73- Initial reboiler duty profile and optimised reboiler duty profile for medium and light component distillation optimisation

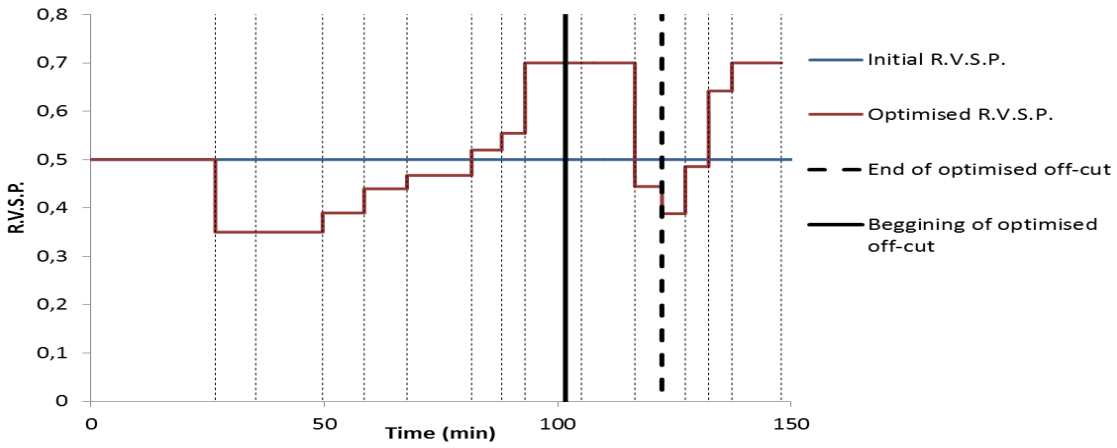

Figure 74 - Initial reflux valve stem position profile and optimised reflux valve stem position profile for medium and light component distillation optimisation

Table 30 - Optimisation results for the optimised control variables in the medium and light component distillation problem, for 14 time intervals

Interval	Duration (s)	Final time (min)	PI_2 setpoint (kmol/hr)	RVSP	Reboiler heat duty setpoint (kJ/s)
1	518	35.3	0.030	0.35	0.85
2	859	49.7	0.030	0.35	0.85
3	534	58.6	0.026	0.39	0.85
4	550	67.7	0.020	0.44	0.85
5	830	81.6	0.008	0.47	0.85
6	385	88.0	0.010	0.52	0.85
7	300	93.0	0.030	0.55	0.40
8	724	105.1	0.030	0.70	0.40
9	687	116.5	0.006	0.70	0.85
10	347	122.3	0.006	0.44	0.85
11	300	127.3	0.030	0.39	0.85
12	300	132.3	0.030	0.49	0.85
13	300	137.3	0.030	0.64	0.85
14	633	147.9	0.030	0.7	0.40

A.6 – Full distillation problem

In this appendix the control variables optimised profiles for the full distillation problem are presented. Additionally, table 31 presents the optimisation result values for the controlled variables for the 10 time intervals optimisation:

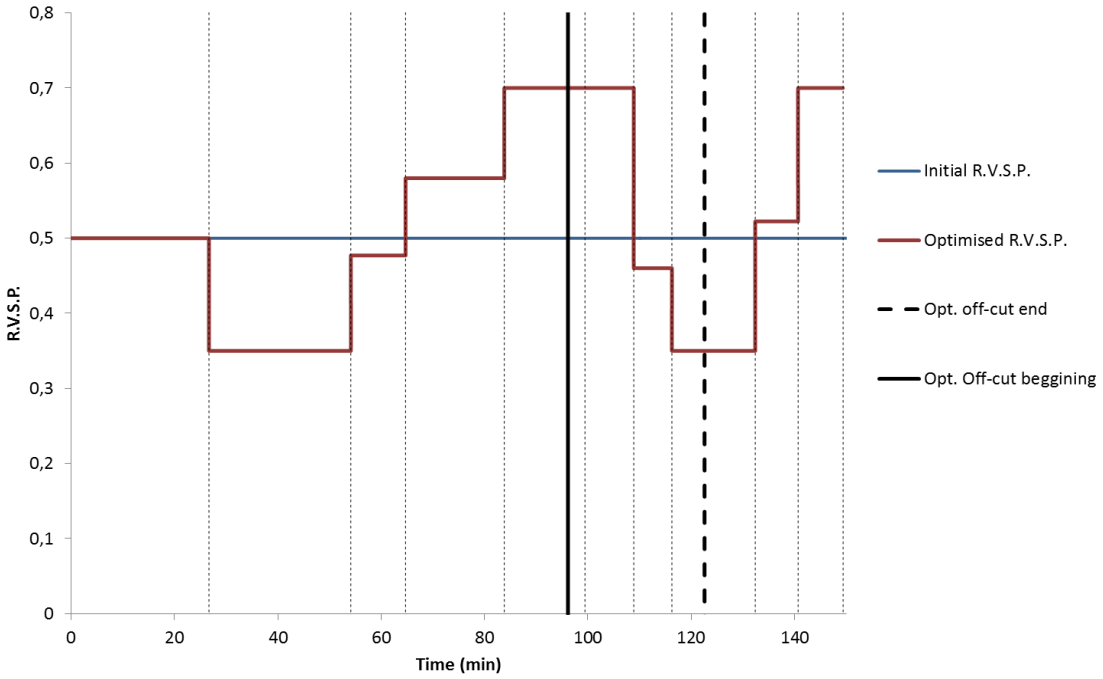

Figure 75 - Initial reflux valve stem position profile and optimised reflux valve stem position profile for distillation distillation optimisation

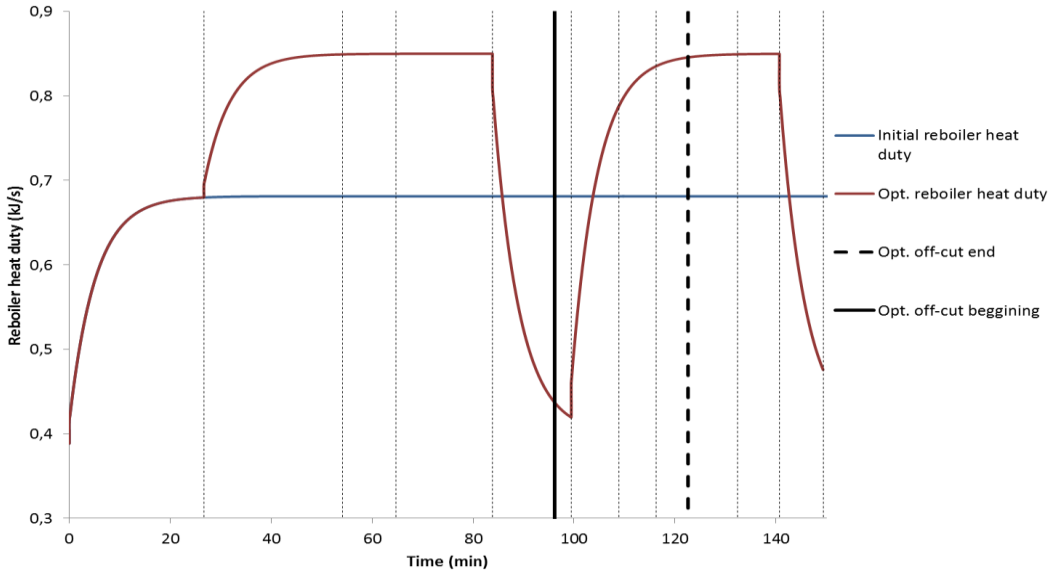

Figure 76 - Initial reboiler heat duty profile and optimised reboiler heat duty profile for full distillation optimisation

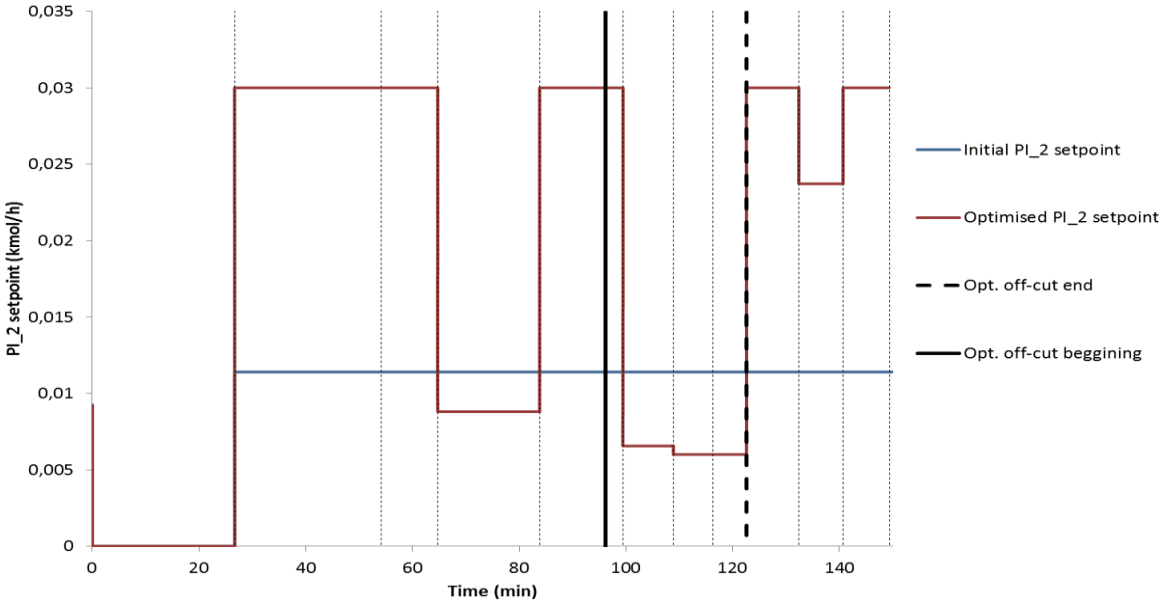

Figure 77 - Initial PI_2 setpoint profile and optimised PI_2 setpoint profile for full distillation optimisation

Table 31 - Optimisation results for the optimised control variables in the full distillation problem, for 14 time intervals

Interval	Duration (s)	Final time (min)	PI_2 setpoint (kmol/hr)	RVSP	Reboiler heat duty (kJ/s)
1	1648	54.1	0.030	0.35	0.85
2	635	64.7	0.030	0.46	0.85
3	1147	83.8	0.009	0.58	0.85
4	937	99.4	0.030	0.70	0.40
5	566	108.9	0.007	0.70	0.85
6	443	116.3	0.006	0.46	0.85
7	379	122.6	0.006	0.35	0.85
8	588	132.4	0.030	0.35	0.85
9	497	140.7	0.024	0.52	0.85
10	523	149.4	0.030	0.70	0.04

A.7 – Pressure drop correlations

In this appendix, the pressure drop correlations from Bernoulli and Bennett for dry vapour and aerated liquid (respectively) are presented.

A.7.1 – Bernoulli dry vapour pressure drop correlation

The dry vapour pressure drop h_d (m) is calculated with the following equation:

$$h_d = \frac{50.8}{C_v^2} * \frac{\rho^V}{\rho^L} * v_h^2 \quad \text{(A.1)}$$

where $\rho^V$is the vapour density (kg/m^3), ρ^L is the liquid density (kg/m^3), and v_h the vapour velocity through the holes (m/s). C_v is the orifice coefficient, and for this correlation, it assumes the constant value of 0.75.

A.7.2 – Bennett aerated liquid pressure drop

The Bennett correlation for the aerated liquid pressure drop h_l (m) is presented below:

$$h_l = h_c + h_\sigma \quad \text{(A.2)}$$

where h_c is the effective clear liquid height (m) and h_σ is the residual pressure drop due to surface tension (m). The former value is calculated as.

$$h_\sigma = \frac{472000*\sigma}{g*\rho^L} * (\frac{g(\rho^L-\rho^V)}{\sigma*d_h*10^6})^{\frac{1}{3}} \quad \text{(A.3)}$$

where g is the gravitational acceleration constant (m/s^2), σ is the surface tension (N/m) and d_h is the hole diameter (m). The effective clear liquid height is based on froth regime, calculated as:

$$h_c = h_f \phi_f \quad \text{(A.4)}$$

$$h_f = h_w + 15.33 * C * (\frac{Q}{\phi_f})^{\frac{2}{3}} \quad \text{(A.5)}$$

$$C = 0.0327 + 0.0286e^{(-0.1378h_w)} \quad \text{(A.6)}$$

$$\phi_f = e^{(-12.55K_s^{0.91})} \quad \text{(A.7)}$$

$$K_s = v_a(\frac{\rho^V}{\rho^L-\rho^V})^{0.5} \quad \text{(A.8)}$$

where h_f is the froth height (m), ϕ_f is the froth density (kg/m^3), Q is the volumetric flowrate (m^3/s), $h_w$is the weir height (m), v_a is the vapour velocity through the active area (m/s).